

ENCLOSURE 2

CNRO-2003-00033

ENGINEERING REPORT M-EP-2003-002, REV. 1

**FRACTURE MECHANICS ANALYSIS FOR THE ASSESSMENT OF THE
POTENTIAL FOR PRIMARY WATER STRESS CORROSION CRACK (PWSCC)
GROWTH IN THE UNINSPECTED REGIONS OF THE
CONTROL ELEMENT DRIVE MECHANISM (CEDM) NOZZLES AT
ARKANSAS NUCLEAR ONE UNIT 2**



ENTERGY NUCLEAR SOUTH
Engineering Report Coversheet

**Fracture Mechanics Analysis for the Assessment
 of the
 Potential for Primary Water Stress Corrosion Crack (PWSCC) Growth
 in the
 Un-Inspected Regions of the Control Element Drive Mechanism (CEDM) Nozzles
 at
 Arkansas Nuclear One Unit 2**

Engineering Report Type:

New Revision Deleted Superseded

Applicable Site(s)

ANO Echelon GGNS RBS WF3

Report Origin: ENS Vendor **Safety-Related:** Yes No

Vendor Document No. _____

		Date:	Comments:	Attached:
Prepared by:	<u>J. S. Bithman-Lesau</u>	<u>8/26/2003</u>	<input type="checkbox"/> Yes	<input type="checkbox"/> Yes
	Responsible Engineer		<input type="checkbox"/> No	<input type="checkbox"/> No
Verified/ Reviewed by:	<u>Brian C. Gray</u>	<u>8/26/03</u>	<input checked="" type="checkbox"/> Yes	<input type="checkbox"/> Yes
	Design Verifier/Reviewer		<input type="checkbox"/> No	<input checked="" type="checkbox"/> No
Approved by:	<u>R. S. [Signature]</u>	<u>8/26/03</u>	<input type="checkbox"/> Yes	<input type="checkbox"/> Yes
	Responsible Supervisor or Responsible Central Engineering Manager (for multiple site reports only)		<input checked="" type="checkbox"/> No	<input type="checkbox"/> No

E-M-EP-2003-002 01

Engineering Report No. _____ Rev. _____

Page 2 of 62

RECOMMENDATION FOR APPROVAL FORM

	Date:	Comments:	Attached:
Prepared by: <u>J.S. Bohmleson</u> <u>William Simo 8/26/03</u> Responsible Engineer	<u>8/27/03</u>	<input type="checkbox"/> Yes <input type="checkbox"/> No	<input type="checkbox"/> Yes <input type="checkbox"/> No
Concurrence: <u>Karl Tucker</u> Responsible Engineering Manager, ANO	<u>8/26/03</u>	<input type="checkbox"/> Yes <input checked="" type="checkbox"/> No	<input type="checkbox"/> Yes <input type="checkbox"/> No
Not Applicable	Date: _____	<input type="checkbox"/> Yes <input type="checkbox"/> No	<input type="checkbox"/> Yes <input type="checkbox"/> No
Concurrence: _____ Responsible Engineering Manager, GGNS	Date: _____	<input type="checkbox"/> Yes <input type="checkbox"/> No	<input type="checkbox"/> Yes <input type="checkbox"/> No
Not Applicable	Date: _____	<input type="checkbox"/> Yes <input type="checkbox"/> No	<input type="checkbox"/> Yes <input type="checkbox"/> No
Concurrence: _____ Responsible Engineering Manager, RBS	Date: _____	<input type="checkbox"/> Yes <input type="checkbox"/> No	<input type="checkbox"/> Yes <input type="checkbox"/> No
Not Applicable	Date: _____	<input type="checkbox"/> Yes <input type="checkbox"/> No	<input type="checkbox"/> Yes <input type="checkbox"/> No
Concurrence: _____ Responsible Engineering Manager, WF3	Date: _____	<input type="checkbox"/> Yes <input type="checkbox"/> No	<input type="checkbox"/> Yes <input type="checkbox"/> No

Table of Contents

Section	Title	Page Number
	List of Tables	3
	List of Figures	4
	List of Appendices	6
1.0	Introduction	7
2.0	Stress Analysis	11
3.0	Analytical Basis for Fracture Mechanics and Crack Growth Models	33
4.0	Method of Analysis	38
5.0	Discussion and Results	43
6.0	Conclusions	60
7.0	References	61

List of Tables

Table Number	Title	Page Number
1	Nodal Stress data for 0° Nozzle.	17
2	Nodal Stress data for the 8.8° nozzle at the downhill location.	18
3	Nodal Stress data for the 8.8° nozzle at 22.5° rotated from the downhill location.	19
4	Nodal Stress data for the 8.8° nozzle at 45° rotated from the downhill location.	20
5	Nodal Stress data for the 8.8° nozzle at 67.5° rotated from the downhill location.	21
6	Nodal Stress data for the 8.8° nozzle at the Mid-Plane location.	22
7	Nodal Stress data for the 8.8° nozzle at the uphill location.	23
8	Nodal Stress data for the 28.8° nozzle at the downhill location.	24

List of Tables (continued)

Table Number	Title	Page Number
9	Nodal Stress data for the 28.8° nozzle at 22.5° rotated from the downhill location.	25
10	Nodal Stress data for the 28.8° nozzle at the Mid-Plane location.	26
11	Nodal Stress data for the 28.8° nozzle at the uphill location.	27
12	Nodal Stress data for the 49.6° nozzle at the downhill location.	28
13	Nodal Stress data for the 49.6° nozzle at 22.5° rotated from the downhill location.	29
14	Nodal Stress data for the 49.6° nozzle at 45° rotated from the downhill location.	30
15	Nodal Stress data for the 49.6° nozzle at the Mid-Plane location.	31
16	Nodal Stress data for the 49.6° nozzle at the uphill location.	32
17	Comparison of Fracture Mechanics Models	48
18	Results for compression zone	49
19	ANO-2 As-Built Analyses Results Summary	51
20	Results from Additional Analysis	56
21	Boundaries for Augmented Inspection	57

List of Figures

Figure Number	Title	Page Number
1	Details of guide-cone connection to CEDM [2]. Detail extracted from Drawing M-2001-C2-107 [2]	8
2	Sketch of a typical inspection probe sled [3a].	9
3	Estimated as-built nozzle configuration based on evaluation of the UT and design data.	12
4	Hoop Stress contours for the 0° nozzle.	14
5	Hoop Stress contours for the 8.8° nozzle.	14
6	Hoop Stress contours for the 28.8° nozzle.	15
7	Hoop Stress contours for the 49.6° nozzle.	15
8	Plot showing hoop stress distribution along tube axis for the 0° nozzle.	17
9	Plot showing hoop stress distribution along tube axis for the 8.8° nozzle at the downhill location.	18
10	Plot showing hoop stress distribution along tube axis for the 8.8° nozzle at 22.5° rotated from the downhill location.	19
11	Plot showing hoop stress distribution along tube axis for the 8.8° nozzle at 45° rotated from the downhill location.	20

List of Figures (Continued)

Figure Number	Title	Page Number
12	Plot showing hoop stress distribution along tube axis for the 8.8° nozzle at 67.5° rotated from the downhill location.	21
13	Plot showing hoop stress distribution along tube axis for the 8.8° nozzle at the Mid-Plane location.	22
14	Plot showing hoop stress distribution along tube axis for the 8.8° nozzle at the uphill location.	23
15	Plot showing hoop stress distribution along tube axis for the 28.8° nozzle at the downhill location.	24
16	Plot showing hoop stress distribution along tube axis for the 28.8° nozzle at 22.5° rotated from the downhill location..	25
17	Plot showing hoop stress distribution along tube axis for the 28.8° nozzle at the Mid-Plane location.	26
18	Plot showing hoop stress distribution along tube axis for the 8.8° nozzle at the uphill location.	27
19	Plot showing hoop stress distribution along tube axis for the 49.6° nozzle at the downhill location.	28
20	Plot showing hoop stress distribution along tube axis for the 49.6° nozzle at 22.5° rotated from the downhill location.	29
21	Plot showing hoop stress distribution along tube axis for the 49.6° nozzle at 45° rotated from the downhill location.	30
22	Plot showing hoop stress distribution along tube axis for the 49.6° nozzle at the Mid-Plane location.	31
23	Plot showing hoop stress distribution along tube axis for the 49.6° nozzle at the uphill location.	32
24	SICF shown as a function of normalized crack depth for the "a-tip" and the "c-tip"	34
25	Curve fit equations for the "extension and bending" components in Reference 8.	37
26	Plots showing effect of nodal data selection on the accuracy of polynomial regression fit,	41
27	Comparison of SICF for the edge crack configurations with the membrane SICF for current model.	46
28	Comparison of SIF for the current model and conventional model.	47
29	SIF comparison between current model and conventional model.	48
30	Crack growth and SIF for 0° nozzle – OD surface crack.	52

List of Figures (Continued)

Figure Number	Title	Page Number
31	Crack growth and SIF for 0° nozzle – Through-wall axial crack.	53
32	Crack growth and SIF for 8.8° nozzle – OD surface crack.	53
33	Crack growth and SIF for 8.8° nozzle – Through-wall axial crack.	54
34	Crack growth and SIF for 28.8° nozzle – OD surface crack.	54
35	Crack growth and SIF for 28.8° nozzle – Through-wall axial crack.	55
36	0° Nozzle crack growth at a lowered reference line at 1.25 inches above nozzle bottom.	58
37	8.8° Nozzle crack growth at blind zone elevation of 1.544 inches above nozzle bottom at an azimuth of 67.5°.	58
38	28.8° Nozzle crack growth at blind zone elevation of 1.544 inches above nozzle bottom at an azimuth of 22.5°.	59
39	49.6° Nozzle crack growth at blind zone elevation of 1.544 inches above nozzle bottom at an azimuth of 45°.	60

List of Appendices

Appendix Number	Content of Appendix	Number of Attachments In Appendix
A	Design, UT probe characterization, UT analysis results, and evaluation for as-built configuration	6
B	Mathcad worksheets annotated to describe the three models	3
C	Mathcad worksheets for ANO-2 Analyses	48 ¹
D	Verification and Comparisons (Mathcad worksheets)	4

1) Attachment number 32 is intentionally blank, but is included to keep the sequence in order.

Note:- This document {revision 1} was revised to:

- 1) Make it ANO-2 specific.**
- 2) Revise finite element models and re-analyze residual stresses.**
- 3) Change the surface crack fracture mechanics models.**
- 4) Define augmented inspection regions.**

1.0 Introduction

The US Nuclear Regulatory Commission (NRC) issued Order EA-03-009 [1], which modified licenses, requiring inspection of all Control Element Drive Mechanism (CEDM), In-Core Instrumentation (ICI), and vent penetration nozzles in the reactor vessel head. Paragraph IV.C.1.b of the Order requires the inspection to cover a region from the bottom of the nozzle to two (2.0) inches above the J-groove weld. In the Combustion Engineering (CE) design the CEDM nozzles have a guide-cone attached to the bottom of each CEDM. Figure 1 [2] provides a drawing showing the attachment detail and a sketch showing the typical CEDM arrangement in the reactor vessel head. The attachment is a threaded connection with a securing set-screw between the guide-cone and the CEDM nozzle. The CEDM nozzle is internally threaded and the guide-cone has external threads. Thus, the CEDM nozzles in the region of attachment, including the chamfered region, become inaccessible for Ultrasonic Testing (UT) to interrogate the nozzle base material. The design of the UT probes result in a region above the chamfer (0.200 inch [reference 3a & 3b]) that cannot be inspected. Therefore, the region of the CEDM base metal that can be inspected begins at about 1.544 inches above the bottom of the CEDM nozzle and extends to two (2.0) inches above the J-groove weld. The unexamined length (here after called the blind zone) constitutes the threaded region, the chamfer region, and the UT dead zone ($1.250 + 0.094 + 0.200$). The terms used in this report are defined as follows:

- Freespan = (bottom of weld – blind zone); this area below the weld is accessible for volumetric examination.
- Propagation Length = (bottom of weld –top of crack tip); area available for crack growth.

Note:- for an outside diameter (OD) surface crack, this length is always less than the freespan; for through-wall it is equal to the freespan; and, for an inside diameter (ID) surface crack, the criterion is the propagation length and a through-wall penetration condition.

- Augmented Inspection Area: The axial and circumferential extent of the CEDM below the blind zone subject to an OD surface examination to ensure sufficient region for crack growth in one (1) cycle of operation without compromising the weld. This region may include weld material when the weld extends into the blind zone.

The nozzle as-built dimensions were determined by a detailed review of applicable design drawings and UT data from the previous inspection, which are provided as an attachment in Appendix A. The results of this assessment was used to develop the finite element model which obtains the prevailing stress distribution (Residual+Operating) used in the deterministic fracture mechanics analyses. The deterministic fracture mechanics analyses, in turn, assess the potential for primary water stress corrosion cracking (PWSCC) in the blind zone of the nozzles. This aspect is discussed in more detail in Section 2.

In order to exclude the blind zone from the inspection campaign, a relaxation of the Order is required pursuant to the requirements prescribed in Section IV.F and footnote 2 of the Order [1].

The purpose of this engineering report is to:

1. Determine if sufficient area between the blind zone and the weld exists to facilitate one (1) cycle of axial crack growth without the crack reaching the weld, and
2. For nozzles not meeting 1 above, determine how much of the blind zone combined with the available freespan is required to facilitate 1 cycle of crack growth without the crack reaching the weld. This area is subject to augmented surface examination.

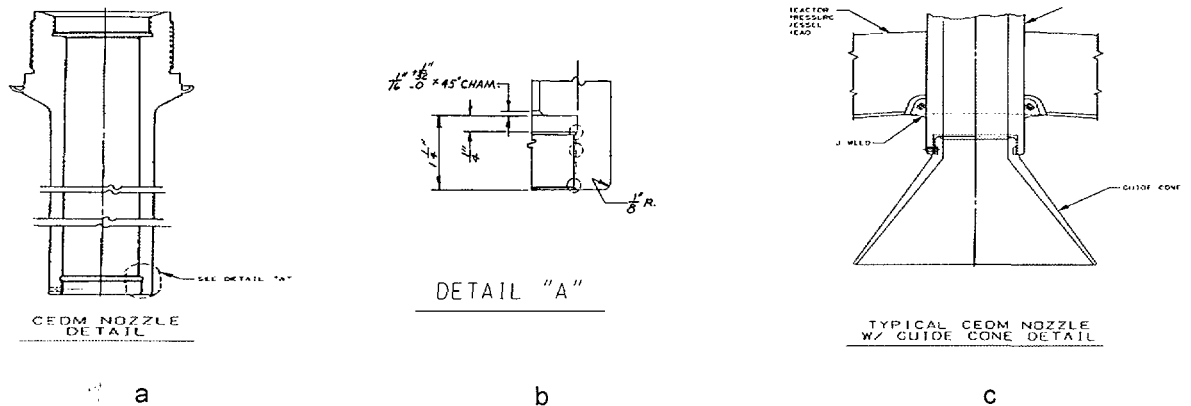
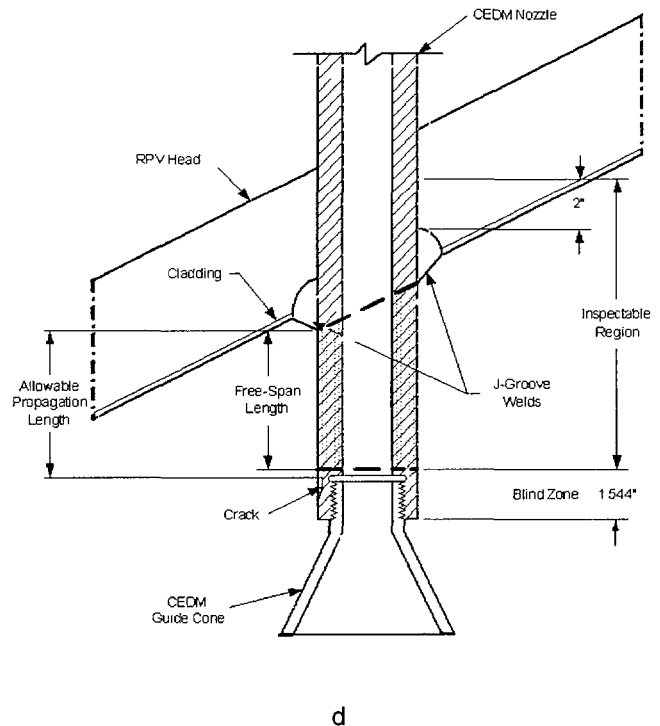


Figure 1:

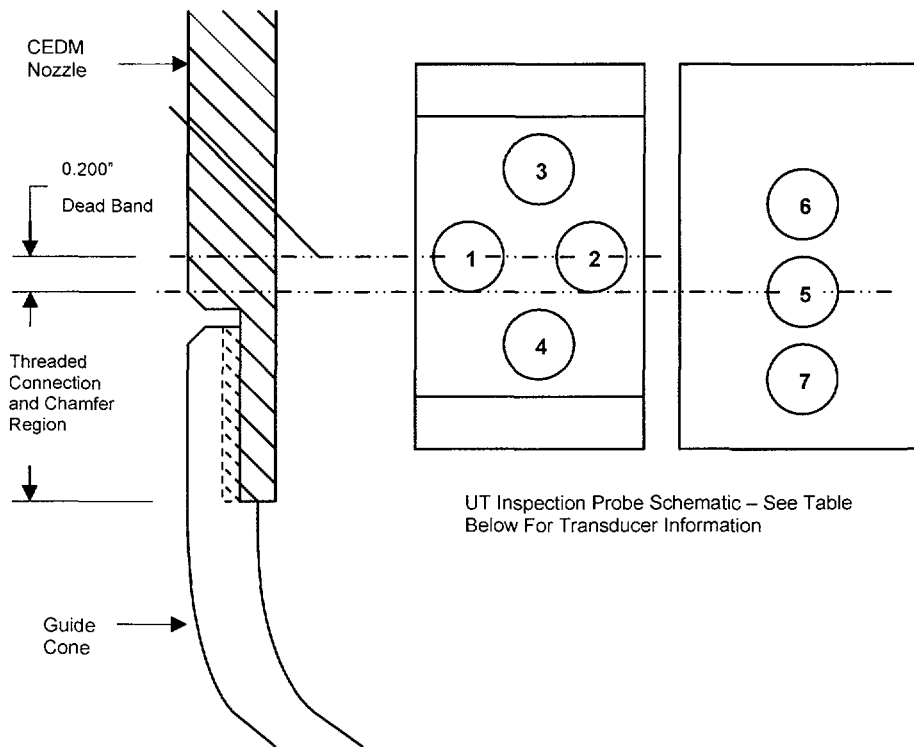
Details of guide cone connection to CEDM[2]. A sketch of a typical CEDM connection showing regions of interest is provided.

- a) CEDM nozzle tube.
- b) Details of the chamfer in the machined recess of the threaded region. Provides dimensions for the threaded and chamfer regions.
- c) Details of guide-cone connection to CEDM [2].
- d) Sketch of a typical CEDM penetration showing the region of interest.

Detail extracted from Drawing M-2001-C2-23 (ANO-2) [2]. The threaded region in the CEDM is 1.344 inches (Threads plus Recess plus chamfer).



The detail of the guide-cone-to-CEDM connection shows that the threaded + chamfer region is 1.344 inches in height. The UT dead band, determined to be 0.200 inch above the top of the threaded plus chamfer region in the CEDM, is based on a typical inspection probe sled design [3b] (shown in Figure 2).



Position	Mode	Diameter	Description
1	Transmit	0.25"	Circumferential Scan Using TOFD
2	Receive	0.25"	Circumferential Scan Using TOFD
3	Transmit	0.25"	Axial Scan Using TOFD
4	Receive	0.25"	Axial Scan Using TOFD
5	Transmit Receive	0.25"	Standard Zero Degree Scan
6	LFEC	NA	Low Frequency Eddy Current Probe
7	EC	NA	Standard Driver/Pickup Eddy Current Probe

Figure 2: Sketch of a typical inspection probe sled [3a]. The UT dead band is shown with respect to the thread + chamfer region

Based on the probe design and the geometry of the nozzle at the threaded connection, the explanation provided in Reference 3b shows the UT dead band to

extend 0.200 inch above the chamfer region immediately above the threads. Therefore, to account for the thread region, chamfer and the UT dead band, the blind zone height is determined to be 1.544 inch ($1.250'' + 0.094'' + 0.2''$) above the bottom of the nozzle.

The analysis used to determine the impact of not examining the blind zone independently evaluates a part through-wall axial crack initiated from the ID, a part through-wall axial crack initiated from the OD, and a through-wall axial crack.

Part Through-Wall Cracks

The initial crack depth obtained from Reference 4 is 0.04627 inch deep for an ID axial crack and 0.07932 inch deep for an OD axial crack. The crack length is based on the detected length of 4 mm (0.157 inch) from Reference 4. In the deterministic fracture mechanics analyses, the part through-wall crack lengths are doubled to 0.32 inch and the crack center is located at the top of the blind zone. Thus, the crack spans both the blind zone and the inspectable region. The postulated crack sizes and depths are two times the detectable limits with one-half (0.16 inch) of the flaw length being located in the examinable area. This provides for a conservative evaluation because:

- A) By extending the postulated crack 0.16 inch into the inspectable region, it places the crack tip closer to the weld where the hoop stresses are higher; and
- B) it assumes that 0.16 inches of the inspectable region is already cracked, reducing the remaining area for crack propagation.

Through-Wall Crack

In addition to evaluating the part through-wall cracks, this evaluation also conservatively evaluates a through-wall axial crack. The through-wall axial crack is postulated to exist from the top of the blind zone down to a point where the hoop stress is ≤ 10 ksi. This is a very conservative assumption, because for a crack to initiate on the surface and propagate through-wall while being totally contained within the blind zone would result in an unrealistic aspect ratio. As can be concluded from the following analysis, the length of a part through-wall crack would propagate into the inspectable region long before its depth reaches a through-wall condition. However, evaluation of the through-wall crack provides completeness to this assessment and ensures all plausible crack propagation modes are considered. Like the part through-wall crack, the hoop stresses at the top of the blind zone were used as the initial stress with adjustments to account for the increased stresses as the crack approaches the weld.

The analyses include a finite element stress analysis of the CEDM nozzles and a fracture mechanics-based crack growth analysis for PWSCC. These analyses are

performed for four nozzles (the nozzles were chosen at four head angles 0° , 8.8° , 28.8° , and 49.6°) in the reactor vessel head to account for the varied geometry of the nozzle penetration. In this manner the analysis provides a bounding evaluation for all nozzles in the reactor vessel head. The sections that follow contain a description of the analyses, the results, and conclusions supported by the analyses.

2.0 Stress Analysis

Finite element-based stress analyses for the ANO-2 CEDM penetrations, using the highest tensile yield strength for each group of nozzles, were performed using the best-estimate geometries based on previous UT and design information. The UT data obtained at the previous refueling outage were reviewed to determine the locations of the top and bottom of the J-weld at two azimuthal locations, downhill (0°) and the uphill (180°). The UT data obtained from this analysis is presented in Appendix A. This UT data were compared to the design information obtained from design drawings using an Excel spreadsheet to estimate the as-built condition. The spreadsheet used in this analysis is presented in Appendix A. This evaluation showed the following:

- 1) The central CEDM nozzles (0° and 8.8°) have weld sizes that are similar in size to the design drawings. However, this analysis also showed that the nozzle length below the ID clad surface to be 2.08 inches (shorter by 0.4 inch) compared to the design length of 2.48 inches.
- 2) The downhill side fillet welds on the peripheral CEDM nozzles (28.8° and 49.6°) have a longer leg than estimated from the design information. A fillet weld radius of $3/8$ inch instead of the specified $3/16$ inch provided the fillet weld leg length that matched the UT data. This evidence was also observed in another CE fabricated reactor vessel head. The fillet weld on the uphill side matched the information on the design drawing. Thus, only the downhill side fillet weld leg was extended for the model. The weld length on the uphill side matched the design information.

The evaluation to estimate the as-built dimensions of the CEDM configuration, taking into consideration the UT data and design information, consisted of the following steps:

- 1) The blind zone elevation of 1.544 inches from the nozzle bottom was taken to exist for all CEDM nozzles.
- 2) The design lengths for freespan at both the downhill and uphill locations were established (design length from weld bottom – blind zone).
- 3) These values were compared to the measurements obtained from the UT data analysis. The differences were recorded.
- 4) The design length to the top of the J-weld was compared to the measured length from the UT data for both the downhill and uphill locations and the differences recorded.

- 5) The weld lengths from design drawings were compared to the as measured data from the UT results. This was done for both the downhill and uphill locations. The differences were recorded.
- 6) The differences were evaluated to assess the variation between the design and as-measured data. This comparison showed that the differences for the central nozzles (8.8°) were consistent but the differences at the uphill location was 0.53 inch and a downhill freespan location was about 0.33 inch. This variation could be reconciled if the nozzle was about 0.4 inch shorter than the design insertion length. Therefore, the design insertion length was reduced by 0.4 inch to minimize the variation between the as-measured and design data. The higher hillside angle nozzles (28.8° and 49.6°) showed the variation to be more on the downhill side indicating a longer fillet weld leg length. This variation was minimized when the fillet weld radius was changed to $3/8$ inch instead of the design specified value of $3/16$ inch. Similar findings have been observed for another reactor vessel head fabricated by CE. Therefore, the increased fillet weld radius reasonably explains the larger fillet weld leg length observed in the UT data. For these nozzles the fillet weld leg length was increased. Figure 3 presents the sketches for the higher hillside angle nozzles (28.8° and 49.6°). This geometry was used to develop the estimated as-built finite element model. For the central nozzle group (0° and 8.8°), the nozzle insertion length was shortened by 0.4 inch to 2.08 inches. Since the weld lengths measured from the UT data matched the design data, the finite element model was developed using the shorter length but using the as-designed fillet weld dimensions.

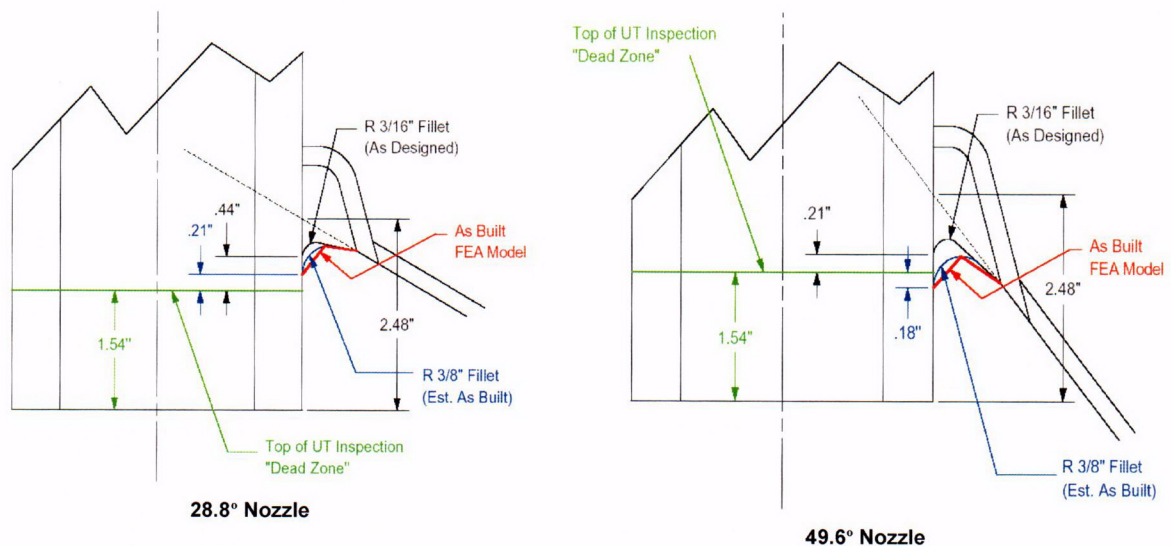


Figure 3: Estimated as-built nozzle configuration based on evaluation of the UT and design data. For the 49.6° nozzle, the bottom of the fillet weld extends 0.18 inch below the blind zone. For the 28.8° nozzle, the freespan length is reduced to 0.21 inch from the as-designed condition of 0.44 inch.

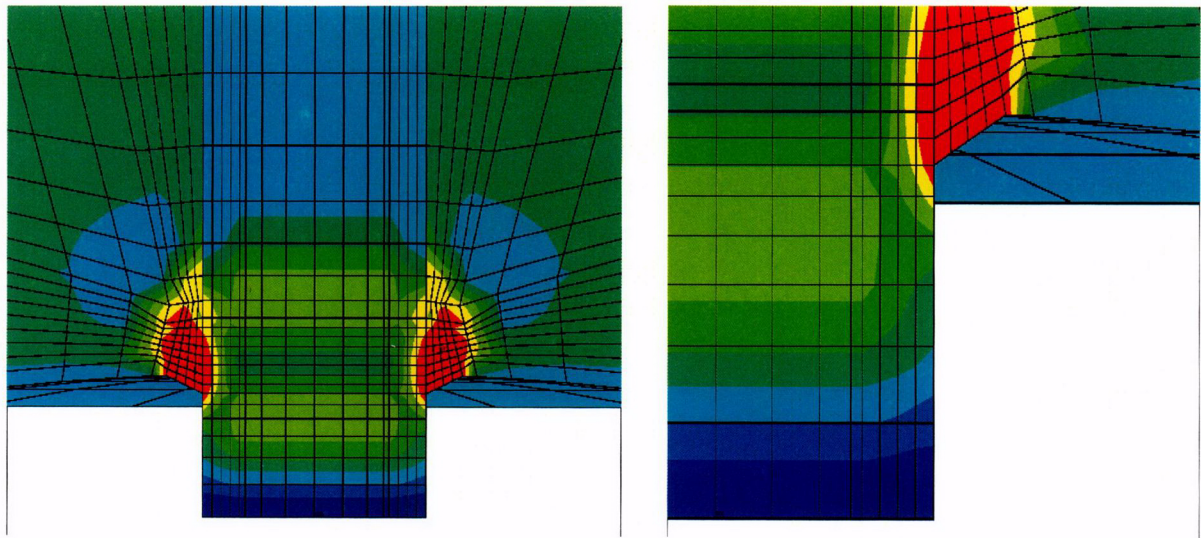
201

The finite element modeling for obtaining the necessary stress (residual+operating) distribution for use in fracture mechanics analysis followed the process and methodology described in Reference 5a. The modeling steps were as follows:

- 1) The finite element mesh consisted of 3-dimensional solid (brick) elements. Four elements were used to model the tube wall and similar refinement was carried to the attaching J-weld.
- 2) The CEDM tube material was modeled with a monotonic stress strain curve. The highest yield strength from the nozzle material bounded by the nozzle group was used. This yield strength was referenced to the room temperature yield strength of the stress-strain curve described in Reference 5a. The temperature dependent stress strain curves were obtained by indexing the temperature dependent drop of yield strength.
- 3) The weld material was modeled as elastic-perfectly plastic for the weld simulation. This approximation is considered reasonable since most of the plastic strain in the weld metal occurs at high temperatures where metals do not work-harden significantly (Reference 5c). The temperature in the weld is always high during the welding process and once the weld begins to cool, the temperatures in the weld at which strain hardening would persist are of limited duration (Reference 5c). This was borne out by the comparison between the analysis based residual stress distribution and that obtained from experiments (Reference 5d).
- 4) The weld is simulated by two passes based on studies presented in Reference 5a.
- 5) After completing the weld, a simulated hydro-test load step is applied to the model. The hydro-test step followed the fabrication practice.
- 6) The model is then subjected to a normal operating schedule of normal heat up to steady state conditions at operating pressure. The residual plus operating stresses, once steady state has been achieved, are obtained for further analysis. The nodal stresses of interest are stored in an output file. These stresses are then transferred to an Excel spreadsheet for use in fracture mechanics analysis.

The stress contours for the four nozzle groups obtained from the finite element analysis are presented in Figures 4 through 7. The stress contour color scheme are as follows:

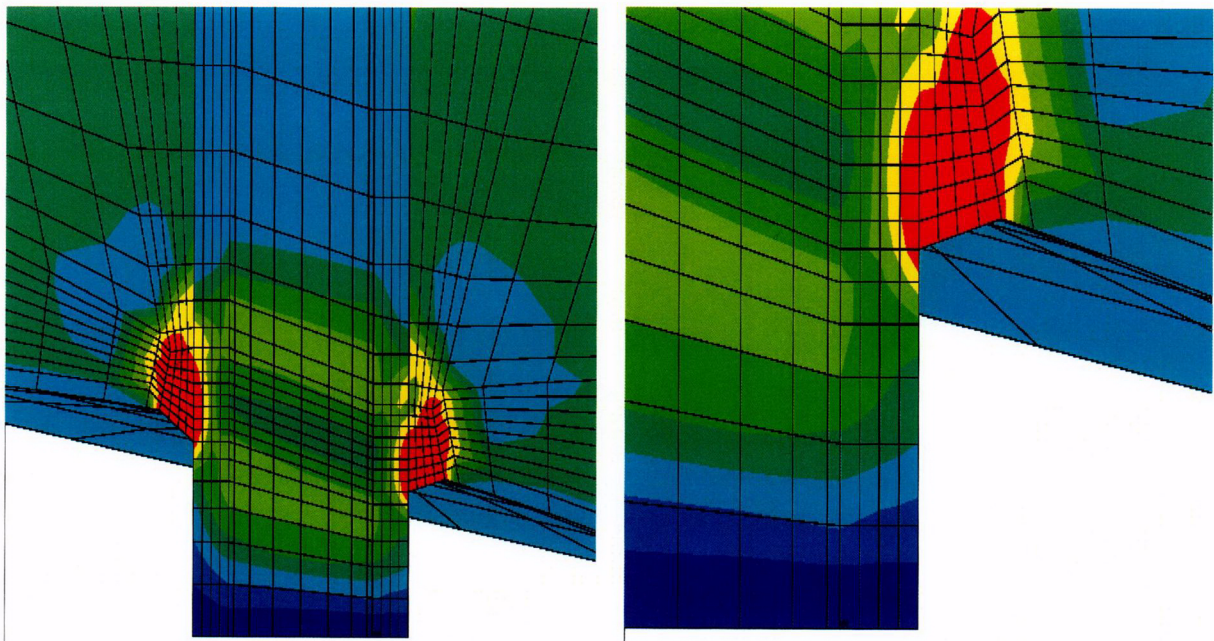
<i>Dark Navy blue</i>	<i>from Minimum (Compression) to -10 ksi</i>
<i>Royal blue</i>	<i>from -10 to 0 ksi</i>
<i>Light blue</i>	<i>from 0 to 10 ksi</i>
<i>Light green</i>	<i>from 10 to 20 ksi</i>
<i>Green</i>	<i>from 20 to 30 ksi</i>
<i>Yellow green</i>	<i>from 30 to 40 ksi</i>
<i>Yellow</i>	<i>from 40 to 50 ksi</i>
<i>Red</i>	<i>from 50 to 100 ksi</i>



Full Cross-section

Zoomed in right weld

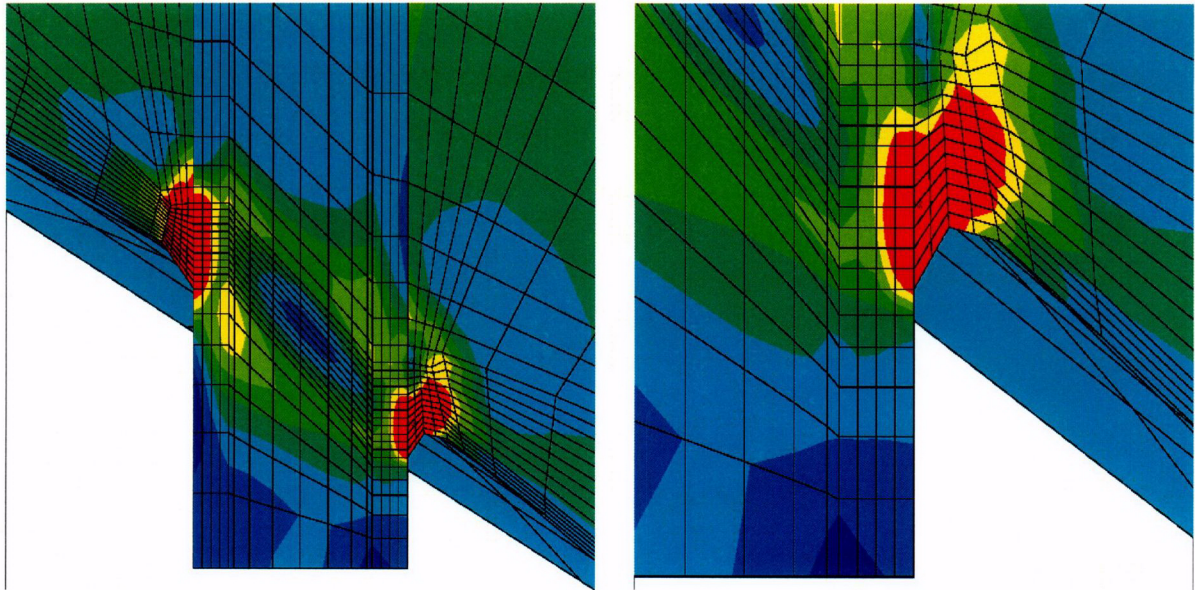
Figure 4: Hoop stress contours for the 0° nozzle. High tensile stresses occur in the weld and adjacent tube material. The bottom of the tube is in compression.



Full cross-section

Zoomed in Downhill side

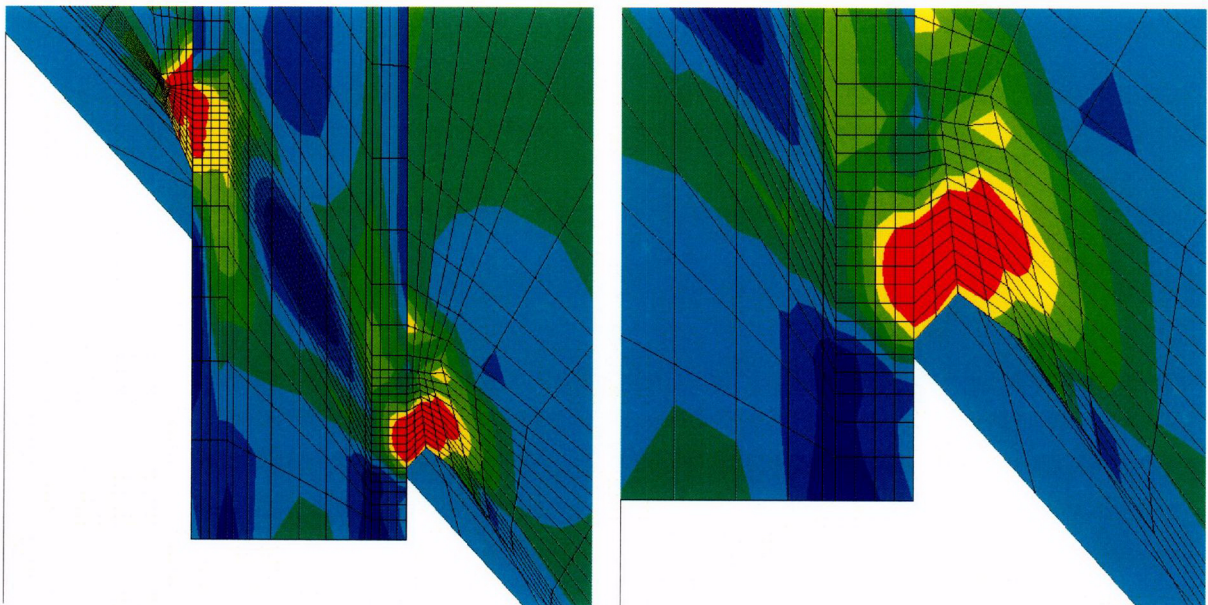
Figure 5: Hoop stress contours for the 8.8° nozzle. High tensile stresses occur in the weld and adjacent tube material. The bottom of the tube is in compression.



Full cross-section

Zoomed in Downhill side

Figure 6: Hoop stress contours for the 28.8° nozzle. High tensile stresses occur in the weld and adjacent tube material. The bottom of the tube is in compression.



Full cross-section

Zoomed in Downhill side

Figure 7: Hoop stress contours for the 49.6° nozzle. High tensile stresses occur in the weld and adjacent tube material. The bottom of the tube is in compression.

The nodal stresses for the locations of interest in each of the four nozzle groups were provided by Dominion Engineering Inc. and were tabulated in Reference

5b. The nodal stresses and associated figures representing the OD and ID distributions along the tube axis are presented in tables and associated figures in the following pages. The location of the weld bottom was maintained at the node row ending with "601". The blind zone location is shown on the associated figure. For the nozzle group at 8.8°, additional azimuthal locations (22.5°, 45° and 67.5°) around the circumference are shown. For the nozzle group at 28.8°, an additional azimuthal location (22.5°) around the circumference is shown. For the nozzle group at 49.6°, additional azimuthal locations (22.5° and 45°) around the circumference are shown. These additional locations are shown since they were evaluated for establishing the augmented inspection scope. The zone of compressive stress is also marked in the figure.

From the tables and associated figures, a full visualization of the stress distribution in the nozzle, from the nozzle bottom (located at 0.0 inch) to the top of the J-weld is obtained. These figures are also shown in the Mathcad worksheets provided in the Appendix "C" attachments. The nodal stress distribution, provided by Dominion Engineering, is used to establish the region of interest and the associated stress distribution that will be utilized in the subsequent analyses. In all cases evaluated but one, the bottom end of the nozzle (free end) is observed to be in compression. This is expected since the tube in the vicinity of the weld is in tension (high hoop tension), and the normal decay of stresses along the length of the tube results in compressive stress at the bottom. When the weld bottom extends lower, the compressive zone is shortened, but there remains a zone of compressive stress at the free end. For the 49.6° nozzle at the 90° rotated from the downhill location, the ID stress remains in tension while the OD stress becomes compressive (Figure 22)

In the following pages, the stress data from the Excel spreadsheet provided by Dominion Engineering (Reference 5b) and plots representing the axial distribution at the ID and OD locations are presented for each nozzle group with the specific azimuthal location that is evaluated. The location of the compression zone the blind zone and bottom of the weld are marked by colored reference lines.

Row	Height	ID	25%	50%	75%	OD
1	0.000	-25.088	-27.546	-27.787	-25.624	-23.763
101	0.485	-0.56305	-0.53856	-2.1108	-4.851	-6.1565
201	0.874	21.515	18.635	17.122	14.843	10.089
301	1.186	32.751	28.494	24.136	19.645	14.45
401	1.436	35.667	29.598	26.166	25.589	28.417
501	1.635	34.244	29.574	28.286	35.408	45.379
601	1.796	29.45	29.814	31.385	43.337	61.713
701	1.932	23.674	26.502	33.261	47.609	64.65
801	2.068	18.928	24.564	33.968	49.071	65.876
901	2.204	16.541	22.854	34.789	49.525	62.795
1001	2.341	17.561	22.683	33.806	47.49	63.558
1101	2.477	22.026	23.229	32.421	44.118	58.478
1201	2.613	26.382	25.611	31.17	41.606	52.552
1301	2.750	30.043	28.69	33.688	38.959	45.295
1401	2.886	33.132	31.073	37.166	43.676	36.261

Table 1: Nodal stress for 0° nozzle. This nozzle is symmetric about the nozzle axis hence these stresses prevail over the entire circumference. The weld location is shown by the shaded row.

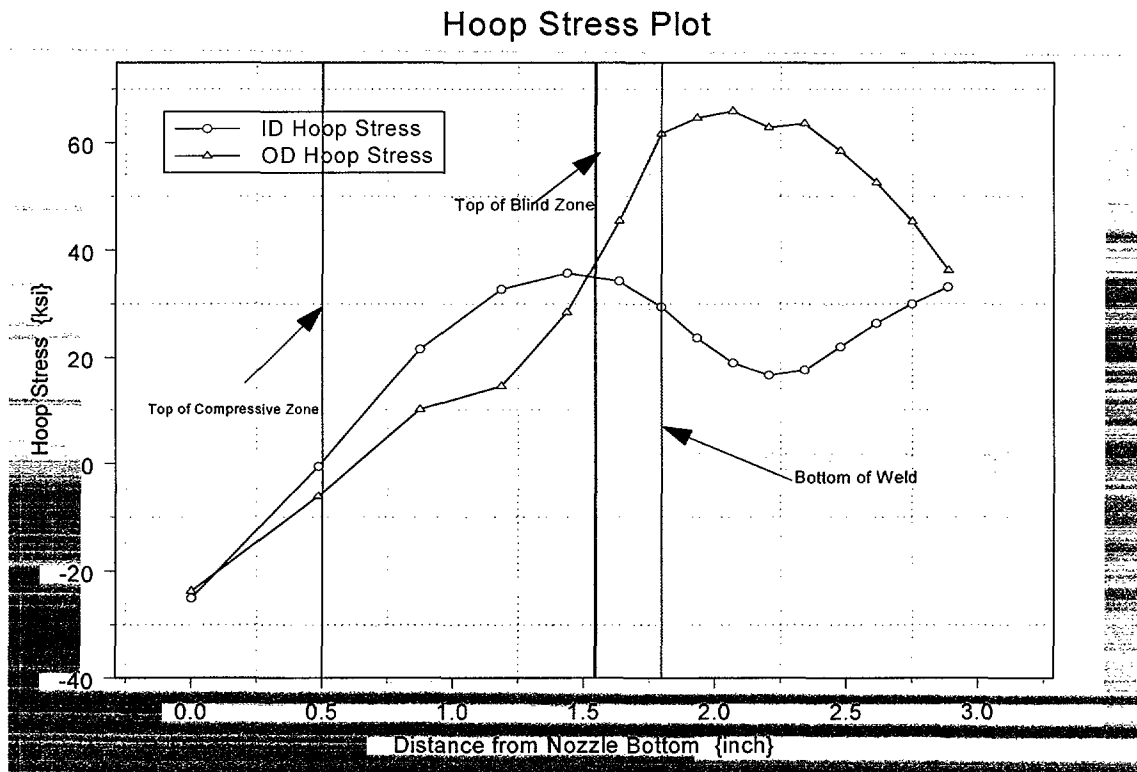


Figure 8: Plot showing hoop stress distribution along tube axis for the 0° nozzle. The top of compressive zone, the top of blind zone, and the bottom of the weld are shown.

Row	Height	ID	25%	50%	75%	OD
1	0.000	-27.404	-24.356	-22.209	-20.407	-18.978
101	0.483	0.63328	-1.486	-3.5987	-4.4402	-5.2679
201	0.870	17.665	16.422	14.61	12.415	9.3756
301	1.180	29.798	26.049	22.723	18.95	14.201
401	1.428	33.623	27.792	24.8	24.321	26.989
501	1.627	32.364	28.469	27.591	34.284	45.104
601	1.786	27.394	28.918	31.388	43.882	63.71
701	1.919	21.498	25.556	33.55	48.089	66.365
801	2.051	16.944	23.793	34.064	49.472	67.672
901	2.183	14.834	22.263	34.779	49.055	63.377
1001	2.315	15.852	21.898	33.764	46.61	61.537
1101	2.448	20.835	22.531	32.095	42.501	53.972
1201	2.580	25.973	25.072	30.748	39.365	47.486
1301	2.712	29.955	28.372	32.593	36.879	39.934
1401	2.844	33.46	31.26	36.351	41.573	31.302

Table 2: Nodal stress for 8.8° nozzle at the downhill location. The weld location is shown by the shaded row.

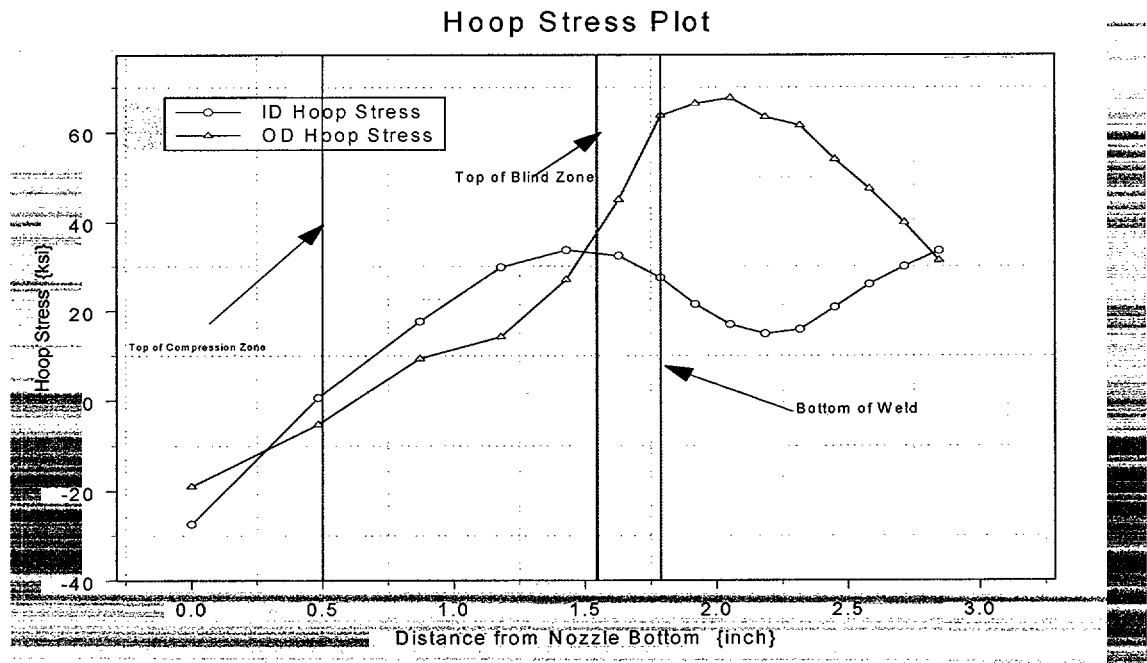


Figure 9: Plot showing hoop stress distribution along tube axis for the 8.8° nozzle at the downhill location. The top of compressive zone, the top of blind zone, and the bottom of the weld are shown.

Row	Height	ID	25%	50%	75%	OD
10001	0	-27.118	-24.146	-22.087	-20.358	-18.981
10101	0.48843	0.64978	-1.526	-3.6985	-4.5989	-5.4683
10201	0.87972	17.955	16.435	14.447	12.118	8.9948
10301	1.1932	29.829	26.102	22.672	18.714	13.833
10401	1.4443	33.679	27.823	24.722	24.104	26.541
10501	1.6455	32.389	28.385	27.447	34.121	44.818
10601	1.8067	27.386	28.803	31.156	43.603	61.245
10701	1.9403	21.477	25.458	33.3	47.738	65.934
10801	2.074	16.919	23.701	33.846	49.217	67.244
10901	2.2076	14.769	22.095	34.557	48.869	62.964
11001	2.3413	15.756	21.725	33.561	46.369	61.153
11101	2.4749	20.717	22.317	31.908	42.308	53.889
11201	2.6085	25.789	24.923	30.579	39.284	47.365
11301	2.7422	29.737	28.248	32.847	37.236	40.412
11401	2.8758	33.001	30.843	35.887	41.552	34.5

Table 3: Nodal stress for 8.8° nozzle at 22.5° rotated from the downhill location. The weld location is shown by the shaded row.

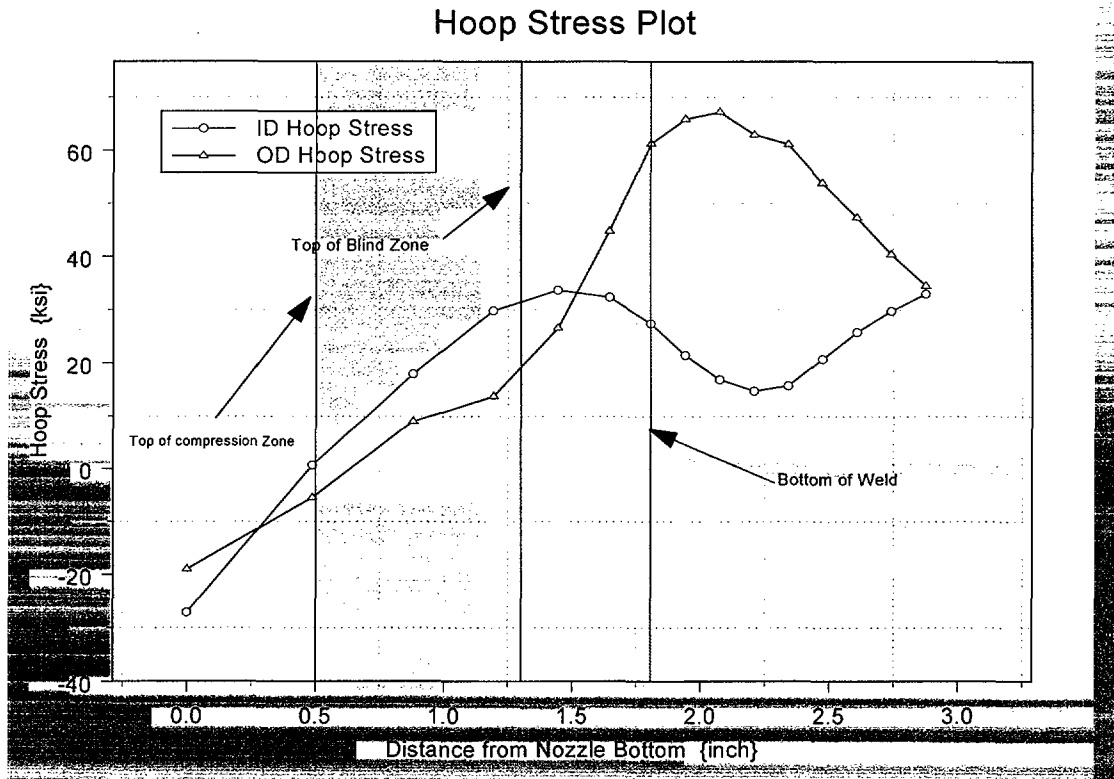


Figure 10: Plot showing hoop stress distribution along tube axis for the 8.8° nozzle at 22.5° rotated from the downhill location. The top of compressive zone, the top of blind zone, and the bottom of the weld are shown.

Row	Height	ID	25%	50%	75%	OD
20001	0	-26.311	-23.544	-21.718	-20.18	-18.943
20101	0.50592	-0.3769	-2.2224	-3.9683	-5.0362	-6.0278
20201	0.91123	20.089	16.851	14.017	11.337	7.9165
20301	1.2359	29.934	26.239	22.486	18.067	12.788
20401	1.4961	33.829	27.906	24.526	23.554	25.421
20501	1.7045	32.487	28.206	27.053	33.58	44.169
20601	1.8714	27.432	28.598	30.659	42.946	60.214
20701	2.0063	21.433	25.168	32.645	46.971	64.949
20801	2.1413	16.793	23.322	33.237	48.59	66.19
20901	2.2762	14.561	21.627	33.983	48.342	62.067
21001	2.4111	15.505	21.303	33.027	45.936	60.887
21101	2.5461	20.329	21.914	31.51	42.056	54.174
21201	2.681	25.223	24.532	30.274	39.283	47.704
21301	2.8159	29.209	27.786	32.709	37.408	41.335
21401	2.9509	32.564	30.324	35.521	41.82	35.243

Table 4: Nodal stress for 8.8° nozzle at 45° rotated from the downhill location. The weld location is shown by the shaded row.

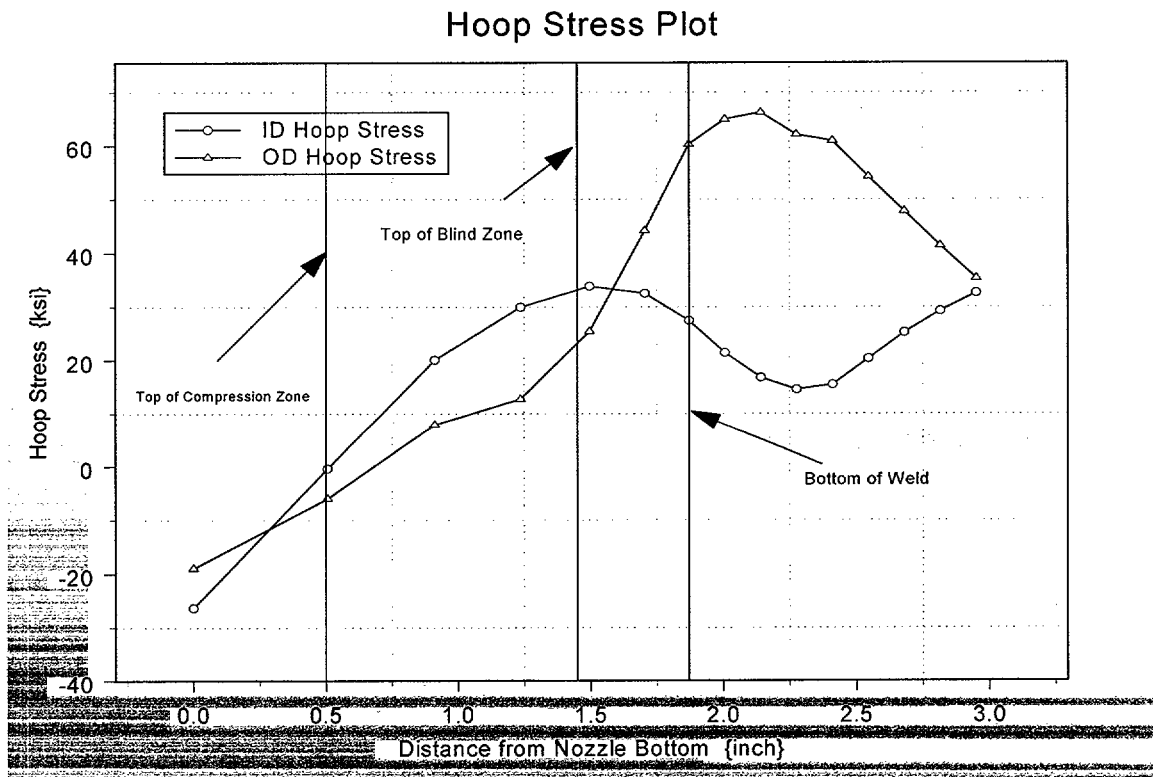


Figure 11: Plot showing hoop stress distribution along tube axis for the 8.8° nozzle at 45° rotated from the downhill location. The top of compressive zone, the top of blind zone, and the bottom of the weld are shown.

Row	Height	ID	25%	50%	75%	OD
30001	0	-25.236	-22.713	-21.175	-19.868	-18.802
30101	0.53254	-1.2673	-2.9633	-4.403	-5.6895	-6.8335
30201	0.95918	21.942	17.089	13.361	10.182	6.3275
30301	1.301	30.023	26.373	22.21	17.121	11.241
30401	1.5748	34.094	28.085	24.306	22.834	23.834
30501	1.7941	32.716	28.035	26.605	32.916	43.289
30601	1.9699	27.602	28.447	30.151	42.181	58.888
30701	2.1061	21.457	24.92	31.944	46.103	63.871
30801	2.2422	16.731	22.988	32.591	47.9	65.049
30901	2.3784	14.342	21.261	33.406	47.848	61.204
31001	2.5145	15.204	20.994	32.436	45.675	60.976
31101	2.6507	19.799	21.653	30.997	42.11	55.015
31201	2.7869	24.558	24.206	29.798	39.607	48.995
31301	2.923	28.72	27.503	32.15	37.459	42.682
31401	3.0592	32.844	30.245	35.773	41.844	36.257

Table 5: Nodal stress for 8.8° nozzle at 67.5° rotated from the downhill location. The weld location is shown by the shaded row.

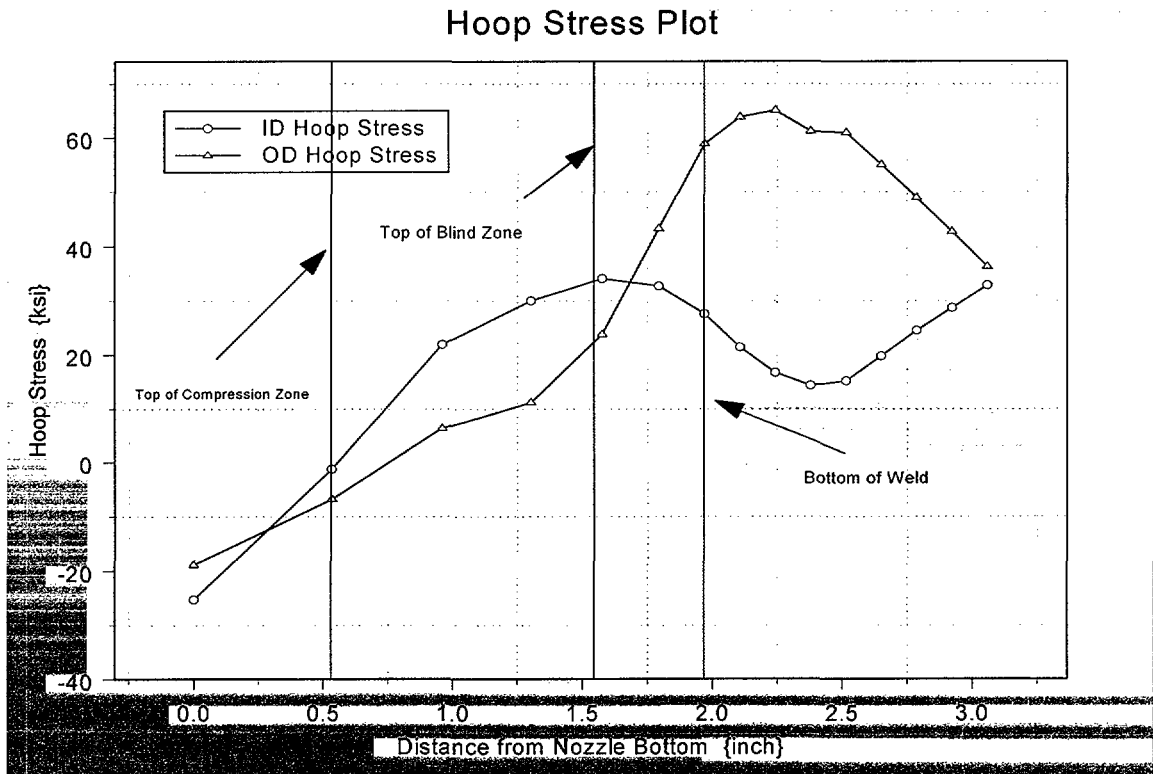


Figure 12: Plot showing hoop stress distribution along tube axis for the 8.8° nozzle at 67.5° rotated from the downhill location. The top of compressive zone, the top of blind zone, and the bottom of the weld are shown.

Row	Height	ID	25%	50%	75%	OD
40001	0.000	-24.18	-21.838	-20.55	-19.438	-18.504
40101	0.564	-1.4119	-3.3196	-4.9822	-6.4762	-7.7535
40201	1.016	22.032	16.773	12.529	8.7215	4.4282
40301	1.378	29.956	26.483	21.849	16.053	9.4283
40401	1.668	34.51	28.439	24.198	22.09	22.082
40501	1.900	33.218	28.069	26.319	32.416	42.48
40601	2.087	28.217	28.594	29.911	41.713	57.592
40701	2.224	22.006	25.059	31.606	45.624	63.118
40801	2.361	17.219	23.064	32.349	47.567	64.115
40901	2.499	14.675	21.28	33.218	47.796	60.65
41001	2.636	15.505	21.064	32.273	45.911	61.401
41101	2.773	19.832	21.649	31.008	42.649	56.171
41201	2.911	24.356	24.044	29.89	40.44	50.554
41301	3.048	28.385	27.206	32.287	37.721	43.702
41401	3.185	31.93	29.733	35.809	42.479	38.37

Table 6: Nodal stress for 8.8° nozzle at (Mid-Plane) 90° rotated from the downhill location. The weld location is shown by the shaded row.

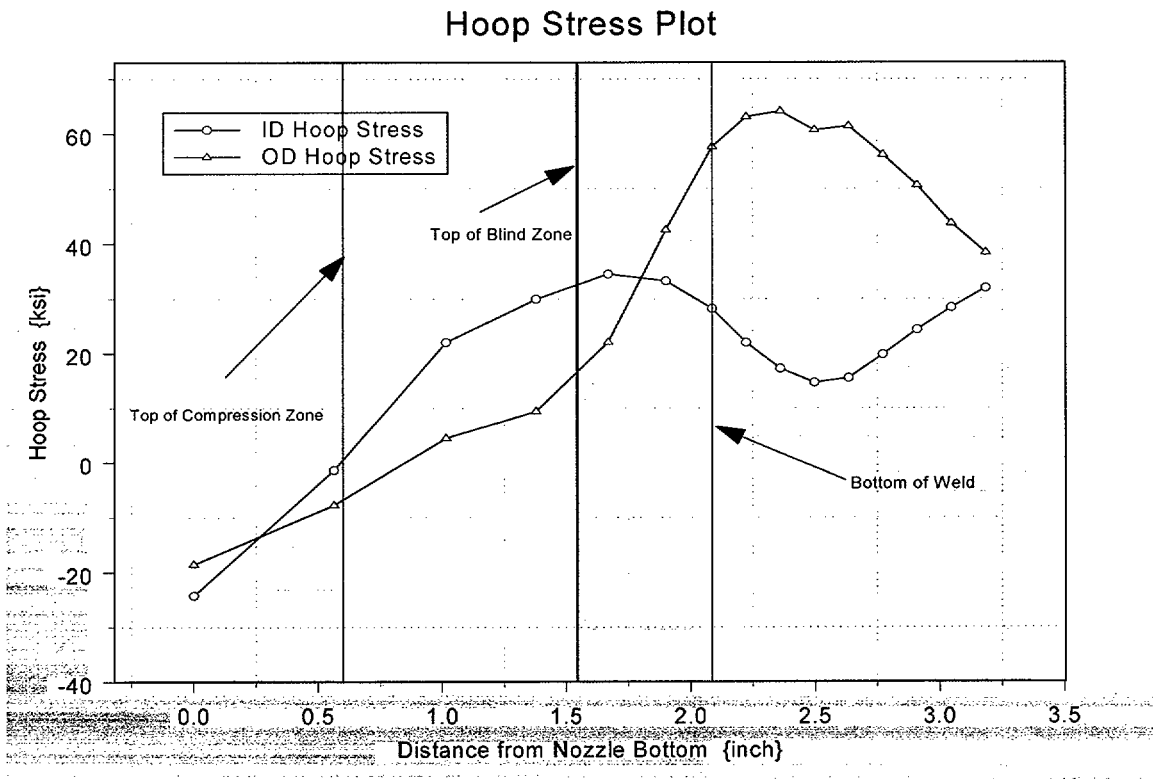


Figure 13: Plot showing hoop stress distribution along tube axis for the 8.8° nozzle at (Mid-Plane) 90° rotated from the downhill location. The top of compressive zone, the top of blind zone, and the bottom of the weld are shown.

Row	Height	ID	25%	50%	75%	OD
80001	0.000	-22.34	-20.022	-18.961	-18.087	-17.153
80101	0.645	-0.72174	-3.6673	-6.8206	-8.6957	-10.19
80201	1.162	17.28	14.912	9.6529	3.7661	-1.2205
80301	1.576	29.359	26.501	20.582	13.796	4.7531
80401	1.907	36.503	30.924	25.411	21.15	18.374
80501	2.173	36.536	30.331	27.24	32.606	41.485
80601	2.386	33.132	31.54	31.442	42.452	57.24
80701	2.528	27.116	28.37	33.434	47.233	63.826
80801	2.670	21.957	26.115	34.408	48.851	63.884
80901	2.813	18.993	24.124	35.202	49.904	62.107
81001	2.955	19.578	24.12	34.376	48.405	64.458
81101	3.098	23.12	24.375	33.301	45.647	61.604
81201	3.240	26.499	26.538	32.257	43.763	56.525
81301	3.382	29.872	29.202	35.086	41.634	49.89
81401	3.525	32.509	30.842	37.607	45.45	40.77

Table 7: Nodal stress for 8.8° nozzle at (Uphill) 180° rotated from the downhill location. The weld location is shown by the shaded row.

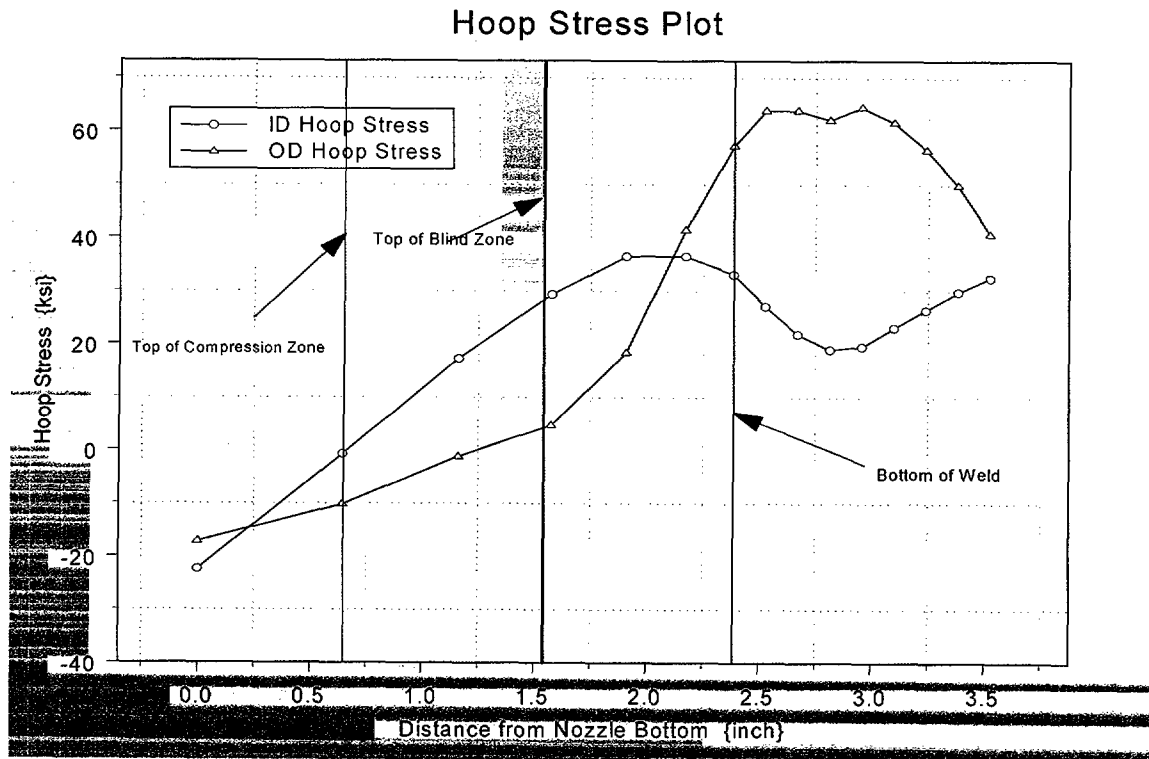


Figure 14: Plot showing hoop stress distribution along tube axis for the 8.8° nozzle at (Uphill) 180° rotated from the downhill location. The top of compressive zone, the top of blind zone, and the bottom of the weld are shown.

Row	Height	ID	25%	50%	75%	OD
1	0.000	-17.414	-13.552	-11.113	-8.8843	-6.6283
101	0.461	-8.4943	-6.31	-4.924	-3.7058	-2.5412
201	0.830	0.088906	0.17947	0.11003	0.18625	0.2839
301	1.126	7.0251	6.9534	6.3144	5.2078	4.6462
401	1.363	8.2154	10.954	10.85	9.5121	5.6465
501	1.552	13.266	16.41	16.061	17.131	25.256
601	1.704	20.627	22.237	25.413	43.58	53.784
701	1.825	29.036	28.83	31.285	53.547	64.082
801	1.946	33.945	30.929	36.407	61.6	71.01
901	2.066	29.591	31.788	40.536	64.612	76.418
1001	2.187	23.26	29.738	41.2	64.193	79.626
1101	2.308	18.689	27.734	41.29	61.777	78.117
1201	2.428	15.391	26.097	40.668	58.596	72.784
1301	2.549	14.546	24.118	39.369	54.107	62.074
1401	2.670	16.833	23.402	37.135	47.479	45.328
1501	2.790	22.94	24.557	33.686	39.867	31.733
1601	2.911	30.347	28.824	34.637	35.903	24.215
1701	3.032	36.319	33.178	37.13	37.761	22.663
1801	3.152	40.587	36.14	41.105	36.249	-4.0021

Table 8: Nodal stress for 28.8° nozzle at downhill location. The weld location is shown by the shaded row.

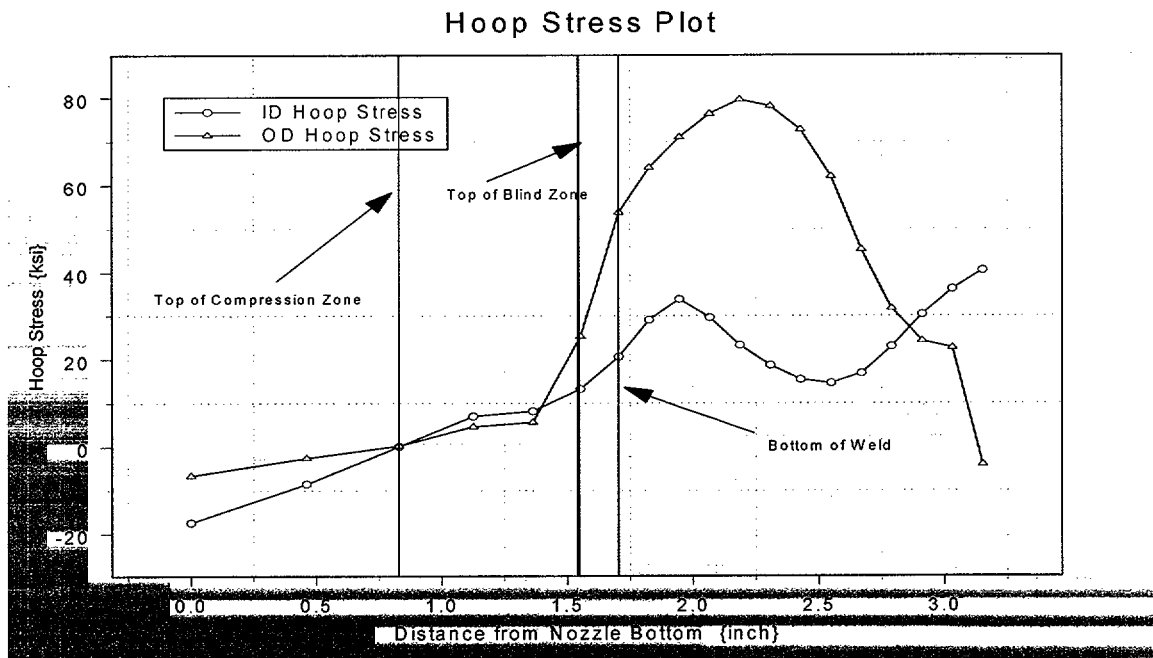


Figure 15: Plot showing hoop stress distribution along tube axis for the 28.8° nozzle at downhill location. The top of compressive zone, the top of blind zone, and the bottom of the weld are shown.

Row	Height	ID	25%	50%	75%	OD
10001	0	-14.205	-11.506	-9.7904	-8.2433	-6.7219
10101	0.49517	-6.4931	-5.1879	-4.4249	-3.7959	-3.1762
10201	0.89187	1.5545	1.0213	0.5647	0.25683	-0.0759
10301	1.2097	8.4295	7.9804	7.1986	6.1861	5.292
10401	1.4643	10.247	12.709	12.22	11.35	8.3641
10501	1.6682	15.665	18.335	18.703	20.835	29.697
10601	1.8317	24.321	24.532	26.71	44.525	57.729
10701	1.9511	31.496	28.696	31.228	53.015	63.555
10801	2.0706	31.975	30.109	35.633	59.449	69.026
10901	2.1901	26.833	29.946	38.369	61.124	72.691
11001	2.3096	20.84	27.287	38.5	59.952	75.043
11101	2.4291	15.99	24.671	38.159	58.169	73.854
11201	2.5486	12.461	22.874	37.588	54.954	67.711
11301	2.6681	11.21	20.931	36.521	51.142	59.155
11401	2.7876	13.526	20.476	34.299	45.784	43.711
11501	2.9071	19.78	22.135	31.566	38.968	31.028
11601	3.0266	26.712	26.192	32.945	36.476	24.484
11701	3.1461	32.478	30.015	35.497	38.328	23.185
11801	3.2656	36.911	32.504	38.269	35.608	2.1982

Table 9: Nodal stress for 28.8° nozzle at 22.5° rotated from the downhill location. The weld location is shown by the shaded row.

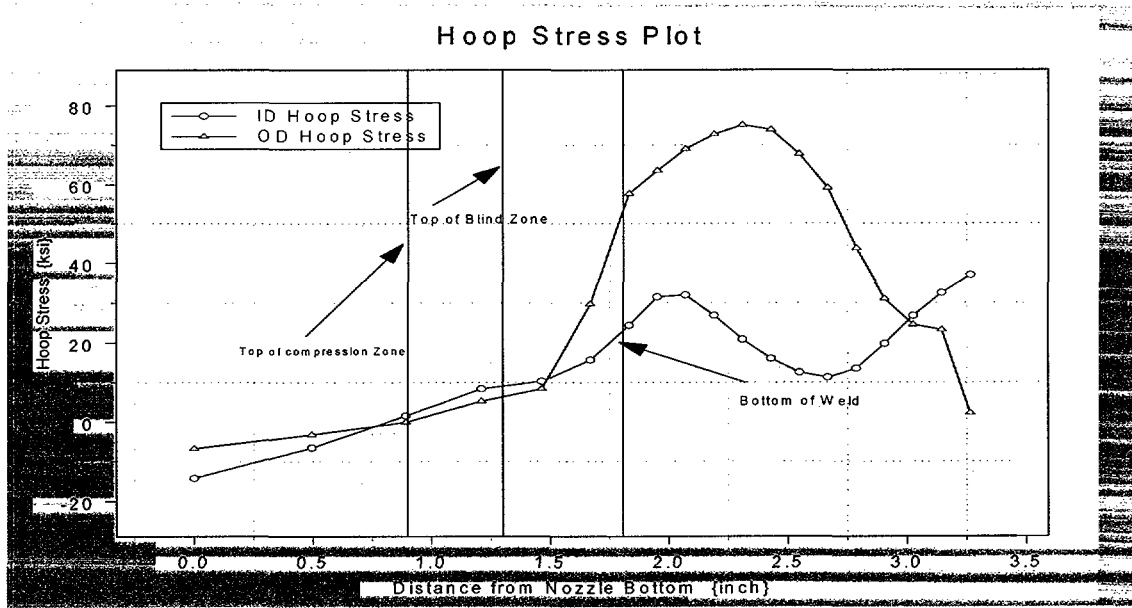


Figure 16: Plot showing hoop stress distribution along tube axis for the 28.8° nozzle at 22.5° rotated from the downhill location. The top of compressive zone, the top of blind zone, and the bottom of the weld are shown.

Row	Height	ID	25%	50%	75%	OD
40001	0.000	2.0791	-0.87476	-2.9601	-4.82	-6.7498
40101	0.811	0.091	-2.3704	-4.267	-6.0042	-7.5523
40201	1.460	5.2826	1.6859	-0.78573	-2.4896	-3.4686
40301	1.980	16.881	12.419	9.564	6.9075	4.3191
40401	2.397	24.144	20.894	18.115	16.59	14.513
40501	2.731	26.962	22.672	20.686	24.842	33.523
40601	2.999	23.279	20.902	21.706	37.111	47.395
40701	3.113	17.161	17.101	20.743	41.091	51.762
40801	3.228	11.722	14.424	21.34	43.543	53.688
40901	3.343	6.0041	11.108	20.912	43.833	54.154
41001	3.457	1.439	8.0852	20.38	43.021	57.025
41101	3.572	-2.1749	5.8905	19.929	42.405	56.415
41201	3.687	-4.7249	4.8584	19.994	40.425	58.85
41301	3.801	-4.9201	4.8793	20.34	38.451	57.617
41401	3.916	-2.8845	6.4727	20.545	37.523	49.152
41501	4.031	0.86049	8.0075	21.386	36.18	40.228
41601	4.145	5.584	11.001	22.915	36.59	35.152
41701	4.260	9.8086	14.62	25.477	36.977	32.699
41801	4.375	17.392	18.195	28.176	40.112	19.759

Table 10: Nodal stress for 28.8° nozzle at (Mid-Plane) 90° rotated from the downhill location. The weld location is shown by the shaded row.

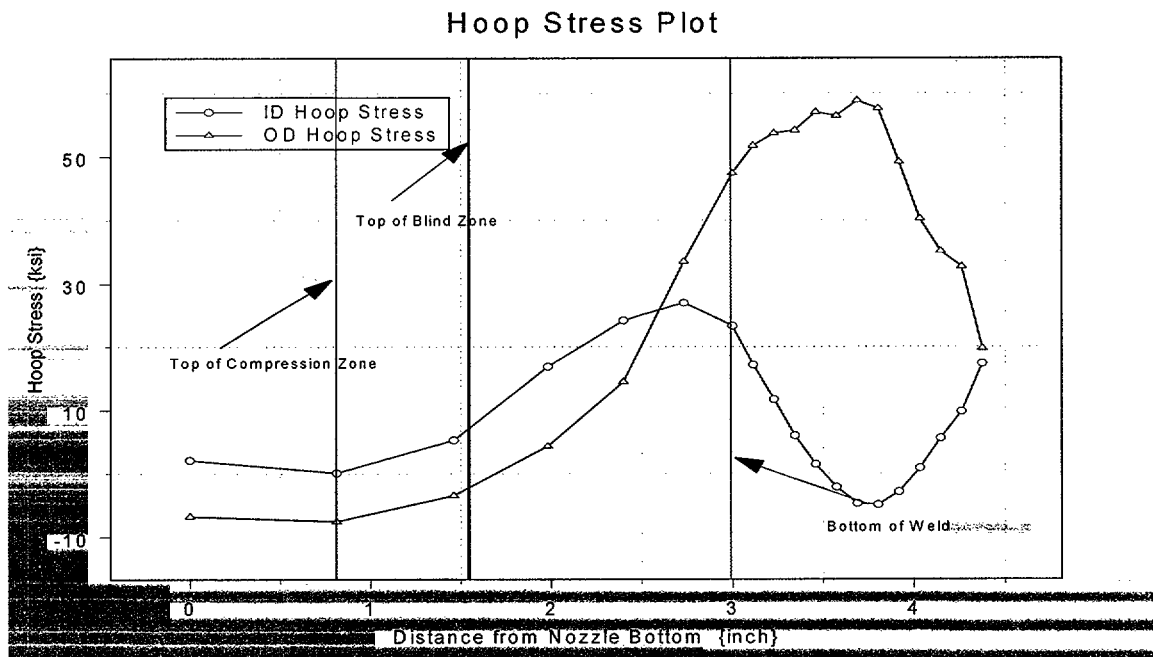


Figure 17: Plot showing hoop stress distribution along tube axis for the 28.8° nozzle at (Mid-Plane) 90° rotated from the downhill location. The top of compressive zone, the top of blind zone, and the bottom of the weld are shown.

Row	Height	ID	25%	50%	75%	OD
80001	0.000	-9.0335	-5.8552	-4.2456	-2.6894	-1.0312
80101	1.154	-6.761	-6.7389	-7.2366	-7.6623	-7.8035
80201	2.078	7.9654	1.7419	-6.2304	-11.848	-16.387
80301	2.819	23.851	21.763	8.5552	-6.3899	-17.647
80401	3.412	43.99	38.072	29.826	13.47	-1.6316
80501	3.888	47.954	41.753	35.453	33.324	35.846
80601	4.268	43.756	39.214	38.4	53.023	57.543
80701	4.377	40.773	36.237	41.27	61.453	62.189
80801	4.486	39.277	35.327	44.863	64.204	63.895
80901	4.595	36.022	35.389	46.842	64.323	62.934
81001	4.704	33.54	36.173	48.06	64.483	66.03
81101	4.813	32.631	36.616	47.779	67.612	70.356
81201	4.922	32.794	36.656	47.356	66.386	72.973
81301	5.031	33.889	36.612	47.548	65.375	77.806
81401	5.140	35.222	36.179	47.538	65.411	75.322
81501	5.249	36.353	35.865	47.964	64.448	70.447
81601	5.358	36.426	36.986	48.341	62.979	62.511
81701	5.467	37.233	38.52	49.064	63.153	61.112
81801	5.575	40.874	39.218	48.17	62.039	57.291

Table 11: Nodal stress for 28.8° nozzle at (Uphill) 180° rotated from the downhill location. The weld location is shown by the shaded row.

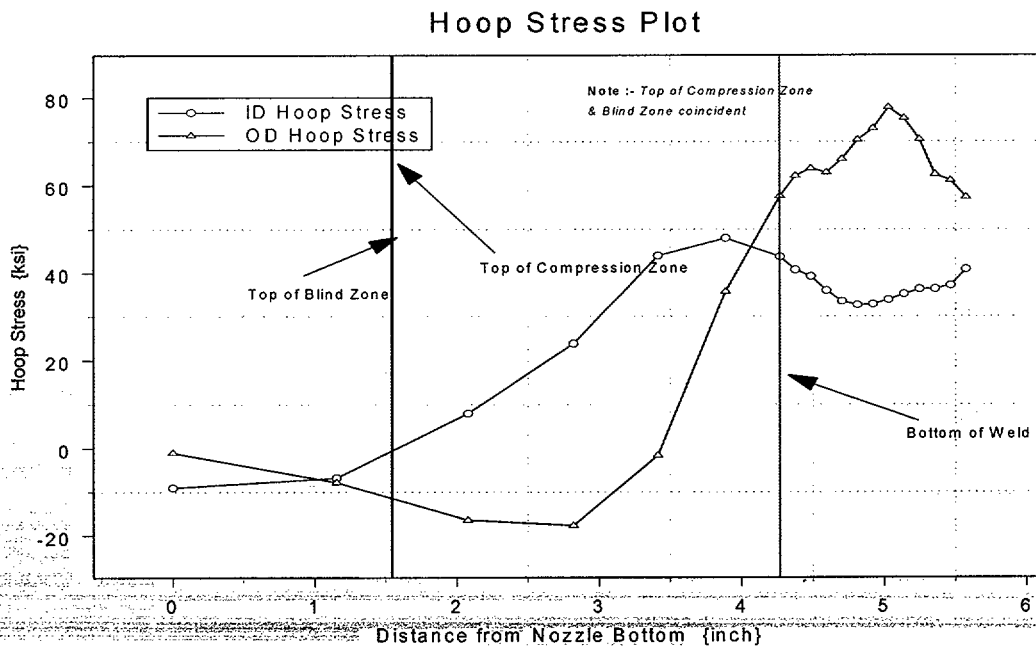


Figure 18: Plot showing hoop stress distribution along tube axis for the 28.8° nozzle at (Uphill) 180° rotated from the downhill location. The top of compressive zone, the top of blind zone, and the bottom of the weld are shown.

Row	Height	ID	25%	50%	75%	OD
1	0.000	-28.324	-18.299	-12.16	-6.2006	-0.02118
101	0.350	-18.794	-12.495	-6.6068	-1.3662	3.655
201	0.630	-17.838	-10.518	-4.4065	-0.47664	2.0799
301	0.854	-20.517	-12.968	-5.9018	-0.87378	-1.5355
401	1.034	-19.663	-11.831	-5.2884	0.22693	1.4602
501	1.178	-17.203	-10.587	-0.51546	16.326	21.019
601	1.293	-8.023	-2.2049	10.461	32.658	37.28
701	1.442	4.7776	9.5574	24.903	38.177	54.089
801	1.591	13.252	18.569	35.278	52.808	66.517
901	1.740	16.001	22.017	39.194	62.945	75.001
1001	1.889	15.857	23.14	40.235	64.335	74.874
1101	2.038	12.629	23.76	41.263	58.673	66.777
1201	2.187	10.061	25.095	39.628	49.272	55.012
1301	2.336	11.161	24.955	35.646	38.588	37.57
1401	2.485	17.623	24.541	31.309	28.654	24.693
1501	2.634	27.264	24.647	26.511	19.508	17.468
1601	2.783	35.465	28.75	27.109	14.597	16.305
1701	2.933	39.949	34.666	31.396	15.64	12.404
1801	3.082	39.547	36.368	37.156	24.257	1.4483

Table 12: Nodal stress for 49.6° nozzle at the downhill location. The weld location is shown by the shaded row.

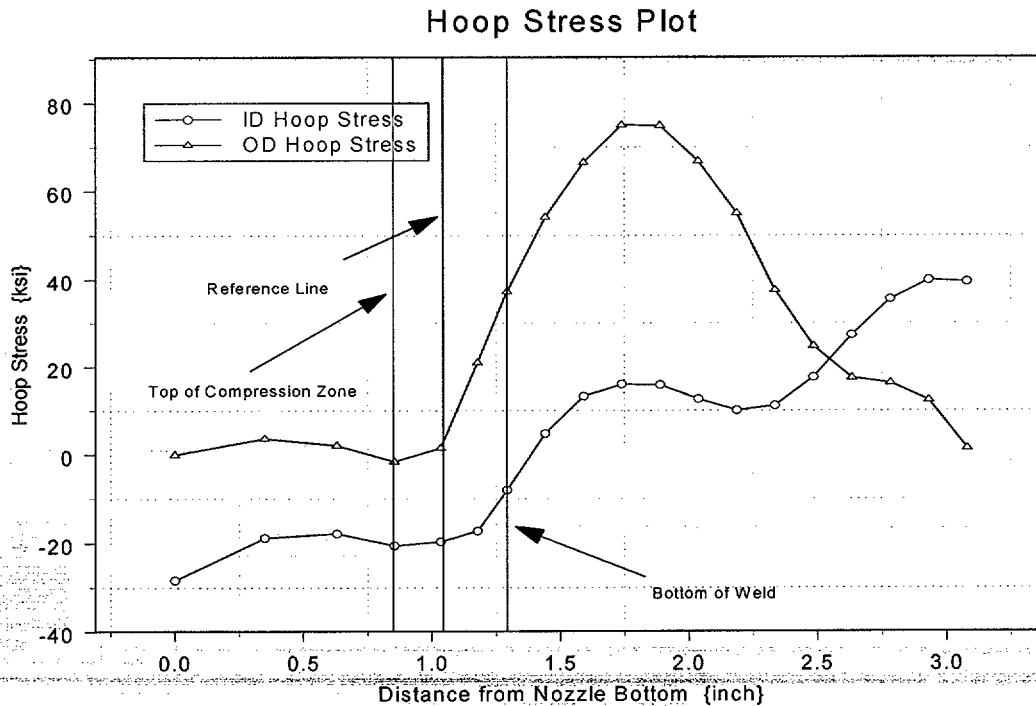


Figure 19: Plot showing hoop stress distribution along tube axis for the 49.6° nozzle at the downhill location. The top of compressive zone, the reference line, and the bottom of the weld are shown.

Row	Height	ID	25%	50%	75%	OD
10001	0	-19.301	-12.523	-8.3043	-4.3142	-0.28909
10101	0.41913	-13.153	-8.5716	-4.6802	-1.2548	1.8343
10201	0.75491	-11.834	-6.958	-2.6848	0.027936	1.4633
10301	1.0239	-14.146	-8.3146	-3.1681	1.1025	1.2206
10401	1.2394	-12.132	-6.552	0.003002	5.7801	7.8584
10501	1.4121	-5.3804	-2.4127	7.4976	23.29	28.718
10601	1.5504	4.3312	6.4775	17.842	35.67	42.74
10701	1.6988	13.644	15.667	27.164	40.65	53.563
10801	1.8473	18.304	21.201	32.424	50.345	61.379
10901	1.9957	18.316	22.292	34.208	53.258	63.464
11001	2.1442	14.517	21.816	35.085	51.479	61.5
11101	2.2926	9.6239	20.816	34.508	47.885	53.875
11201	2.441	6.1777	19.919	32.257	40.249	44.059
11301	2.5895	7.4871	19.244	30.005	33.466	33.498
11401	2.7379	12.725	18.544	26.491	26.271	20.889
11501	2.8864	21.018	19.128	23.312	19.922	13.905
11601	3.0348	27.04	22.243	23.901	17.166	13.045
11701	3.1833	30.565	26.038	26.927	19.252	11.52
11801	3.3317	31.022	26.941	29.307	23.991	3.6688

Table 13: Nodal stress for 49.6° nozzle at the 22.5° rotated from the downhill location. The weld location is shown by the shaded row.

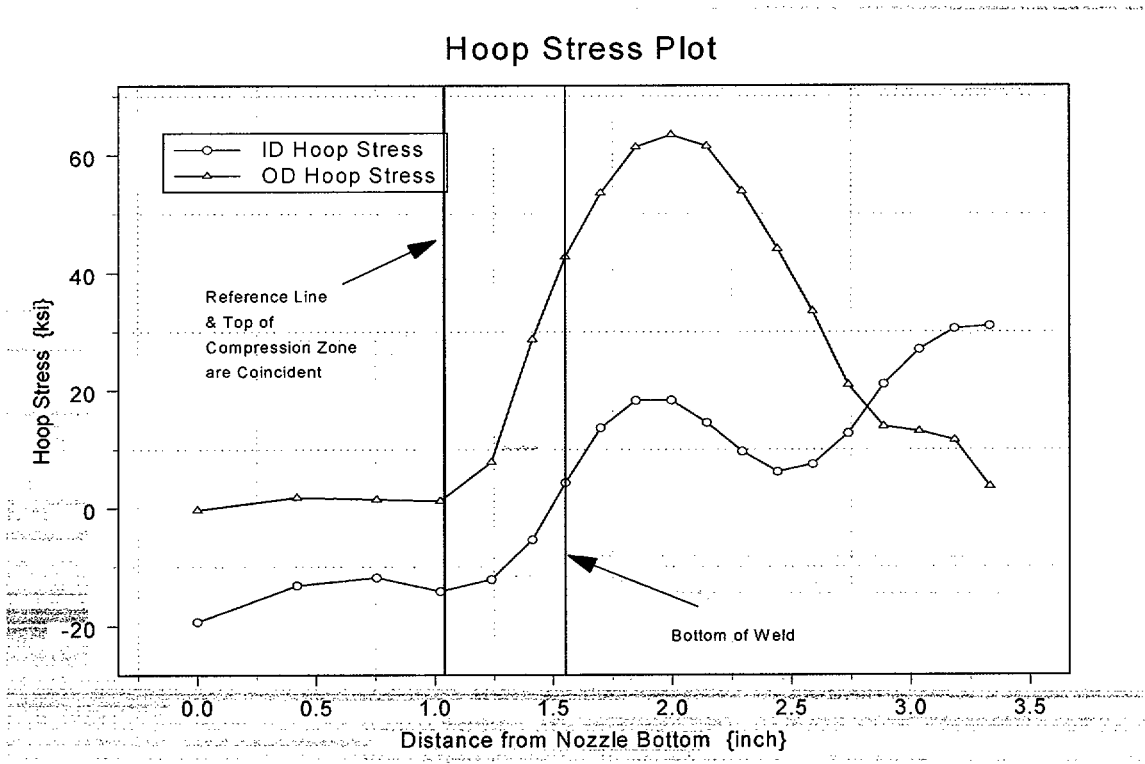


Figure 20: Plot showing hoop stress distribution along tube axis for the 49.6° nozzle at 22.5° rotated from the downhill location. The top of compressive zone, the reference line, and the bottom of the weld are shown.

Row	Height	ID	25%	50%	75%	OD
20001	0	-0.41426	-1.3595	-1.8423	-2.3694	-3.1566
20101	0.58479	-1.2562	-1.4879	-1.714	-1.9503	-2.0734
20201	1.0533	-1.0226	0.22345	0.34713	0.51562	-0.49543
20301	1.4286	-1.5585	0.62217	2.583	4.8953	4.258
20401	1.7293	4.1652	4.3149	8.8598	13.38	15.252
20501	1.9702	16.258	12.541	16.926	28.26	32.667
20601	2.1632	21.131	17.131	20.087	34.279	36.98
20701	2.3099	21.593	19.093	21.933	34.049	41.718
20801	2.4567	17.702	17.82	22.18	34.468	41.213
20901	2.6034	10.688	14.251	21.112	33.319	39.555
21001	2.7502	3.5924	10.953	19.959	31.013	38.939
21101	2.8969	-0.98491	8.7362	18.339	28.346	33.446
21201	3.0437	-2.9447	7.0211	18.062	25.996	29.853
21301	3.1905	-2.6882	5.4512	16.967	23.256	22.48
21401	3.3372	-0.60958	5.0995	15.966	21.557	15.04
21501	3.484	3.0879	4.9369	15.116	19.082	11.629
21601	3.6307	7.3077	6.878	15.74	18.42	10.876
21701	3.7775	10.628	9.0825	17.263	20.586	10.946
21801	3.9242	13.502	11.129	17.922	23.742	3.2671

Table 14: Nodal stress for 49.6° nozzle at the 45° rotated from the downhill location. The weld location is shown by the shaded row.

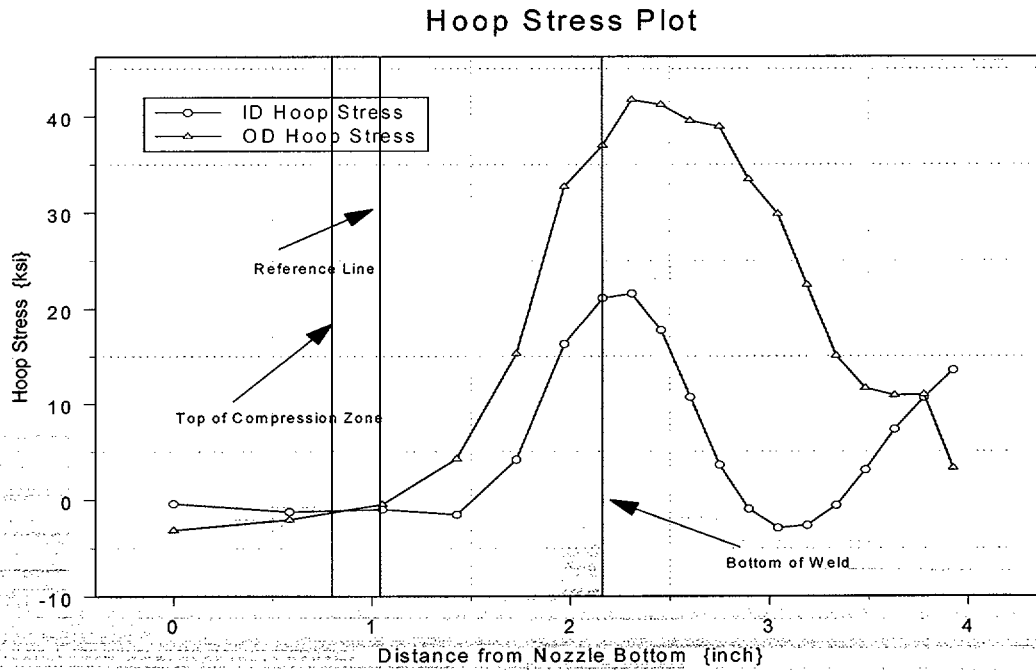


Figure 21: Plot showing hoop stress distribution along tube axis for the 49.6° nozzle at 45° rotated from the downhill location. The top of compressive zone, the reference line, and the bottom of the weld are shown.

Row	Height	ID	25%	50%	75%	OD
40001	0.000	17.354	8.1856	2.2843	-3.0637	-8.6374
40101	1.091	6.8916	1.4705	-2.2239	-5.4445	-7.1995
40201	1.964	5.7811	2.359	0.75379	-0.955	-3.2318
40301	2.664	10.289	7.1481	5.3241	3.4277	0.49388
40401	3.225	12.243	7.028	6.8287	7.2436	5.9517
40501	3.674	6.5788	4.6585	5.8654	12.453	16.377
40601	4.034	-5.6212	-1.2955	4.1843	17.859	24.27
40701	4.176	-12.251	-6.006	2.7409	20.517	31.88
40801	4.318	-15.641	-9.1309	2.2005	21.496	30.446
40901	4.459	-18.614	-11.785	1.3186	20.216	30.786
41001	4.601	-21.257	-13.548	0.57363	19.393	32.088
41101	4.743	-24.142	-14.864	0.3385	19.564	27.322
41201	4.884	-26.133	-15.268	-0.15264	17.776	31.244
41301	5.026	-25.615	-14.158	0.78773	15.555	27.871
41401	5.167	-23.831	-12.25	1.7886	16.579	22.427
41501	5.309	-20.331	-10.681	3.0892	16.489	17.553
41601	5.451	-16.345	-8.6522	4.4543	17.912	15.75
41701	5.592	-12.679	-6.5122	5.5067	16.075	15.827
41801	5.734	-7.2577	-2.477	7.8649	19.847	6.0174

Table 15: Nodal stress for 49.6° nozzle at the (Mid-Plane) 90° rotated from the downhill location. The weld location is shown by the shaded row.

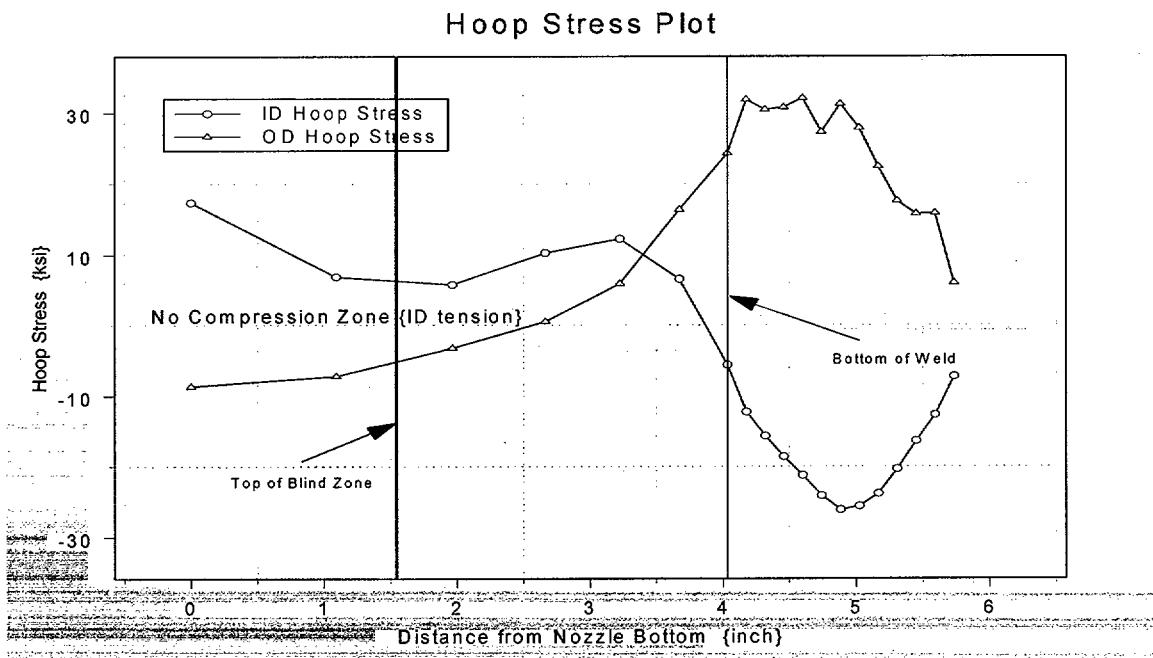


Figure 22: Plot showing hoop stress distribution along tube axis for the 49.6° nozzle at (Mid-Plane) 90° rotated from the downhill location. The top of blind zone, and the bottom of the weld are shown. There is no compression zone since the ID is in tension.

Row	Height	ID	25%	50%	75%	OD
80001	0.000	-20.175	-11.45	-5.9403	-1.1628	3.7037
80101	1.792	-3.0237	-4.3776	-5.4433	-5.5114	-5.3415
80201	3.228	9.3983	12.134	-0.25796	-12.622	-20.232
80301	4.378	25.65	24.71	14.577	-15.299	-25.689
80401	5.299	36.179	33.787	26.287	-5.9249	-24.306
80501	6.037	38.106	35.028	31.43	21.215	8.834
80601	6.628	42.186	38.102	36.248	40.684	36.405
80701	6.764	45.067	42.217	42.736	47.553	44.235
80801	6.899	44.968	43.606	46.007	49.995	48.803
80901	7.035	44.695	44.12	47.021	51.043	54.113
81001	7.170	43.723	43.973	47.639	50.172	54.17
81101	7.305	42.926	43.816	47.515	52.325	56.546
81201	7.441	42.312	43.142	47.497	51.329	55.754
81301	7.576	41.252	42.489	47.751	53.141	58.971
81401	7.712	40.403	41.864	46.936	54.111	57.676
81501	7.847	40.359	40.735	47.685	56.669	64.401
81601	7.982	39.39	39.72	46.452	53.712	57.649
81701	8.118	38.459	37.5	43.25	47.79	52.344
81801	8.253	35.922	35.062	36.626	38.139	49.538

Table 16: Nodal stress for 49.6° nozzle at the (Uphill) 180° rotated from the downhill location. The weld location is shown by the shaded row.

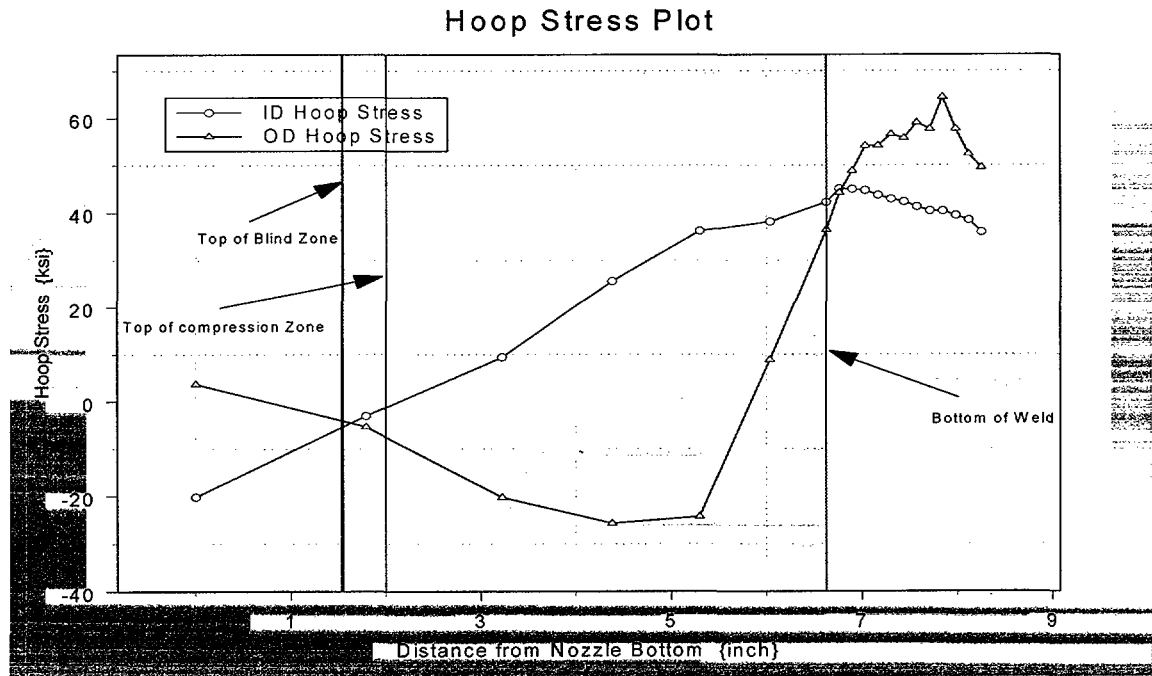


Figure 23: Plot showing hoop stress distribution along tube axis for the 49.6° nozzle at (Uphill) 180° rotated from the downhill location. The top of the compression zone, the top of blind zone, and the bottom of the weld are shown.

The nodal stress data presented in the previous pages are the data imported into the respective Mathcad worksheet (discussed later) for further processing to obtain the pertinent stress distributions required for the fracture mechanics analysis. The processing of the nodal stress data is described in Section 4.

3.0 Analytical Basis for Fracture Mechanics and Crack Growth Models

Fracture Mechanics Models

Surface Crack

The mean radius-to-thickness ratio (R_m/t) for the CEDM nozzle was about 1.7. The fracture mechanics equation used in the proposed revision to the ASME Code Section XI is based on the solution from Reference 6. This solution is valid for an outside radius-to-thickness (" R_o/t ") ratio from 4.0 to 10.0. The CEDM nozzle " R_o/t " ratio is lower (3.06), indicating that the CEDM nozzle is a thicker wall cylinder than those considered in Reference 6. Therefore, the fracture mechanics formulations presented in Reference 7 were chosen (the applicable " R_m/t " ratio is from 1.0 to 300.0).

The stress intensity factor (SIF) for the postulated crack under an arbitrary stress distribution was obtained from Reference 7. The model was for both an internal and external part through-wall surface crack subjected to an arbitrary stress distribution. This model is valid for a ratio of mean radius (R_{mean})-to-thickness (t) between 1.0 and 300.0. Since the ratio for the CEDM nozzle is about 1.7, this model is considered applicable.

The equation for the SIF for the deepest point of the crack is given as [7]:

$$K_I = \left(\frac{\pi}{Q} a\right)^{0.5} * \left[\sum_{i=0}^3 \sigma_i G_i\right]$$

Where:

$$K_I = SIF \text{ \{ksi}\sqrt{\text{in.}}\}$$

Q = Crack shape factor; defined as

$$Q = 1 + 1.464 * \left(\frac{a}{c}\right)^{1.65} \text{ when } a/c \leq 1.0 \text{ and,}$$

$$Q = 1 + 1.464 * \left(\frac{c}{a}\right)^{1.65} \text{ when } a/c > 1.0$$

a = Crack depth \{inch\}

σ_i = Coefficients of the stress polynomial describing the hoop stress variation through the crack depth. Describes the power loading on the crack face.

G_i = Stress Intensity Correction Factors (SICF), which are provided in tables in Reference 7.

In Reference 7 SICF is presented for both the depth point of the crack (“a-tip”) and for the surface point of the crack (“c-tip”). Separate tables are provided for the internal (ID) and external (OD) surface cracks. In addition the values are provided in association with the R_m/t ratio, a/c ratio (crack aspect ratio), and a/t ratio (normalized crack depth). The SICF tables are large and a suitable interpolation scheme is necessary to obtain proper coefficients dependent on crack size and shape for a given cylindrical geometry. Selected SICF from the tables for internal cracks for two different R_m/t ratios and a/c ratios are presented in Figure 24 below.

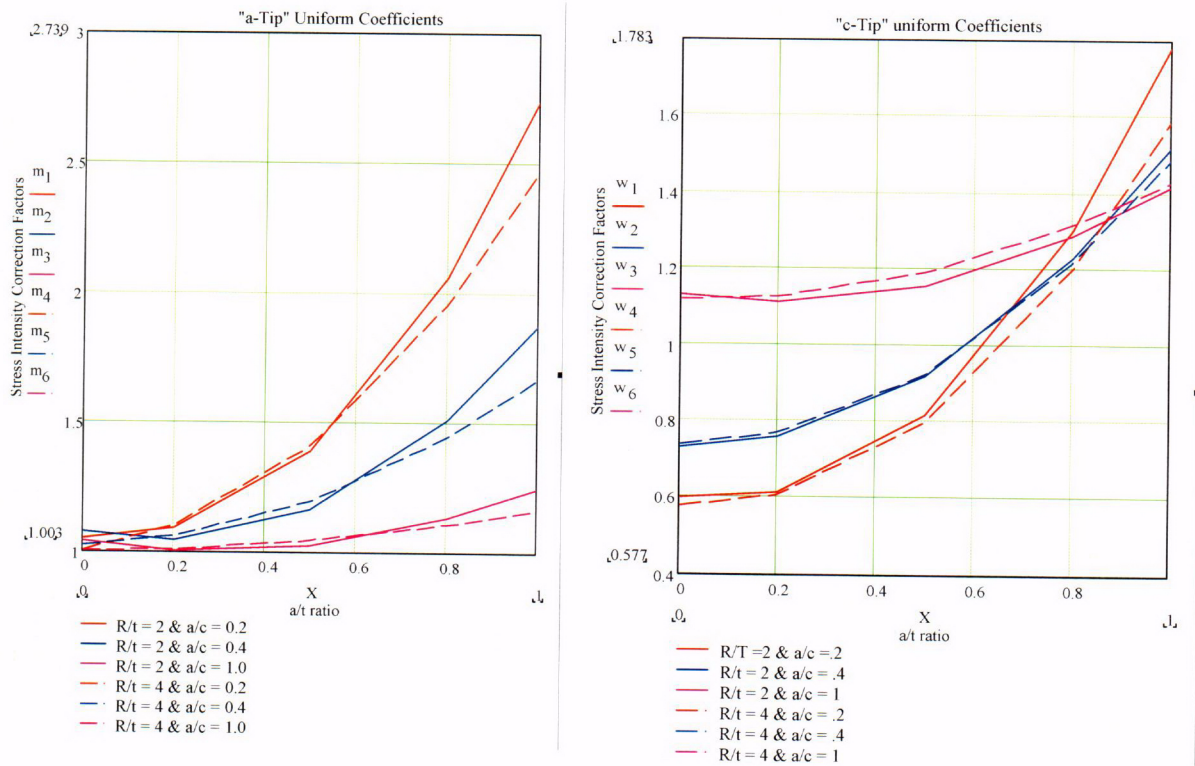


Figure 24: SICF shown as a function of normalized crack depth for the “a-tip” (left figure) and the “c-tip” right figure. These figures show that simple linear interpolation would not provide accurate coefficients. These figures also show that a proper R_m/t is essential to provide a reasonably accurate estimate of the SIF.

The figure above shows two features that are significant;

- 1) The interpolation used to obtain the SICF must be carefully performed such that the value accurately represents the crack geometry. This is accommodated by selecting a suitable order for the polynomial prior to performing an interpolation to obtain the specific value. This aspect is discussed in further detail in the section describing the analysis method.
- 2) The correct R_m/t ratio is essential for obtaining a reasonably accurate estimate of the SIF. Using a higher ratio will tend to underestimate the SIF and hence under predict the crack growth.

Both these features have been considered in the development of the analysis model such that a reasonable, yet conservative, estimate of the SIF is obtained.

Through-Wall Axial Crack

The analysis for a through-wall axial crack was evaluated using the formulation of Reference 8. This formulation was chosen since the underlying analysis was performed considering thick-wall cylinders that had " R_o/t " ratio in the range of the application herein. The analysis used the outside surface (OD) as the reference surface and, hence, the same notation is used here.

It was noted in Reference 8 that the formulations based on thin shell theory do not consider the complete three-dimensional nature of the highly localized stress distribution. This would be the case for the residual stress distribution from welding. The nonlinear three-dimensional stress distribution coupled with shell curvature must be properly addressed to account for the material behavior at the crack tip, which controls the SIF, such that the SIF is not underestimated. The information presented in Reference 8 compared the results from formulations derived using thin shell theory and those derived using thick shell formulation, these results highlighted the need to use thick shell based formulation for situations such as the current application to CEDM nozzle through-wall axial cracks.

The formulation provides the correction factors, which account for the " R_o/t " ratio and crack geometry (λ), that are used to correct the SIF for a flat plate solution subjected to similar loadings. The correction factors were given for both "extension" and "bending" components. The flat plate solutions for both membrane and bending loads were to be used to obtain the applied SIF. The formulations for SIF were given as [8]:

$$K_{outer} = \{ A_e + A_b \} * K_p \quad \text{for the OD surface;}$$

and,

$$K_{Inner} = \{A_e - A_b\} * K_p \text{ for the ID surface;}$$

where:

A_e and A_b are the "extension" and "bending" components; and,
 K_p is the SIF for a cracked Flat Plate subject to the same boundary condition and loading as the cracked cylinder.

The flat plate SIF solutions are written as:

$$K_{p-Membrane} = \sigma_h * \sqrt{\pi * l} \text{ for membrane loading, and}$$

$$K_{p-Bending} = \sigma_b * \sqrt{\pi * l} \text{ for bending loading.}$$

Where:

σ_h and σ_b are the membrane and bending stresses and " l " is one-half the crack length.

The reference surface used in the evaluation was the OD surface. The stresses at the ID and OD at the axial elevation of interest were decomposed into membrane and bending components as follows:

$$\sigma_h = \frac{\sigma_{res-OD} + \sigma_{res-ID}}{2} \text{ for membrane loading; and}$$

$$\sigma_b = \frac{\sigma_{res-OD} - \sigma_{res-ID}}{2} \text{ for bending loading.}$$

where:

σ_{res-OD} is the stress (residual+operating) on the OD surface; and,

σ_{res-ID} is the stress (residual+operating) on the ID surface.

The data presented in the tables in Reference 8 for determining the A_e and A_b components were curve fit using a fifth order polynomial such that they could be calculated knowing the parameter λ , which is defined as [8]:

$$\lambda = \{[12 * (1 - \nu^2)]^{0.25} * \frac{l}{(R * t)^{0.5}}\}$$

where ν is Poisson's ratio and R is the mean radius.

The data obtained from the tables in Reference 8 were curve fit using a fifth order polynomial. The curve fitting was accomplished using Axum 7 [9]. The curve fit results for the components are presented in Figure 25 below.

Extension and Bending Constants for Throughwall Axial Flaws R/t = 3.0
(ASME PVP 350, 1997; pp 143)

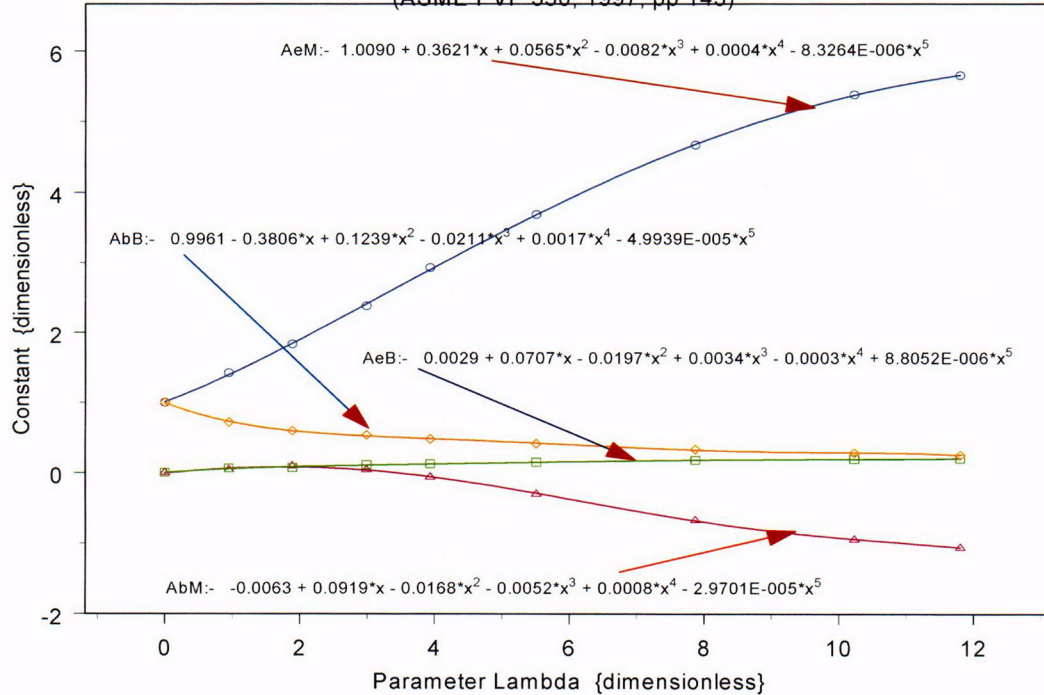


Figure 25: Curve fit equations for the “extension and “bending” components in Reference 8. Tables 1c and 1d for membrane loading and Tables 1g and 1h for bending loading of Reference 8 were used.

Crack Growth Model

To evaluate the potential for crack growth due to PWSCC, the crack growth rate equation from EPRI-MRP 55 [10] was used. The crack growth rate as a function of the SIF with a correction for temperature effects is given as [10]:

$$\frac{da}{dt} = \exp\left[-\frac{Q_g}{R} \left(\frac{1}{T} - \frac{1}{T_{ref}}\right)\right] \alpha (K - K_{th})^\beta$$

Where:

da/dt = crack growth rate at temperature T {m/s}

Q_g = thermal activation energy for crack growth {31.0 kcal/mole}
 R = universal gas constant $\{1.103 \times 10^{-3} \text{ kcal/mole-}^\circ\text{R}\}$
 T = absolute operating temperature at crack tip $\{^\circ\text{R}\}$
 T_0 = absolute reference temperature for data normalization $\{1076.67 \text{ }^\circ\text{R}\}$
 a = crack growth amplitude $\{2.67 \times 10^{-12}\}$
 K = crack tip SIF $\{\text{Mpa}\sqrt{\text{m}}\}$
 K_{th} = threshold SIF for crack growth $\{\text{MPa}\sqrt{\text{m}}\}$
 β = exponent $\{1.16\}$

The above equation represents the seventy-fifth percentile curve. Since the PWSCC crack growth of interest is in the primary water, this model would provide a reasonably conservative crack growth.

4.0 Method of Analysis

Mathcad Worksheet Format

The analytical scheme was developed using Mathcad [11] which facilitates calculations (including recursive) in a logical manner. Appendix B provides annotated versions of the three sets of worksheets used in the current analysis. The three sets are for the ID surface crack, the OD surface crack and for the through-wall crack. In the paragraphs below the general approach used to develop the worksheet is presented.

The first part of the worksheet is common to all three sets and requires the proper identification for the analysis being performed. In this region the component and the reference location in that component are identified. Immediately below the identification entry are the geometric landmark entries. For the surface cracks three entries are required and these are:

- 1) The location of a reference line (e.g. blind zone location) referenced to the nozzle bottom $\{\text{Ref}_{\text{Point}}\}$.
- 2) The location of the crack with respect to the reference line (Upper crack tip at the reference line, center of crack at the reference line or lower crack tip at the reference line) $\{\text{Val}\}$;
- 3) The location of the bottom of the weld measured upwards from the nozzle bottom $\{\text{UL}_{\text{Strs.Dist}}\}$.

For the through-wall crack the location of the crack upper tip is always at the reference line, while the two other landmark entries are similar to that for the surface crack. This completes the entries on the first page of the worksheet.

The second page of each Mathcad worksheet contains the inputs for crack dimensions, tube geometry, internal pressure, years of operation, iteration limit, operating temperature, and the constants for the PWSCC crack growth parameters. It should be noted that the crack growth is performed using metric units; hence, those constants are required to be in metric units. The remainder of this sheet does not require user input. The calculation shown is simple arithmetic to determine the values necessary for the analysis.

The third page of each worksheet is designed to import the entire nodal stress data from the Excel spreadsheet provided by Dominion Engineering (described earlier). After the required data has been imported, the graph below the data table depicts the ID and OD stress distributions along the axial length of the nozzle. This graph is needed to aid in the selection of the nodal stress data to be used in the subsequent analysis. Once the data needed for the evaluation has been selected, it is pasted onto the third sheet at a variable defined as "Data". No further user input is required. The worksheets presented in Appendix C reflect this design.

Determination of Stress Field (Distributions)

The first step in the analysis is to develop the appropriate stress distribution to be used in the determination of the SIF. This is needed because the SIF formulation is based on use of a uniform stress distribution along the length of the tube. However, the stress field at the bottom portion of the nozzle, starting from the nozzle bottom, increases in magnitude as the bottom of the weld is approached. Consequently, if an assumed crack located in the vicinity of the reference line were to grow by PWSCC, it would be subjected to an increasing stress field. Thus, to use the stress distribution at the initial crack location would lead to an underestimate of the SIF since the SIF is directly proportional to the applied stress. In order to obtain a reasonably representative SIF under the prevailing stress field variation, a moving average scheme was developed. This scheme is as follows:

- 1) For the initial crack location the stress distribution at the two crack tips (lower and upper) and the crack center are averaged to produce an average stress field that is applied to the crack. It is this stress distribution that is used to ascertain whether there exists a potential for PWSCC crack growth. This method is considered reasonable since it is similar to the superposition principle used in finite element based SICF determination.
- 2) The remaining portion of the nozzle extending from the upper crack tip to the bottom of the weld is divided into twenty (20) equal segments.
- 3) The stress distribution in the first segment, above the upper crack tip, is an arithmetic average of the first three initial crack region distribution (Lower tip, center of crack and the upper tip) plus the distribution in the first segment. Thus, when the crack enters the first segment the magnitude of the stress distribution is appropriately increased to account for the increased applied stress. Similarly, as the crack progresses upward to the weld bottom through the various segments, the applied stress distribution is adjusted accordingly. The small extent of the length between the reference

line and the bottom of the weld can be sufficiently accommodated by the twenty-segment characterization.

To accomplish this averaging scheme, the nodal stresses at the five (5) nodal locations through the tube thickness and its variation along the length of the nozzle are individually regressed with a third order polynomial. Hence, it is important to ensure that the axial distribution can be described by a third-order polynomial. The regression is performed along the nozzle axis at each of the five (5) locations individually. The result of the regression provides the spatial coefficients required to describe the stress distribution. The nodal stress data representing the region of interest, from the nozzle bottom to an elevation just above the bottom of the weld, is selected. In this manner, it is expected that proper representation of the stress distribution, pertinent to crack initiation and growth, can be accurately described.

An example of this approach is presented in Figure 26 below. In this example, the stress at the ID and the OD locations were selected from a typical set of nodal stress data. The graphs immediately below show the individual stress distribution and the result from the third-order polynomial fit. In the first set, the entire data set from the bottom of the nozzle to the top of the J-weld was used. The regression curve shows that the general trend is captured; however, the fit in localized regions are not accurate representation of the original data. Significant variation that might cause errors in the determination of the SIF could occur, which in turn could lead to an inaccurate estimate in crack growth.

The two lower plots follow the scheme utilized in the current analysis. In this process the nodal stress data from the bottom of the nozzle to an elevation just above the bottom of the J-weld is selected. In this manner the stress distribution in the region of interest is chosen for the regressed curve fitting. This is necessary since the stresses in the weld region show significant variation (top plot) and cannot be adequately represented by a third-order polynomial. Limiting the stress distribution data to the region of interest would limit the variation and results in a more accurate fit. The plots in the lowest row, in Figure 26, show the improvement in the accuracy of fitting. The regression fit does provide an accurate representation of the stress distribution of the region. Therefore, the stress distribution used in the fracture mechanics analysis would be a reasonably accurate representation of the actual stress distribution in the region where the initial crack and subsequent crack growth are of interest.

This example and the associated plots in Figure 26 show that the regression method, as developed for the current analyses, provides an adequate representation of the stress distribution.

The analysis worksheets (Appendix C) contain a cautionary statement such that inaccurate regression is avoided. The Mathcad worksheet used to develop this example is presented in Appendix D, Attachment 1. However, it should be

noted that this attachment is not annotated but does follow the method used in the analysis worksheets.

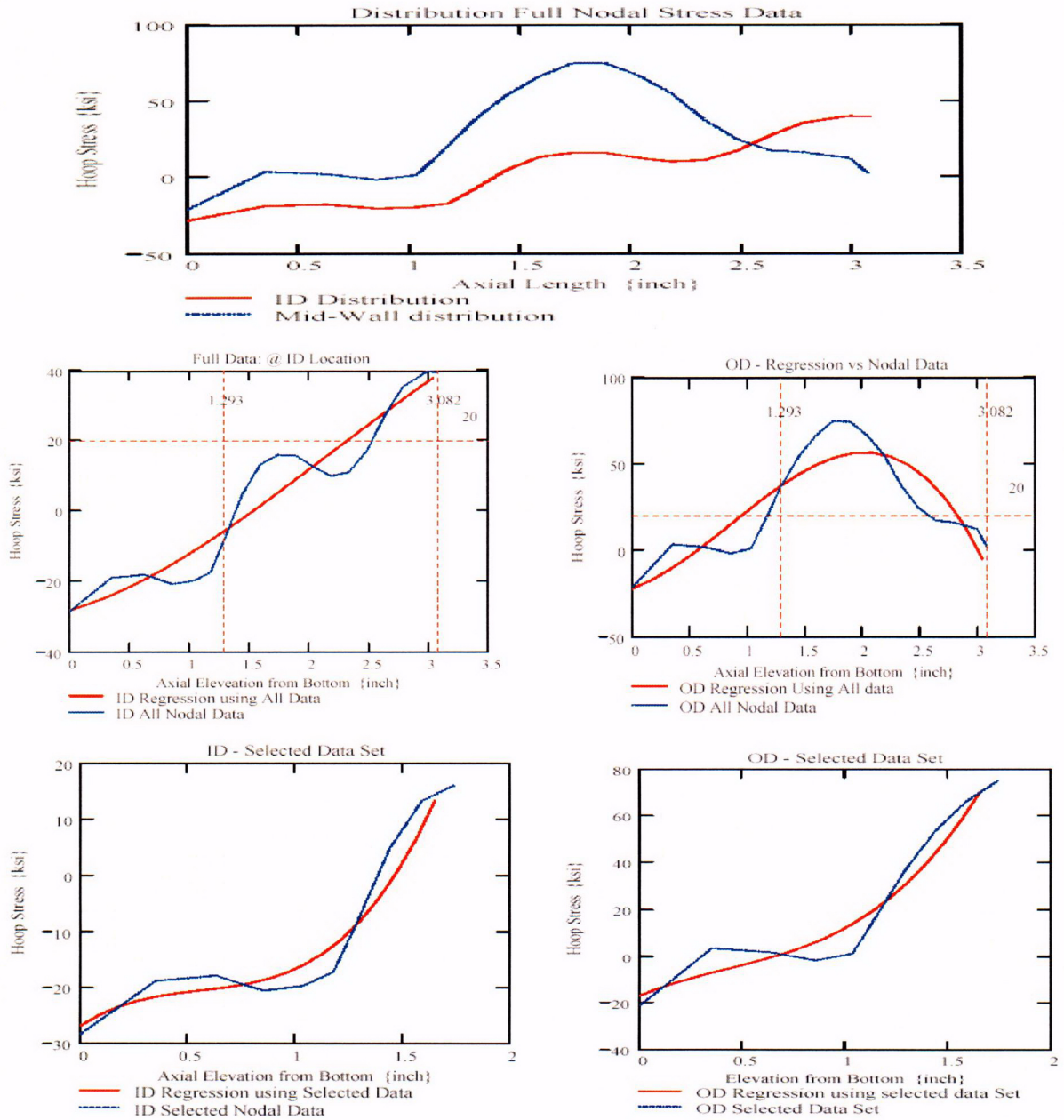


Figure 26: Plots showing effect of nodal data selection on the accuracy of polynomial regression fit. The first plot represents all nodal stress data from the nozzle bottom to the top of the J-weld.

The two plots, in the middle row, are the comparison of regression fit with nodal stress data; the full data set of nodal data for the ID and OD distribution was used.

The two plots, in the lower row, use a limited data set comprising the axial length to the bottom of the weld. The regression curve shows a significantly improved fit to the data.

Once the five polynomial equations for the axial distribution are established, the through-wall stress distribution for the three locations defined by the crack and the twenty segments are established. The distributions at the twenty-three locations are subjected to a third order polynomial regression to obtain the coefficients describing the through-wall distributions. These coefficients are used within the recursive loop to assign the coefficients based on the current crack location. The five axial distributions are used for the surface cracks (ID and OD) whereas only two are required for the through-wall crack (ID and OD distributions).

Iterative Analysis to Determine SICF

For the surface cracks (ID and OD) the SICF coefficients were incorporated in two data tables. The first table contains the geometry data (R_m/t , a/c and a/t) and the second table consists of the SICF data for the appropriate cylinder and crack geometry. The values for the data were obtained from Reference 7. The data contained in the two tables were regressed into function statements with an appropriate polynomial order. The data for cylinder geometries from R_m/t ranging from one (1) to four (4) were regressed with a third-order polynomial, and for those above four, a second-order polynomial was used. The selection of the polynomial order was based on matching the value in the table given, for a selected set of independent variables, with that obtained from the interpolation performed using the regressed coefficients. In this manner the accuracy of the regression-interpolation method was established. The interpolation equation was defined outside the recursive loop and function call was made inside the loop using the pertinent variables at the time of the call.

The through-wall crack SICF was obtained using the fifth-order polynomial equation presented earlier. These equations were provided inside of the recursive loop.

The recursive loop starts the calculation scheme to determine the crack growth for a specified time period under the prevailing conditions of applied stress. The first few statements are the initialization parameters. The calculation algorithm begins with the assignment of the through-wall stress coefficients based on the current crack location. Once the four coefficients (uniform, linear, quadratic and cubic) are assigned, the through-wall stress distribution is used as the basis to establish the stress distribution along the crack face in the crack depth direction. That is, the stresses through the thickness are used to determine the stress along the crack face for application in the determination of the SIF in accordance with Reference 7. Once again, five locations along the crack depth were used to define the crack face distribution. The stresses representing the crack face values were regressed with a third-order polynomial to obtain the stress coefficients that would be used in the determination. At this point, the internal pressure is added to the stress coefficient (SCIF) for the uniform term. Therefore, the crack face is subjected to an additional stress representing the internal pressure.

Following the determination of the stress coefficients, the function call to obtain the four SICF coefficients is made. In this case the two function calls were necessary to account for the "a-tip" and the "c-tip". The crack shape factor ("Q") was then computed using the appropriate crack dimensions. The SIF is calculated separately for the "a-tip" and the "c-tip" using the stress coefficients, appropriate SICFs and crack dimensions.

In the through-wall crack solution; the fifth-order polynomial equations were solved using the current crack dimensions. The SIFs were computed for both the ID and OD locations and were then averaged. This averaged SIF was used for crack growth calculation. The crack growth calculation and the remainder of the program for both the surface cracks (ID and OD) and through-wall crack are identical.

The calculated SIFs were converted to metric unit for the computation of crack growth. The crack growth rate, based on the prevailing SIF was computed in metric units. Once this was done, a conditional branch statement was used to calculate the crack growth within the prescribed time increment. The crack growth was computed in English units by converting the calculated crack growth rate in meters-per-second to inches-per-hour. Thus, the crack growth extent was obtained in inches for the specified time period. Since the operating time was selected to be four years and the number of iterations chosen at one thousand five hundred (1500), the time increment for each crack growth block was about twenty-four (24) hours. After the calculations were performed, all necessary information (crack growth, SIFs etc.) was assigned to an output variable such that it is stored in an array. The last step of the recursive loop consisted of updating the essential parameters (namely, the index, crack length, time increment etc.).

Graphical displays of the results using both Mathcad and Axum plots complete the work sheet. The Mathcad plots are used to determine whether or not the crack reached the bottom of the weld in one operating fuel cycle and the Axum plots were generated for incorporation into this report.

The three attachments in Appendix B are sufficiently annotated to provide summary details for each major step in the program.

5.0 Discussion and Results

Discussion

The goal of the inspection program designed for the reactor vessel head penetrations is to ensure that the postulated crack in the vicinity of the blind zone does not reach the weld during the upcoming operating cycle following the refueling outage when the inspections are performed. Safety analyses performed by the MRP have demonstrated that axial cracks in the nozzle tube material do not pose a challenge to the structural integrity of the nozzle. Axial cracks, if allowed to exist undetected for sufficient periods of time can produce a primary boundary leak that can cause damage to the reactor vessel head (carbon steel) and create a conducive environment for initiating and propagating OD circumferential cracks. These conditions challenge

the pressure boundary; hence, critical importance is paid to proper periodic inspection and to the disposition of cracks that may be discovered. Therefore, proper analyses are essential to ascertain the nature of axial crack growth such that appropriate determination can be accomplished.

The analyses performed in this report were designed to capture the behavior of postulated cracks that might exist in the blind zone for the CEDM nozzle. The growth region for the postulated cracks was to the bottom of the weld along the tube OD.

The design review of the reactor vessel head construction, the detailed residual stress analyses, the selection of representative nozzle locations, selection of representative fracture mechanics models, and the application of a suitable crack growth law has provided the bases for arriving at a comprehensive and prudent decision.

The axial crack geometry is selected for evaluation because this crack has the potential for propagation into the pressure boundary weld (the J-groove weld); and since the circumferentially oriented cracks will not propagate towards the pressure boundary weld, this crack type is not evaluated. The hoop stress distribution at the downhill location (0°), at the Mid-Plane location (90° rotated from the downhill), and at the uphill (180°) location were chosen for evaluation. The axial distribution of the hoop stress magnitude for both the ID and OD surfaces shows that at axial location below the evaluated elevation, the stresses drop off significantly and become compressive except for the mid-plane location on the 49.6° nozzle group where the ID stays in tension; hence, the potential for PWSCC crack growth would be significantly low to non-existent in these locations.

The fracture mechanics evaluation considered the crack face to be subjected to the operating reactor coolant system (RCS) pressure. This is accomplished by arithmetically adding the RCS pressure to the uniform stress coefficient in the surface crack analysis and to the membrane stress for the through-wall crack analysis. In this manner, the stress imposed on the crack is accurately and conservatively modeled.

In order to ensure that the moving average technique did not create numerical errors, a Mathcad worksheet was created by using the stress averaging portion of the regular analysis worksheet. In this worksheet, the data table, which is used to import data from an Excel spreadsheet, was entirely populated with a linear through-wall stress distribution. The axial distribution of the stresses along the axis was kept constant. In this manner, the moving average method should provide results that have the same distribution at all locations along the tube axis. This implies the through-wall distribution is invariant along the length of the tube. The example and the associated worksheet are provided in Appendix D, Attachment 2. The results of the experiment show that the stress distribution across the wall remained unchanged along the axis of the tube. Therefore the moving stress averaging method is validated.

The through-wall axial crack could have been considered as a single edge crack in a plate. For this model to work properly, it is essential that the plate geometry be described accurately. The CEDM nozzle is welded to the head; hence the nozzle OD surface is clamped at the bottom of the weld. Therefore, the plate height would be equal to the length of the nozzle from the bottom of the nozzle to the bottom of the J-weld. When this plate height is assumed and the length of the through-wall axial crack is taken to be the length (height) of the blind zone, then the ratio of crack length to the plate height (assumed) violates the pre-requisite for the SICF of 0.6. It is possible to assume the plate height to be equal to the nozzle height or some smaller elevation (e.g. length equal to top of the J-weld). These assumptions tend to keep the crack-to-plate height ratio within the limit; however, the resulting SICF is lower than the membrane SICF from the model used in this analysis. A Mathcad worksheet showing the comparison is presented in Appendix D, Attachment 3. The results presented in this attachment demonstrate that the SICF for the model used in the current analysis is higher than the SICF produced by an edge crack model with longer plate lengths. In addition, the bottom zone of the CEDM nozzle is in compression, as shown in Figures 8-23, which further argues against postulating an edge crack for evaluating a through-wall crack. Therefore, for the two reasons cited herein the model developed for through-wall crack is considered valid and provides an accurate (but conservative) estimate of the SIF. The SICF comparison is presented in Figure 27 below.

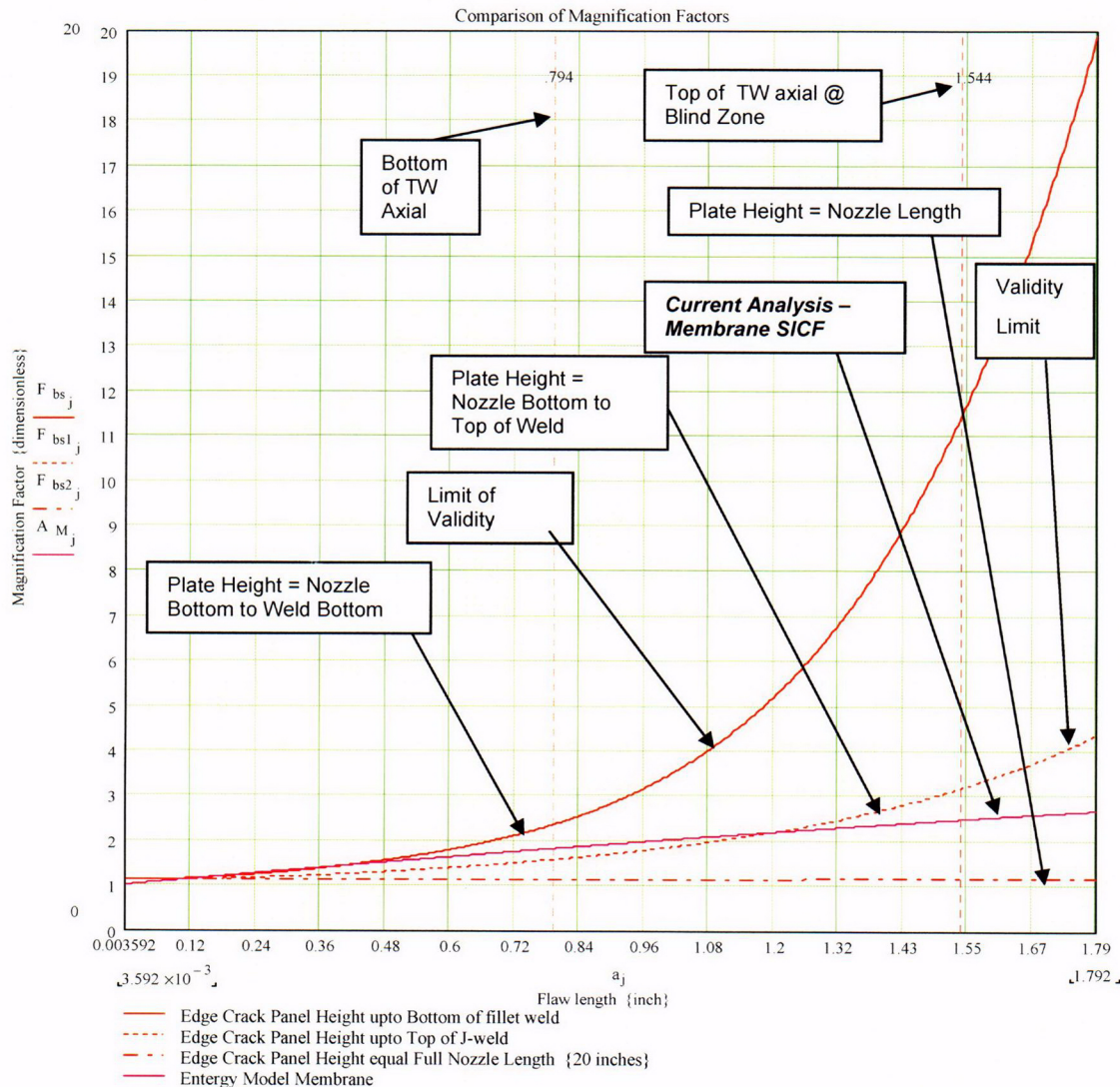


Figure 27: Comparison of SICF for the edge crack configurations with the membrane SICF for current model. The current model results in a higher SICF value for the application considered.

The models used in the analysis presented here were compared with the conventional approach used by the industry. The OD surface crack evaluated shows that the model used provides a higher SIF and, in addition, has the capability of separately evaluating the SIF at the two crack locations (the “a-tip” and the “c-tip”). The SIF comparison for a sample case from Appendix D, Attachment 4 is shown in Figure 28.

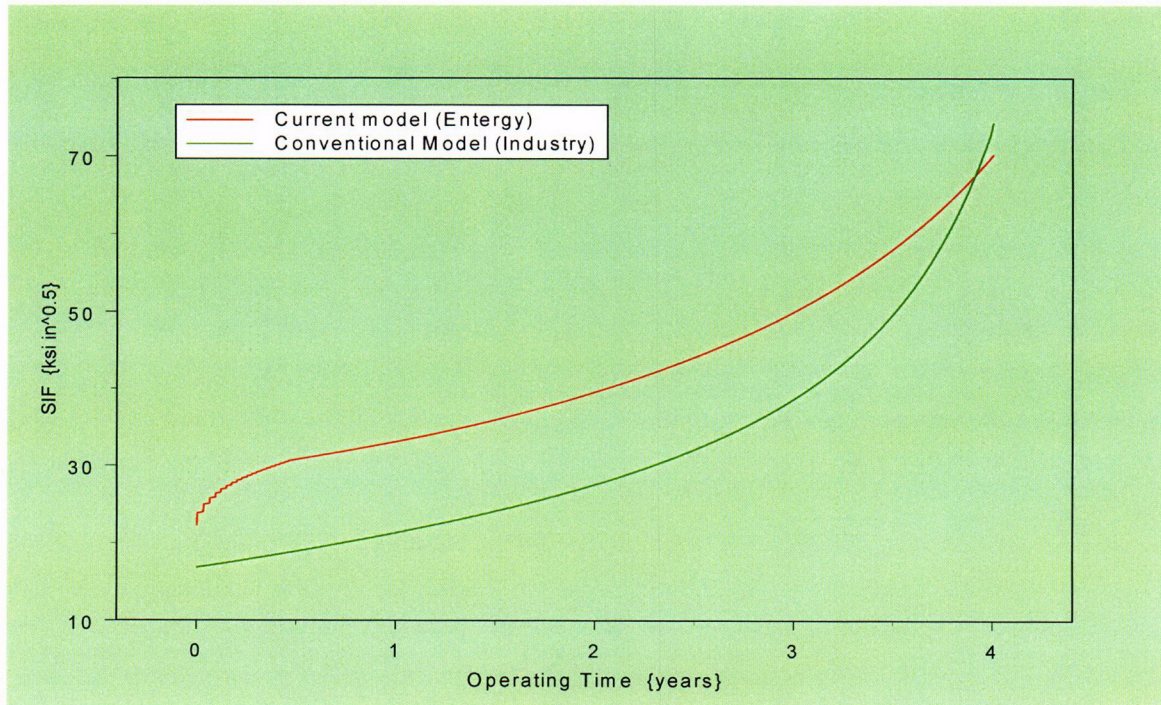


Figure 28: Comparison of SIF for the current model and conventional model.

The conventional approach for the through-wall axial crack is the Center Cracked Panel (CCP) with an SICF of one ($\text{SICF} = 1.0$). This conventional model is compared to the current model used within this analysis. The Mathcad worksheet for this comparison is presented in Appendix D, Attachment 5. The results presented in this attachment clearly demonstrate that the SIF obtained by the current model is significantly higher than that from the conventional approach. Therefore, the estimated crack growth would be higher for the current model than that estimated using the conventional approach. This would lead to an underestimate of the crack growth, by the conventional model, leading to a non-conservative propagation length estimate. Figure 29 shows a comparison between the conventional and current models.

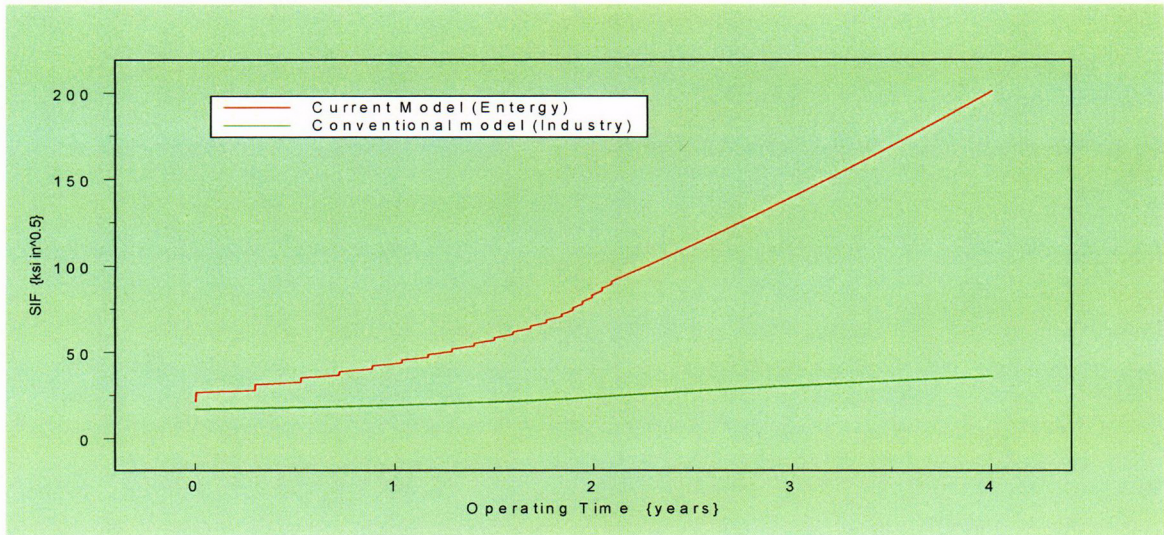


Figure 29: SIF comparison between current model and conventional model.

A comparison of the fracture mechanics models for the current analyses and the conventional method are summarized in Table 17. The comparison shows that the models used in the current analyses would provide a higher estimate for the SIF. The net result would be a higher crack growth rate and hence a larger crack propagation length for one (1) cycle of operation. These improvements in analysis methods are believed to more accurately predict crack behavior in the CEDM configuration and may be conservative compared to the conventional approach.

Table 17 Comparison of Fracture Mechanics Models

Flaw Type	Feature	Conventional Approach	Energy Approach
Surface Flaws (ID & OD) Part Throughwall	Stress	Distribution Fixed a Initial flaw Location	Variable Distribution along Length of Tube & Flaw face Pressurized
	Cylinder Geometry	Fixed "R/t" ratio of 4.0	Variable "R/t" ratio from 1 to 300
	Flaw Geometry	Fixed Aspect Ratio; "a/c" = 0.33	Variable Aspect Ratio; "a/c" from 0.2 to 1.0
	Flaw Growth	Only Growth in Depth direction Evaluated	Growth both in the Depth and Length directions evaluated Independently
Throughwall Axial Flaws	Stress	Uniform Tension @ Initial flaw Location	Variable along Length; Both Membrane and Bending components considered; Flaw face Pressurized
	Model	Center Cracked Panel without Correction Factors	Thick Cylinder with correction for Flaw/Tube geometry

Results

Analysis for the As-Built Condition

The first set of analyses was performed using the as-built dimensions for the welds which were estimated from the review of UT data. In addition, these analyses were performed by setting the blind zone elevation at 1.544 inches above the nozzle bottom. These analyses were performed at three azimuthal locations on the nozzle (downhill, mid-plane, and uphill). At each location, three crack geometries (ID surface, OD surface, and through-wall) were evaluated. The extent of the compression zone in each nozzle group at the three locations was obtained from the stress distributions presented in Figures 8-23. From these figures, the compression zone at the three azimuthal locations is presented in Table 18, below. In these regions of compression, no PWSCC-assisted crack growth is possible; therefore, these zones can be excluded from consideration for inspection.

Table 18: Results for Compression Zone

Nozzle Group (Head Angle – Degrees)	Azimuthal Location	Height of Compression Zone (inch) (Measured from Nozzle Bottom)
0	All (360°)	0.5
8.8	Downhill	0.5
	Mid-Plane	0.6
	Uphill	0.68
28.8	Downhill	0.8
	Mid-Plane	0.81
	Uphill	1.55
49.6	Downhill	0.8
	Mid-Plane	0 (ID is in Tension)
	Uphill	3.25

For nozzles 0° through and including 28.8°, the as-built nozzle and weld dimensions showed some nozzles with a measurable freespan length. For these nozzles, the representing nozzle groups (0°, 8.8°, and 28.8°) were evaluated for both part through-wall cracks and the through-wall crack. For the nozzles beyond 28.8°, the UT data indicates that on the downhill side of the nozzle that the weld extends to or into the blind zone. Therefore, the downhill side of nozzle group 49.6° has been excluded from the OD surface and through-wall crack analysis and has been addressed in the “Additional Analysis” portion of this report.

Twenty eight (28) analyses cases were performed. The worksheets representing these evaluations are presented in Appendix C, Attachments 1 - 28. The

results from this set of analyses are summarized in Table 19. Table 19 provides the "Propagation Dimension" which represents the available freespan for the limiting nozzle within the specific nozzle group. For the OD Crack Type, the length dimension excludes the 0.16 inches that was assumed for the portion of the crack that extends into the freespan. This information represents the limiting condition and is used to identify where "Additional Analysis" is needed to determine augmented surface examination requirements.

Table 19 also provides "Growth/Cycle" dimensions. This is the calculated crack growth for one cycle of operation and is used to evaluate the available freespan of each individual nozzle (as determined from the UT data). This is done by comparing the available nozzle freespan to the "Growth/Cycle" dimension. Where the freespan is larger, adequate margin for flaw growth is available without compromising the weld. When comparing the OD surface crack, 0.16 inch is subtracted from the available freespan to account for the portion of the assumed crack that extends into the freespan.

The analysis results indicate that one or more nozzles from each nozzle group does not possess sufficient free span to facilitate one cycle of crack growth. As evidenced in Table 18, it is either the OD part through-wall crack or through-wall crack that limits the nozzle group. In all cases evaluated, the ID part through-wall crack provides acceptable results for one cycle of operation. None of the postulated ID part through-wall cracks came close to reaching the bottom of the weld or penetrating through the wall to meet the weld. There is no evidence to support that an ID initiated part through-wall crack would provide a leak path or reach the weld within one operating cycle.

Because at least one nozzle in each nozzle group does not have sufficient freespan to accommodate crack growth and for many nozzles, the weld actually reaches to or into the blind zone, additional analysis have been performed for each nozzle group to identify the amount of area below the available freespan or below the weld when there is no freespan that is required to accommodate one cycle of crack growth.

Table 19: ANO-2 As-Built Analyses Results Summary

Nozzle Angle (Reactor Vessel Head)	Azimuth Location	Crack Type	Fracture Mechanics Analysis Results		Attachment Number in Appendix C
			Propagation Dimension (L= length; D= depth) (inch)	Growth / Cycle (inch)	
0 Degree	All	ID	0.092L/0.661D	.054L/.081D *	1
		OD	0.092	0.101	2
		TW	0.252	0.576	3
8.8 Degree	Downhill	ID	0.082L/0.661D	.042L/.074D *	4
		OD	0.082	0.105	5
		TW	0.242	0.560	6
	Uphill	ID	0.682/0.661D	.041L/.072D *	7
		OD	0.682	0	8
		TW	0.842	0.043	9
	Mid-Plane	ID	0.383L/0.661D	.053L/.081D *	10
		OD	0.383	0.02	11
		TW	0.543	0.229	12
28.8 Degree	Downhill	ID	0L/0.661	.010L/.048D *	13
		OD	0	0.086	14
		TW	0.16	0.083	15
	Uphill	ID	2.564L/0.661D	0L/0D *	16
		OD	2.564	0	17
		TW	2.724	0	18
	Mid-Plane	ID	1.295L/0.661D	0L/0D *	19
		OD	1.295	0	20
		TW	1.455	0	21
49.6 Degree	Downhill	ID	na-L/0.661D	0L/0D *	22
		ID	4.924L/0.661D	0L/0D *	23
	Uphill	OD	4.924	0	24
		TW	5.084	0	25
		ID	2.33L/0.661D	0L/0D *	26
	Mid-Plane	OD	2.33	0	27
		TW	2.49	0	28

* For ID Surface Cracks the dimensions for both in Length (L) and Depth (D) are provided.

The graphical presentation of results for those nozzle groups which showed insufficient propagation length are discussed below, by nozzle group. In the graph for length growth, a vertical red line represents one fuel cycle and a horizontal blue line representing available propagation length. When the curve is above the intersection point of these two lines, the analysis indicates that the postulated crack would reach the bottom of the weld in one operating cycle.

0° Nozzle

This nozzle was shown to be shorter than the design specified length. The reduction in the length negatively affected the freespan length. Therefore, there was insufficient propagation length to accommodate the expected crack growth for one fuel cycle. Figure 30 and 31 show the results for the OD surface crack and the through-wall crack, respectively.

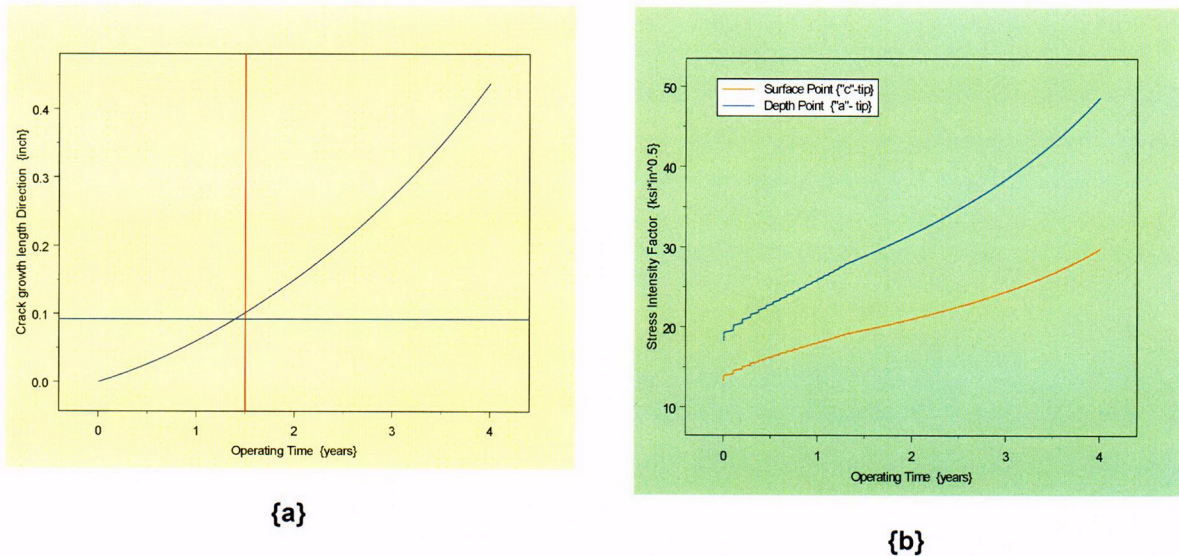
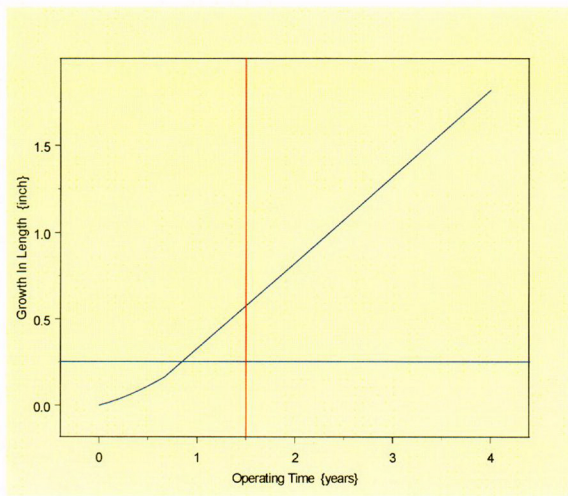
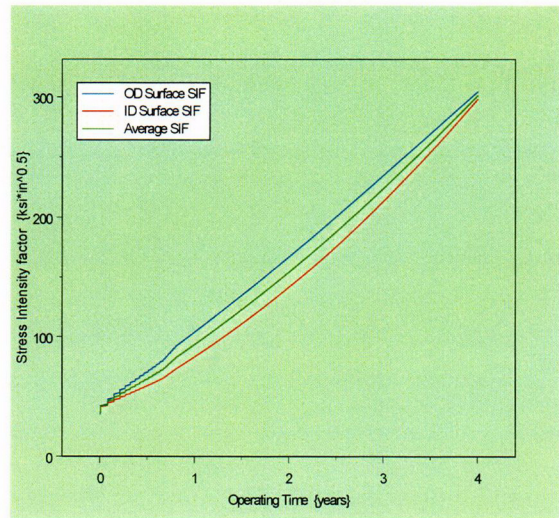


Figure 30: Nozzle at 0°; Crack growth (a) and SIF (b) plots for an OD surface crack.



{a}

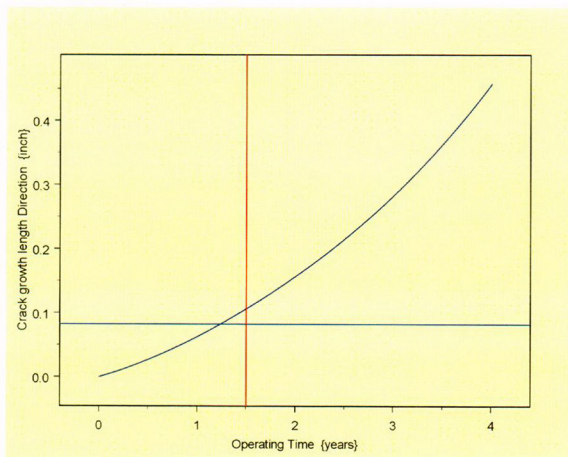


{b}

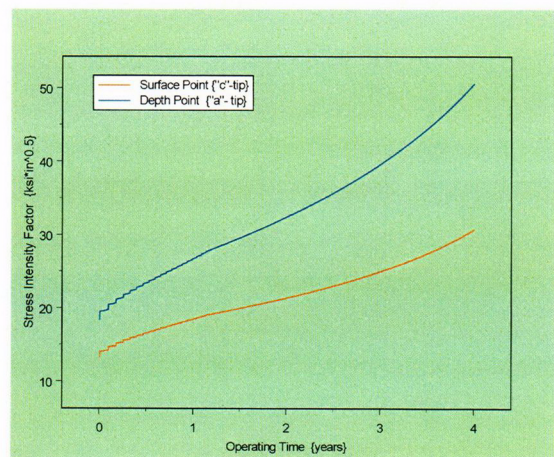
Figure 31: Nozzle at 0°; Crack growth (a) and SIF (b) plots for a through-wall crack.

8.8° Nozzle Group

This nozzle was determined, based on a comparison of UT and design information, to be shorter than the design specified length. The reduction in the length negatively affected the freespan length. Therefore, there was insufficient propagation length to accommodate the expected crack growth for one operating cycle. Figures 32 and 33 show the results for the OD surface crack and the through-wall crack, respectively.

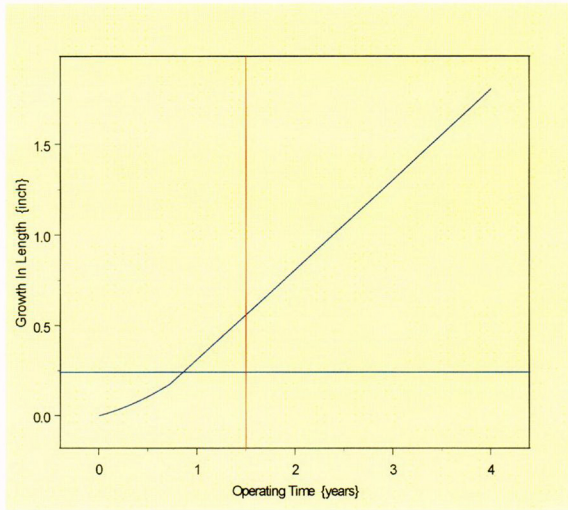


{a}

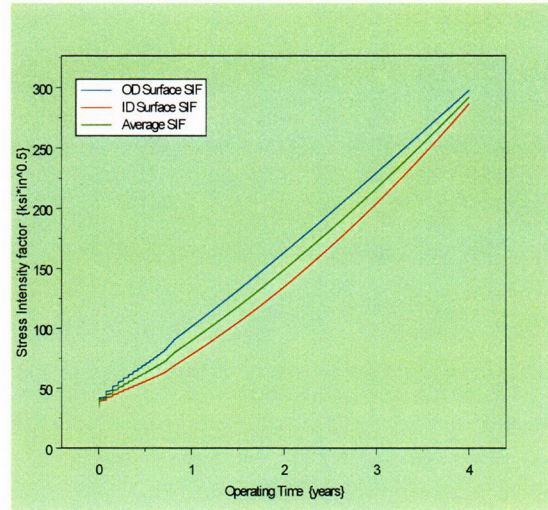


{b}

Figure 32: Nozzle at 8.8°; Crack growth (a) and SIF (b) plots for an OD surface crack



{a}

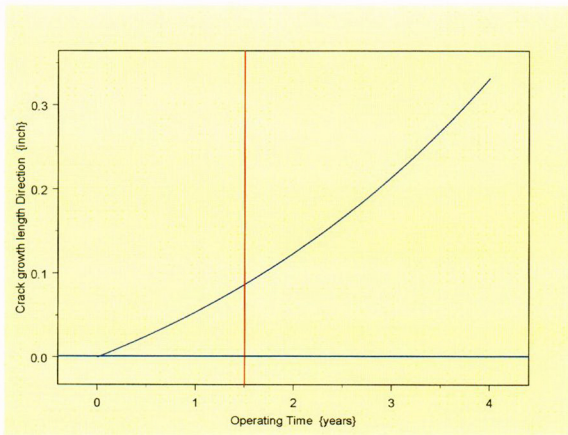


{b}

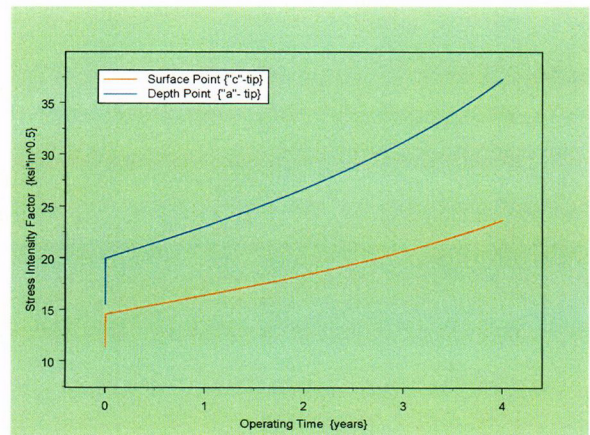
Figure 33: Nozzle at 8.8°; Crack growth (a) and SIF (b) plots for a through-wall crack.

28.8° Nozzle Group

The results for this nozzle location at the downhill position showed the crack growth for the OD surface crack to be greater than the available propagation length in one operating cycle. As stated earlier the through-wall crack growth was within the available propagation length. In Figures 34 and 35 the graphical presentation for the OD surface crack and the through-wall crack are provided. A comparison of the two figures shows that the growth is marginal and is the result of the crack placement in the analysis.



{a}



{b}

Figure 34: Nozzle at 28.8°; Crack growth (a) and SIF (b) plots for an OD surface crack

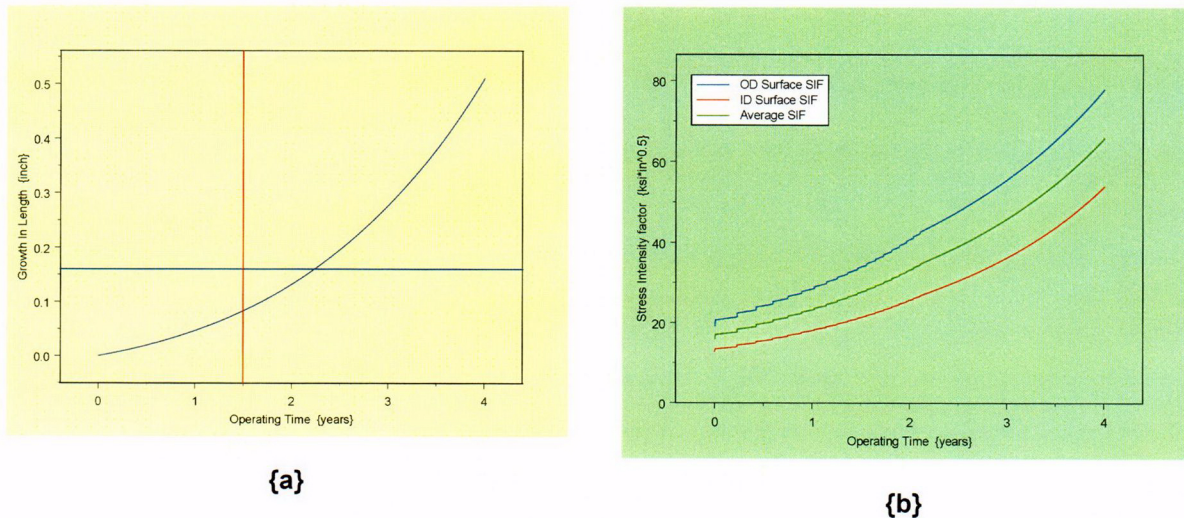


Figure 35: Nozzle at 28.8°; Crack growth (a) and SIF (b) plots for a Through-wall crack.

Comparing Figures 34 and 35 it is observed that the through-wall crack growth does not reach the weld bottom within two years and the SIF for the two crack types are very similar (25-30 ksi√in). The marginal crack growth for both crack types coupled with the acceptable result for the through-wall crack provides reasonable assurance that for this nozzle group the OD crack result would not be controlling.

Additional Analysis

The failure to achieve acceptable crack growth for the postulated cracks in all the nozzle groups necessitated additional analysis to ascertain the augmented inspection region. Since the unacceptable condition related to the OD surface and through-wall crack types, these crack types were reevaluated to define a new region, an extended inspection area, such that acceptable crack growth for one cycle of operation was obtained. In the additional evaluations, the reference line was lowered (below the original blind zone) and the circumferential extent, around the nozzle OD circumference, was iteratively evaluated such that the original UT blind zone was recovered. In this manner the available freespan above the original blind zone and below the weld was sufficient to accommodate one (1) cycle of crack growth.

In this additional evaluation the 49.6° nozzle group at the downhill location, for OD surface and through-wall cracks were also included, since these cracks could not be evaluated using as-built conditions as the weld bottom was below the original blind zone elevation. The additional analysis for the downhill location was similar to that for the analyses process described above. Thus the augmented inspection zone for this group of nozzles was defined in a similar manner.

Results from the additional analysis performed on select nozzle groups are presented in Table 20.

Table 20: Results from Additional Analysis

Nozzle Group Head angle (Degrees)	Azimuthal Location (Degrees)	Reference Line ¹ Above Nozzle Bottom (inch)	Crack Type Evaluated	Propagation Length Available (inch)	Crack Growth in One Cycle (inch)	Appendix C Attachment Number
0	All	1.25	OD	0.386	0.0275	39
	All	1.25	TW	0.546	0.2257	33
8.8	0 (downhill)	1.25	OD	.376	0.026	40
	0 (downhill)	1.25	TW	.536	0.202	34
	DH±22.5	1.3	OD	0.347	0.30	41
	DH±22.5	1.3	TW	0.507	.227	43
	DH±45	1.544	OD	0.167	0.071	42
	DH±45	1.45	TW	0.421	0.345	44
	DH±67.5	1.544	OD	0.263	0.044	46
	DH±67.5	1.544	TW	0.426	0.354	45
28.8	0 (downhill)	1.384	OD	0.16	0.0267	47
	DH±22.5	1.544	OD	0.128	0.05	31
	DH±22.5	1.544	TW	0.288	0.15	48
49.6	0 (downhill)	1.043	OD	0.09	0	29
	0 (downhill)	1.043	TW	0.25	0	30
	DH±22.5	1.3	OD	0.09	0.028	35
	DH±22.5	1.3	TW	0.25	0	37
	DH±45	1.544	OD	0.459	0	36
	DH±45	1.544	TW	0.619	0	38

1) Input to analysis to adjust postulated crack location to identify the axial extent required for one (1) cycle of crack growth.

The analysis results presented in the table above were obtained from specific analysis worksheets provided as Attachments 29 through 48 of Appendix C.

The blue text color in the column labeled "Reference Line" indicates the lowest location of the reference line required to provide sufficient propagation length to support one cycle of operation. The rows colored in yellow show the circumferential (azimuthal) extent required to recover the original blind zone of 1.544 inches. Thus, the two required boundaries for the candidate nozzles are obtained and the required

augmented inspection zone, for OD-based surface examination, can be defined. It is important to note that the OD surface crack's upper half-length is placed above the reference line, hence the axial elevation for the augmented inspection is reduced by the OD crack half-length (0.16 inch). Conversely the axial extent for the augmented inspection is increased by 0.16 inch. The boundaries of the augmented inspection are provided in Table 21 below. The location of the lower extent for the augmented inspection (that is the lower boundary), defined as an elevation above the nozzle bottom, was based on the necessary propagation length for the OD surface crack. Therefore, the boundary is conservative for a through-wall axial crack. Recall that the modeling for an OD surface crack assumes that the lower tip and the upper tip of the crack are placed 0.16 inch below and above the reference line respectively. In the additional analyses the reference line was located below the elevation for the top of the blind zone. The dimension for the axial boundary locations (bottom and top boundary), in Table 21, is the elevation above the nozzle bottom. Hence the full extent of the assumed surface crack is covered. Likewise, the circumferential extent forms an arc on either side of the downhill (0°) location. The included angle of the arc is twice (2) the angle dimension in Table 21. That is the reason for the sign in front of the angle number.

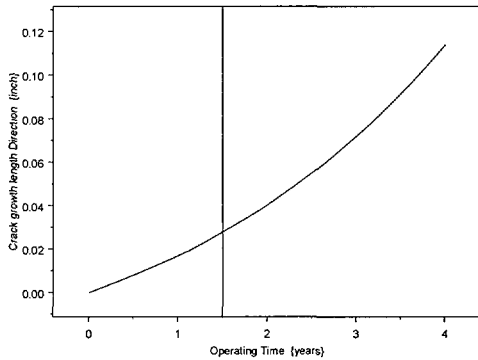
Table 21: Boundaries for Augmented Inspection (OD Surface Examination)

Nozzle Group	Specified Boundary for Augmented Surface Examination (OD)	
	Head Angle (Degrees)	Bottom and Top Boundary for Augmented Examination (Axial Elevation from Nozzle Bottom) (inch)
0	1.09 to 1.544	± 180 (full circumference)
8.8	1.09 to 1.544	± 67.5
28.8	1.224 to 1.544	± 22.5
49.6	0.883 to 1.544	± 45

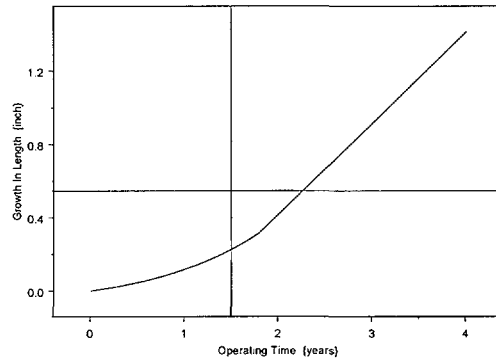
The discussion and graphical presentation below are categorized by nozzle group. Only graphs for crack growth are provided, because these graphs are pertinent to the discussion. The other graphs are available in the attachments provided in Appendix C.

0° Nozzle

This nozzle had insufficient freespan to accommodate one cycle of postulated crack growth. In addition, this nozzle is axi-symmetric about the nozzle axis, hence, the augmented inspection region is the full circumference of the defined region. Figure 36 presents the crack growth behavior at the lowered reference line for both the OD surface and through-wall crack geometry.



OD Surface Crack; Propagation Length = 0.386"

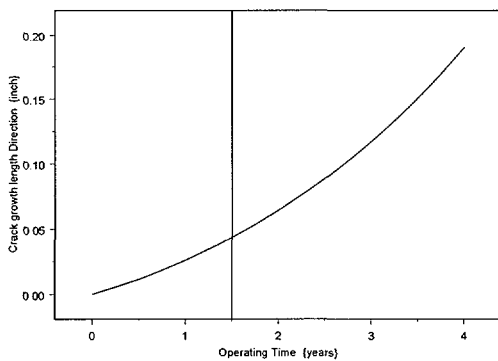


Through-wall Crack

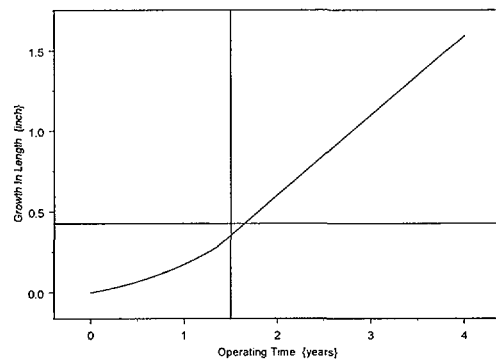
Figure 36: 0° Nozzle crack growth at lowered reference line at 1.25 inches above nozzle bottom. The augmented inspection coverage in the azimuthal direction is the full circumference.

8.8° Nozzle Group

This nozzle group had insufficient propagation length to accommodate one cycle of postulated crack growth. The augmented inspection region in the azimuthal direction is an arc of 135° centered about the downhill location (0°). Figure 37 presents the crack growth behavior at the original blind zone at 1.544 inches above nozzle bottom and the 67.5° azimuth for both the OD surface and through-wall crack geometry.



OD Surface Crack; Propagation Length = 0.263'



Through-wall Crack

Figure 37: 8.8° Nozzle crack growth at blind zone elevation of 1.544 inches above nozzle bottom and at an azimuth of 67.5°. The augmented inspection coverage in the azimuthal direction is a 135° arc centered at the downhill location (0°).

28.8° Nozzle Group

This nozzle group had insufficient propagation length to accommodate one cycle of postulated crack growth for the OD surface crack. The through-wall crack had sufficient propagation length to accommodate one cycle of postulated crack growth. The augmented inspection region in the azimuthal direction is an arc of 45° centered about the downhill location (0°). Figure 38 presents the crack growth behavior at the original blind zone at 1.544 inches above nozzle bottom and the 22.5° azimuth, for both the OD surface and through-wall crack geometry.

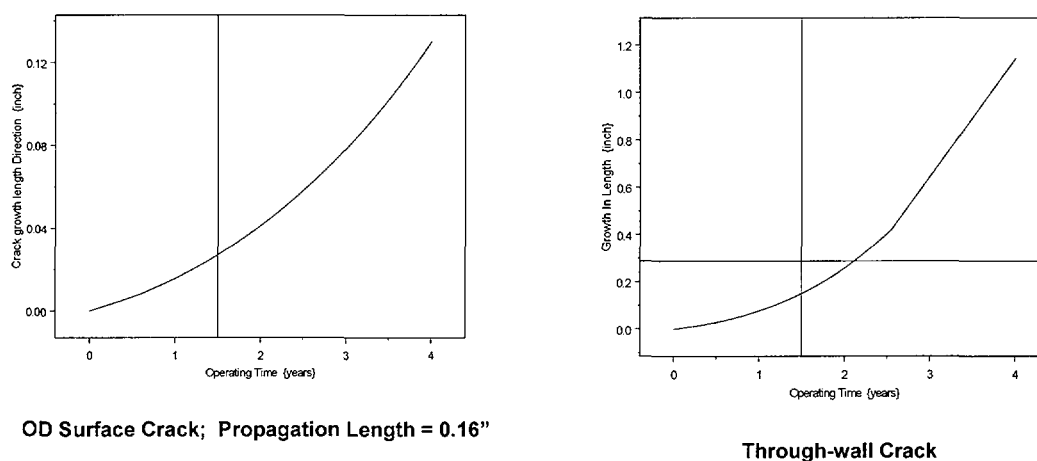


Figure 38: 28.8° Nozzle crack growth at the blind zone elevation of 1.544 inches above nozzle bottom and at an azimuth of 22.5°. The augmented inspection coverage in the azimuthal direction is a 45° arc centered at the downhill location (0°).

49.6° Nozzle Group

This nozzle group had the weld bottom extend into the blind zone at the downhill location. Hence, a lowered reference line was used to define the augmented inspection zone. The analysis was performed at the two different azimuthal locations to ensure the recovery of available propagation length above the original blind zone at 1.544 inches above nozzle bottom. At an azimuth of 45°, the analysis showed that there exists sufficient propagation length above the original blind zone to accommodate one cycle of postulated crack growth. The augmented inspection region in the azimuthal direction is an arc of 90° centered about the downhill location (0°). Figure 39 presents the crack growth behavior at the original blind zone and the 45° azimuth, for both the OD surface and through-wall crack geometry.

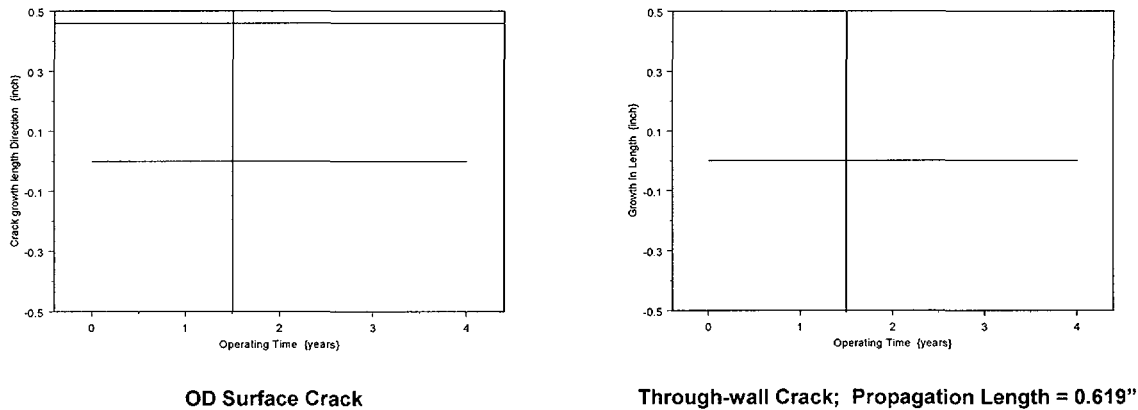


Figure 39: 49.6° Nozzle crack growth at the blind zone elevation of 1.544 inches above nozzle bottom and at an azimuth of 45°. The augmented inspection coverage in the azimuthal direction is a 90° arc centered at the downhill location (0°).

6.0 Conclusions

The evaluation performed and presented in the preceding sections support the following conclusions:

- 1) The detailed deterministic analyses incorporating the as-built dimensions for the weld and nozzle length were used to accurately define the inspection zones for the CEDM nozzle groups.
- 2) The developed models, incorporating a method to account for applied stress distribution variation along the nozzle length, have been shown to be a reasonably realistic but conservative representation of the expected phenomenon. The models are generalized and have the potential to be used at other locations of the nozzles.
- 3) The fracture mechanics models were shown to be representative of the expected crack and nozzle configurations. A review of the current model results and that from the conventional approach showed that the current model produced higher SIF than the conventional model. Therefore, the current model provides a more accurate and conservative estimate of crack growth.
- 4) The conservatism used in the analysis provide assurance that an undetected crack at the lowest elevation for inspection will not reach the weld bottom within one operating cycle.
- 5) The regions below the lowest inspection elevation experience lower stresses and except for the one exception noted within the report, there exists a defined compressive zone at the nozzle bottom. Hence, at elevations below the lowest inspection elevation, a significantly lower

potential for crack growth by PWSCC exists. Thus, at these lower locations PWSCC, crack growth is not expected.

- 6) The ID surface cracks either did not show any potential for crack growth, or the crack growth was well within acceptable limits. Hence, ID surface cracks in a region below the weld are not significant.
- 7) The augmented inspection region, developed by the deterministic analysis, will provide assurance that a postulated crack below the proposed inspection zone will not reach the bottom of the weld in one operating cycle.

References

- 1) NRC Order; Issued by letter EA-03-009 addressed to "Holders of Licenses for Operating Pressurized Water Reactors"; dated February 11, 2003.
- 2) Drawing Number M-2001-C2-23, ANO Design Engineering Drawing files & 1564-506 WSES-3 Design Engineering Drawing files.
- 3) a: E-mail from R. V. Swain (Entergy) to J. G. Weicks (Entergy); Dated 5/15/2003.
b: E-mail from R. V. Swain to J. G. Weicks; Dated 5/12/2003.
- 4) EPRI NDE Demonstration Report; "MRP Inspection Demonstration Program – Wesdyne Qualification": Transmitted by e-mail from B. Rassler (EPRI) to K. C. Panther (Entergy); Dated 3/27/2003.
- 5) a: "PWSCC of Alloy 600 Materials in PWR Primary System Penetrations"; EPRI TR-103696; Electric Power Research Institute, Palo Alto, CA; July 1994.
b: DEI E-Mail containing the Nodal Stress Data for ANO-2 CEDM Analysis; J. Broussard (DEI) to J. S. Brihmadebam (Entergy); Dated 8/17/2003
c: "BWR Vessel and Internals Project – Evaluation of crack growth in BWR Stainless Steel RPV Internals (BWRVIP-14)"; EPRI TR-105873; Electric Power Research Institute, Palo Alto, CA; March 1996.
d: "BWR Vessel and Internals Project – Evaluation of crack growth in BWR Nickel Base Austenitic Alloys in RPV Internals (BWRVIP-59)"; EPRI TR-108710; Electric Power Research Institute, Palo Alto, CA; December 1998.
- 6) "Stress Intensity Factor Influence Coefficients for Internal and External Surface Cracks in Cylindrical Vessels"; I. S. Raju and J. C. Newman, Jr.; ASME PVP Volume 58 "Aspects of Fracture Mechanics in Pressure Vessels and Piping"; 1982.
- 7) "Stress Intensity Factors for Part-Through Surface Cracks in Hollow Cylinders": S. R. Mettu et al; NASA TM-111707; Prepared by Lockheed Engineering & Science Services; Houston, Texas; July 1992.
- 8) "New Stress Intensity factor and Crack Opening Area Solutions for Through Wall Cracks in Pipes and cylinders": Christine C. France, et al.; ASME PVP Volume 350 "Fatigue and Fracture"; 1997.

- 9) Axum 7; Data Analysis Products Division, Mathsoft Inc., Seattle, WA; February 1999.
- 10) "Materials reliability Program (MRP) Crack Growth Rates for Evaluating Primary Water Stress Corrosion cracking (PWSCC) of Thick Wall Alloy 600 Material": MRP-55 Revision 1; Electric Power Research Institute; May 2002.
- 11) Mathcad – 11; Data Analysis Products Division; Mathsoft Inc.; Seattle WA; November 2002.
- 12) "Stress Intensity Factors Handbook Volume 1"; Y. Murakami, Editor-in-Chief; Pergamon Press ; 1986; Section 1.3.

May 29, 2003

Mr. J. A. Stall
Senior Vice President, Nuclear and
Chief Nuclear Officer
Florida Power and Light Company
P.O. Box 14000
Juno Beach, Florida 33408-0420

SUBJECT: SAINT LUCIE NUCLEAR PLANT, UNIT 2 - ORDER EA-03-009 RELAXATION
REQUESTS NOS. 1 AND 2 REGARDING EXAMINATION COVERAGE OF
REACTOR PRESSURE VESSEL HEAD PENETRATION NOZZLES
(TAC NOS. MB8165 AND MB8166)

Dear Mr. Stall:

By letter dated March 28, 2003, Florida Power and Light Company (FPL) submitted two requests for relaxation from the inspection requirements of the U.S. Nuclear Regulatory Commission (NRC) Order EA-03-009 for St. Lucie Unit 2. Pursuant to the procedure specified in Section IV, paragraph F of the Order, FPL requested relaxation from the requirements specified in Section IV, paragraph C.(1)(b)(i) for the reactor pressure vessel head (RPVH) penetration nozzles for which ultrasonic testing requirements cannot be completed as required. Relaxation was also requested from the requirements specified in Section IV, paragraph C.(1)(a) for the area of the RPVH surface that is inaccessible for visual inspection.

These requests were discussed with the NRC staff in a public meeting on April 14, 2003, during which it was determined that additional information was needed. A Request for Additional Information was issued on April 18, 2003. FPL provided the additional information in a letter dated April 18, 2003. Following subsequent telephone discussions with the NRC staff, the requests were further supplemented in letters dated April 29, May 4 and May 11, 2003. The May 11, 2003, letter completely revised the previous requests and provided additional information based on actual inspection results.

We have reviewed and evaluated the information provided in support of your requests for relaxation and have found that FPL has demonstrated good cause for the requested relaxation. FPL has demonstrated that compliance with the Order would result in hardship without a compensating increase in the level of quality and safety. Therefore, pursuant to Section IV.F of the Order and Title 10, *Code of Federal Regulations*, Section 50.55a(a)(3), the NRC staff approves for one 18-month operating cycle, commencing with startup from the spring 2003 (SL2-14) refueling outage, your requests for relaxation and authorizes the proposed alternatives to item IV.C.(1)(b)(i) with respect to ultrasonic testing of RPVH penetration nozzles and item IV.C.(1)(a) with respect to bare metal visual examination of the RPVH surface at St. Lucie Unit 2, contingent on the following conditions:

- a. If the NRC staff finds that the crack growth formula in industry report MRP-55 is unacceptable, the licensee shall revise its analysis that justifies relaxation of the Order within 30 days after the NRC informs the licensee of an NRC-approved crack growth formula. If the licensee's revised analysis shows that the crack

growth acceptance criteria are exceeded prior to the end of the current operating cycle, this relaxation is rescinded and the licensee shall, within 72 hours, submit to the NRC written justification for continued operation. If the revised analysis shows that the crack growth acceptance criteria are exceeded during the subsequent operating cycle, the licensee shall, within 30 days, submit the revised analysis for NRC review. If the revised analysis shows that the crack growth acceptance criteria are not exceeded during either the current operating cycle or the subsequent operating cycle, the licensee shall, within 30 days, submit a letter to the NRC confirming that its analysis has been revised.

- b. Should there be any evidence of corrosive product upslope or downslope of the inaccessible areas, the relaxation is rescinded until such time that the licensee can provide adequate information to the staff that ensures that the RPVH is not degraded in the inaccessible areas.

Further details on the bases for the NRC staff's conclusions are contained in the enclosed safety evaluation. If you have any questions regarding this issue, please contact Brendan Moroney at (301) 415-3974.

Sincerely,

/RA/

Scott W. Moore, Acting Director
Project Directorate II
Division of Licensing Project Management
Office of Nuclear Reactor Regulation

Docket No. 50-389

Enclosure: Safety Evaluation

cc: See next page

growth acceptance criteria are exceeded prior to the end of the current operating cycle, this relaxation is rescinded and the licensee shall, within 72 hours, submit to the NRC written justification for continued operation. If the revised analysis shows that the crack growth acceptance criteria are exceeded during the subsequent operating cycle, the licensee shall, within 30 days, submit the revised analysis for NRC review. If the revised analysis shows that the crack growth acceptance criteria are not exceeded during either the current operating cycle or the subsequent operating cycle, the licensee shall, within 30 days, submit a letter to the NRC confirming that its analysis has been revised.

- B. Should there be any evidence of corrosive product upslope or downslope of the inaccessible areas, the relaxation is rescinded until such time that the licensee can provide adequate information to the staff that ensures that the RPVH is not degraded in the inaccessible areas.

Further details on the bases for the NRC staff's conclusions are contained in the enclosed safety evaluation. If you have any questions regarding this issue, please contact Brendan Moroney at (301) 415-3974.

Sincerely,

/RA/

Scott W. Moore, Acting Director
Project Directorate II
Division of Licensing Project Management
Office of Nuclear Reactor Regulation

Docket No. 50-389

Enclosure: Safety Evaluation

cc: See next page

Distribution:

PUBLIC SMOore AHowe EBrown BMoroney
PDII-2 R/F OGC ACRS BBateman TChan
AHiser RDavis SBloom BSmith, EDO JMunday, RII
BClayton (Hard copy)

ADAMS ACCESSION NUMBER:ML031500489

OFFICE	PDII-2/PM	PDII-2/LA	OGC	EMCB/SC	PDII-2/SC	PDII/D
NAME	BMoroney	BClayton	GLongo-NLO	TChan	AHowe	SMoore
DATE	5/28/03	5/28/03	05/27/03	memo 05/15 /03	5/29/03	5/29/03

OFFICIAL RECORD COPY

Mr. J. A. Stall
Florida Power and Light Company

cc:
Senior Resident Inspector
St. Lucie Plant
U.S. Nuclear Regulatory Commission
P.O. Box 6090
Jensen Beach, Florida 34957

Craig Fugate, Director
Division of Emergency Preparedness
Department of Community Affairs
2740 Centerview Drive
Tallahassee, Florida 32399-2100

M. S. Ross, Attorney
Florida Power & Light Company
P.O. Box 14000
Juno Beach, FL 33408-0420

Mr. Douglas Anderson
County Administrator
St. Lucie County
2300 Virginia Avenue
Fort Pierce, Florida 34982

Mr. William A. Passetti, Chief
Department of Health
Bureau of Radiation Control
2020 Capital Circle, SE, Bin #C21
Tallahassee, Florida 32399-1741

Site Vice President
St. Lucie Nuclear Plant
6351 South Ocean Drive
Jensen Beach, Florida 34957

ST. LUCIE PLANT

Mr. R. E. Rose
Plant General Manager
St. Lucie Nuclear Plant
6351 South Ocean Drive
Jensen Beach, Florida 34957

Licensing Manager
St. Lucie Nuclear Plant
6351 South Ocean Drive
Jensen Beach, Florida 34957

Vice President, Nuclear Operations Support
Florida Power & Light Company
P.O. Box 14000
Juno Beach, FL 33408-0420

Mr. Rajiv S. Kundalkar
Vice President - Nuclear Engineering
Florida Power & Light Company
P.O. Box 14000
Juno Beach, FL 33408-0420

Mr. J. Kammel
Radiological Emergency
Planning Administrator
Department of Public Safety
6000 SE. Tower Drive
Stuart, Florida 34997

SAFETY EVALUATION BY THE OFFICE OF NUCLEAR REACTOR REGULATION

RELAXATION REQUEST NO. 1 AND 2

FLORIDA POWER AND LIGHT COMPANY, ET AL.

SAINT LUCIE NUCLEAR PLANT, UNIT 2

DOCKET NO. 50-389

1.0 INTRODUCTION

By letter dated March 28, 2003, Florida Power and Light Company, et al. (FPL, the licensee) submitted two requests for relaxation from the inspection requirements of the U.S. Nuclear Regulatory Commission (NRC) Order EA-03-009 for St. Lucie Unit 2. Pursuant to the procedure specified in Section IV, paragraph F of the Order, FPL requested relaxation from the requirements specified in Section IV, paragraph C.(1)(b)(i) for the reactor pressure vessel head (RPVH) penetration nozzles for which ultrasonic testing requirements cannot be completed as required. Relaxation was also requested from the requirements specified in Section IV, paragraph C.(1)(a) for the area of the RPVH surface that is inaccessible for visual inspection.

These requests were discussed with the NRC staff in a public meeting on April 14, 2003, during which it was determined that additional information was needed. A Request for Additional Information was issued on April 18, 2003. FPL provided the additional information in a letter dated April 18, 2003. Following subsequent telephone discussions with the NRC staff, the requests were further supplemented in letters dated April 29, May 4 and May 11, 2003. The May 11, 2003, letter completely revised the previous requests and provided additional information based on actual inspection results.

2.0 REGULATORY EVALUATION

Order EA-03-009, issued on February 11, 2003, requires specific examinations of the reactor pressure vessel (RPV) head and vessel head penetration (VHP) nozzles of all pressurized water reactor plants. Section IV, paragraph F, of the Order states that requests for relaxation of the Order associated with specific penetration nozzles will be evaluated by the NRC staff using the procedure for evaluating proposed alternatives to the American Society of Mechanical Engineers Code in accordance with Title 10 of the *Code of Federal Regulations* (10 CFR) Section 50.55a(a)(3). Section IV, paragraph F, of the Order states that a request for relaxation regarding inspection of specific nozzles shall address the following criteria: (1) the proposed alternative(s) for inspection of specific nozzles will provide an acceptable level of quality and safety, or (2) compliance with this Order for specific nozzles would result in hardship or unusual difficulty without a compensating increase in the level of quality and safety.

For St. Lucie Unit 2, and similar plants determined to have a high susceptibility to primary water stress corrosion cracking in accordance with Section IV, paragraphs A and B, of the Order, the

following inspections are required to be performed every refueling outage in accordance with Section IV, paragraph C.(1) of the Order:

- (a) Bare metal visual (BMV) examination of 100 percent of the RPV head surface (including 360° around each RPV head penetration nozzle), AND
- (b) Either:
 - (i) Ultrasonic testing of each RPV head penetration nozzle (i.e., nozzle base material) from two (2) inches above the J-groove weld to the bottom of the nozzle and an assessment to determine if leakage has occurred into the interference fit zone, OR
 - (ii) Eddy current testing or dye penetrant testing of the wetted surface of each J-Groove weld and RPV head penetration nozzle base material to at least two (2) inches above the J-groove weld.

Footnote 3 of the Order provides specific criteria for examination of repaired VHP nozzles.

3.0 TECHNICAL EVALUATION

3.1 Order Requirements for which Relaxation is Requested

Section IV.C.(1) of Order EA-03-009 requires, in part, that the following inspections be performed every refueling outage for high susceptibility plants similar to St Lucie Unit 2:

- (a) Bare metal visual (BMV) examination of 100 percent of the RPV head surface (including 360° around each RPV head penetration nozzle), AND
- (b) Either:
 - (i) Ultrasonic testing of each RPV head penetration nozzle (i.e., nozzle base material) from two (2) inches above the J-groove weld to the bottom of the nozzle and an assessment to determine if leakage has occurred into the interference fit zone, OR
 - (ii) Eddy current testing or dye penetrant testing of the wetted surface of each J-Groove weld and RPV head penetration nozzle base material to at least two (2) inches above the J-groove weld.

Request 1:

The licensee has requested relaxation from Section IV.C.(1)(b)(i) of the Order to perform ultrasonic testing (UT) of the RPV head penetration inside the tube from 2 inches above the J-groove weld to the bottom of the penetration. Specifically, the relaxation is related to UT examination of the bottom portion (threaded area) of all 91 Control Element Drive Mechanism (CEDM) penetration nozzles. Relaxation has not been requested for the remaining 11 RPV head penetrations (10 incore instrumentation penetrations and one RPV head vent line).

Request 2:

The licensee has requested relaxation from Section IV.C.(1)(a) of the Order to perform BMV examination of 100 percent of the RPV head surface. Specifically, the licensee is unable to comply with the 100 percent visual examination requirement due to inaccessibility of a small portion of the RPV head. The inaccessible areas are behind the twelve 6-inch wide shroud lugs and under the horizontal reflective metal insulation (RMI) support legs.

Both of these relaxations were requested for one 18-month operating cycle.

3.2 Licensee's Proposed Alternative Method

Request 1:

The licensee proposed to perform UT examination from 2 inches above the weld to below the weld to the extent possible. Nozzles that cannot be UT examined at least 0.41 inches below the weld would receive a supplemental outside diameter (OD) dye penetrant test (PT) extending from the end of the UT coverage to the bottom of the nozzle for approximately a 90° arc of the nozzle, centered on the downhill side of the nozzle.

Request 2:

The licensee proposes to achieve substantial compliance with the 100 percent requirement by conducting a BMV examination of the RPV head surface to the extent practical, excluding the inside of the 54 RPV stud holes. Specifically, the licensee stated that the examination will include a visual examination of 360° around each RPV head penetration nozzle for evidence of leakage and examination of approximately 99 percent of the bare head surface. The examination will include areas uphill and downhill of inaccessible areas identified by the licensee to be under the horizontal RMI support legs and under vertical panels at 12 shroud lug locations. The licensee stated that the BMV inspection will cover more area than was stated in the licensee's original relaxation request submitted on March 28, 2003. The additional coverage was obtained by removal of the 12 flashing panels attached directly under the shroud support ring, and lifting of the vertical insulation panels that were in contact with the RPV head base material to obtain visual access for remote equipment to inspect areas previously thought inaccessible.

3.3 Licensee's Basis for Relaxation

Request 1:

The licensee stated that the CEDM RPV nozzles have inside-threaded ends that are used to permanently attach externally-threaded guide cones which prevent UT examination to the bottom of the nozzle. According to the licensee, this design condition will prevent current UT examination technology available for CEDM nozzle inspections from collecting UT data to the end of the nozzles. The licensee stated that inspecting the nonpressure boundary area of the threaded portion of the CEDM nozzles would result in a hardship or unusual difficulty without a compensating increase in the level of quality and safety. In particular, the threaded guide cones would have to be removed and special tooling would have to be developed to inspect the threaded nozzle surface in order to implement an inspection in accordance with Section IV,

paragraph C.(1)(b)(i) of the Order. The licensee originally requested relief to inspect from 2 inches above the weld to a minimum of 1 inch below the weld. The 1-inch minimum originally requested by the licensee in a letter dated March 28, 2003, was based on measurements taken from a generic Combustion Engineering Owners Group report. The licensee stated that, during the RPV head inspection, it was discovered that the distance from the toe of the weld on the OD of the nozzle to the start of the internally-threaded area (inside diameter (ID) of nozzle) on the downhill side of most of the CEDM nozzles was generally less than 1 inch.

As an alternative to the UT examination of Order Section IV.C.(1)(b)(i), compliance with Order EA-03-009 can be achieved by eddy current testing (ET) or PT of the wetted surfaces of each J-groove weld and RPV head penetration nozzle base material as described in Order Section IV.C.(1)(b)(ii). However, the licensee stated that its inspection vendor does not have the capability to perform ET, and preparation and performing PT would only be applicable to the outside diameter of the CEDM nozzles. Performing a PT on the outside surfaces would increase personnel radiation exposure. The licensee stated that implementation of surface examinations in accordance with Section IV.C.(1)(b)(ii) of the Order, creates a hardship.

The licensee stated that during its inspection of the 91 CEDM nozzles, there were 9 nozzles that had UT examination coverage less than 0.41 inches from the bottom of the J-groove weld. The 9 nozzles received a PT examination on the OD that overlapped the UT coverage area and extended to the bottom of the nozzle. The licensee stated that the PT enveloped the width (vertical) of UT coverage area that was less than 0.50 inches below the weld for these 9 nozzles. The circumferential width of the PT examination area was limited to 45° on each side of the 0° downhill location. The PT examination found no recordable indications on any of the nine nozzles. The licensee stated that performing PT on the aforementioned 9 nozzles resulted in a radiation exposure of approximately 2.45 person rem.

The licensee's request for the reduction of the examination coverage area is based on a flaw tolerance approach. The licensee stated that its approach will provide an acceptable level of quality and safety with respect to reactor vessel structural integrity and leak integrity. The basis for this approach is provided in Westinghouse Electric Co. LLC, WCAP-16038-P, Revision 0, March 2003, "Structural Integrity Evaluation of Reactor Vessel Upper Head Penetrations to Support Continued Operations: St. Lucie Unit 2."

The licensee stated that, for the limiting nozzle location, a postulated axial through-wall flaw at a distance of 0.28 inches from the bottom of the weld will take 18 months of operation to reach the weld. The licensee, therefore, asserts that a UT inspection that includes an area at least 0.41 inches below the weld will support one 18-month period of operation (one refueling cycle) for St. Lucie Unit 2 with at least an additional 19.4 months of operating margin (37.4 months total). The licensee stated that for the nine nozzles that had UT examination coverage less than 0.41 inches below the weld, a PT examination of these nozzles was performed and included areas that did not receive a minimum UT coverage of 0.50 inch. The licensee states that its analysis shows that a through-wall flaw that is 0.50 inch from the weld toe would take 5 years of operating time to propagate to the toe of the weld.

The licensee stated that according to its analysis, the stresses on the OD surface of the nozzle decrease rapidly as the distance below the weld increases. For the nozzles with limited coverage (intersection angles with the head of 33.8° and higher), the hoop stresses were reported by the licensee to be bounded by 31 ksi on the ID and 30 ksi on the OD at 0.41 inches

below the weld. This calculation is for an intersection angle of 29.1° and at higher intersection angles the stresses are lower.

The licensee stated that additional efforts to achieve the Order-required examination area (below the weld) will result in a hardship or unusual difficulty without a compensating increase in the level of quality and safety.

Request 2:

The licensee stated that inspecting 100 percent of the BMV examination required by the Order would result in a hardship or unusual difficulty without a compensating increase in the level of quality and safety. The licensee stated that the lack of access created by the presence of the twelve 6-inch shroud lugs and the horizontal RMI panel support legs prevent a 100 percent BMV examination. The licensee stated that improving access to these inaccessible areas, including removal of the horizontal panel support legs for visual examination, would require major disassembly of the CEDM stacks and lifting of the shroud and shroud ring to allow access for the destructive RMI removal, resulting in a substantial increase in radiation dose and the potential for damage to removed components.

The licensee stated that in November 2001, during refueling outage SL2-13, a BMV examination was performed of the accessible portions of the RPV head inside the RMI, including 360° visual examination around each RPV head penetration nozzle, to identify leakage from the 102 penetrations. The licensee stated that there were no indications of staining leading downhill on the head surface or evidence of leakage identified around the 102 RPV head penetrations.

By letter dated April 29, 2003, the licensee committed to the following condition:

Should there be any evidence of corrosive product upslope or downslope of the inaccessible areas, the relaxation is rescinded until such time that the licensee can provide adequate information to the staff that ensures that the RPVH is not degraded in the inaccessible areas.

During the current SL2-14 refueling outage, the licensee stated that the visual examination performed included approximately 99 percent of the RPV head excluding the aforementioned areas. The inspection included a 100 percent inspection (360°) of the RPV head and RPV nozzle interface areas. Head surfaces immediately uphill and downhill of the inaccessible areas were examined for evidence of boric acid leakage under the vertical insulation panels at 12 shroud lug locations, and horizontal RMI panel legs. The licensee stated that no evidence of corrosive products were identified.

The licensee concluded that a hardship or unusual difficulty without a compensating increase in level of quality and safety would result if physical modifications were performed to achieve the complete coverage of the RPV head base material required by the order.

3.4 Evaluation

Request 1

The NRC staff's review of this request was based on criterion (2) of paragraph F of Section IV of the Order, which states:

Compliance with this Order for specific nozzles would result in hardship or unusual difficulty without a compensating increase in the level of quality and safety.

In supporting its request for approval of a proposed alternative examination of the RPV penetration nozzles, the licensee has demonstrated the hardship that would result from implementing examinations to the bottom-end of these nozzles. The hardship identified by the licensee includes the nozzle configuration and the limitation of the UT probe used for nozzle examination. The staff finds that the nozzles' threaded areas that mate with guide cones make inspection of these nozzles in accordance with Order EA-03-009 very difficult and would involve a hardship. This evaluation focuses on the issue of whether there is a compensating increase in the level of quality and safety such that these nozzles should be inspected despite this hardship.

The licensee's request to limit the examination of the nozzle base material to at least 0.41 inches below the weld on the downhill side of the CEDM nozzles is appropriately supported by the licensee's analysis (WCAP-1608-P), which indicates that no flaw below that portion of the nozzle would propagate to a level adjacent to the J-groove weld within an 18-month operating period with a margin of 19.4 months. The 9 nozzles that have less than 0.41-inch examination coverage with UT and are supplemented to greater than 0.5 inches with PT of the OD surface have an 18-month operating period but the margin may be different from 19.4 months as stated by the licensee. UT examination is a volumetric examination of the base metal and gives a higher level of interrogation than a PT examination, which inspects the surface only, therefore the margin claimed by the licensee may be less than stated. However, the analysis assumes a through-wall flaw at 0.41 inches below the weld, and the PT examination to at least 0.5 inches below the weld means that the assumption is conservative. The licensee proposes to perform a UT examination to the extent possible, which has been shown to be a minimum of 0.30 inch on the downhill side of the CEDM nozzle 88. The supplemental PT examination technique was applied to CEDM nozzles 54, 59, 66, 70, 78, 86, 87, 88 and 91. The remaining 82 CEDM nozzles received UT examination to a minimum distance of 0.41 inches below the weld on the downhill side. For the 9 nozzles inspected to the requested minimum on the downhill side using a combination of UT and PT, the area that was UT examined was greater on the uphill side of the nozzles.

The aforementioned crack growth analysis used the approach described in Footnote 1 of the Order as the criteria to set the necessary height of the surface examination. Therefore, the coverage addressed by this request provides reasonable assurance of structural integrity of the component. However, this analysis incorporates a crack-growth formula different from that described in Footnote 1 of the Order, as provided in the Electric Power Research Institute Report, "Material Reliability Program (MRP) Crack Growth Rates for Evaluating Primary Water Stress Corrosion Cracking (PWSCC) of Thick Wall Alloy 600 Material (MRP-55), Revision 1." The NRC staff has completed a preliminary review of the crack-growth formula but has not yet made a final assessment regarding the acceptability of the report. If the NRC staff finds that

the crack-growth formula in industry report MRP-55 is unacceptable, the licensee shall revise its analysis that justifies relaxation of the Order within 30 days after the NRC informs the licensee of an NRC-approved crack-growth formula. If the licensee's revised analysis shows that the crack growth acceptance criteria are exceeded prior to the end of the current operating cycle, this relaxation is rescinded and the licensee shall, within 72 hours, submit to the NRC written justification for continued operation. If the revised analysis shows that the crack growth acceptance criteria are exceeded during the subsequent operating cycle, the licensee shall, within 30 days, submit the revised analysis for NRC review. If the revised analysis shows that the crack growth acceptance criteria are not exceeded during either the current operating cycle or the subsequent operating cycle, the licensee shall, within 30 days, submit a letter to the NRC confirming that its analysis has been revised. Any future crack-growth analyses performed for this and future cycles for RPV head penetrations must be based on an acceptable crack growth rate formula. The licensee accepted this condition by letter dated April 29, 2003.

The licensee did not provide calculated stress information directly applicable to all nozzles with coverage less than 0.5 inches below the weld. The licensee provided stress analysis of four intersection angles that represent the range of intersection angles on the RPV head. From the information provided by the licensee, the hoop stress at operating conditions for a nozzle with an intersection angle of 29.1° with the RPV head is 31 ksi on the ID surface and 29.3 ksi on the OD surface at 0.41 inches below the weld. Other information provided by the licensee indicates that the stress levels are reduced as the nozzle intersection angle with the RPV head increases, and the stress levels generally decrease rapidly as the location increases beyond 0.41 inches below the J-groove weld. Based on a review of the information provided by the licensee, it is likely that the areas uninspected by either UT or PT have operational hoop stress levels that are relatively low, possibly less than 25 ksi. Based on the results from the crack growth analysis and these expected stress levels, there is reasonable assurance of structural integrity for the uninspected portions of the nozzles. Therefore, performance of UT beyond 0.41 inches below the J-groove weld would result in hardship without a compensating increase in the level of quality and safety.

Request 2

The NRC staff's review of this request was based on criterion (2) of paragraph F of Section IV of the Order, which states:

Compliance with this Order for specific nozzles would result in hardship or unusual difficulty without a compensating increase in the level of quality and safety.

In supporting its request for approval of a proposed alternative examination to inspect less than 100 percent of the RPV head outer surface, the licensee has demonstrated that hardship would result from implementing a visual examination of 100 percent of the RPV head. The hardship identified by the licensee is caused by the inaccessible area on the RPV head because of twelve 6-inch shroud lugs and the horizontal RMI panel support legs. The staff finds that the access under the vertical insulation panels at the 12 shroud lug locations and the horizontal RMI support legs makes inspection of the RPV head in accordance with Order EA-03-009 very difficult and removal of the necessary interferences to accomplish the examination required by the Order would involve a hardship. This evaluation focuses on the issue of whether there is a compensating increase in the level of quality and safety such that the RPV head should be inspected in accordance with Order EA-03-009 despite this hardship.

The purpose of the BMV examination is to inspect for evidence of head penetration nozzle leakage as well as evidence of degradation on the vessel head surface. Since the examination covers approximately 99 percent of the head surface, including all areas adjacent to each of the head penetration nozzles and 100 percent of the RPV head penetrations 360° at the nozzle/RPV head interface, any evidence of nozzle leaks should be detected. In addition, the licensee's inspection covers those portions of the RPV head which are immediately upslope and downslope of the inaccessible areas. Evidence of boric acid leaks or corrosion would be visible in the examined areas. Therefore, the proposed alternative provides reasonable assurance of the structural integrity of the RPV head.

The licensee agreed by letter dated April 29, 2003 to the following condition:

Should there be any evidence of corrosive product upslope or downslope of the inaccessible areas, the relaxation is rescinded until such time that the licensee can provide adequate information to the staff that ensures that the RPV head is not degraded in the inaccessible areas.

Because the alternative proposed by the licensee in the relaxation request provides reasonable assurance of structural integrity of the component, and subject to the aforementioned condition, the staff finds that the licensee has demonstrated hardship without a compensating increase in the level of quality and safety.

4.0 CONCLUSION

The staff concludes that the licensee's proposed alternative examination of 91 CEDM RPV head penetration nozzles to a level at least 0.41 inches below the J-groove weld (more area will be covered if possible) on the downhill side of the nozzles, and the proposed alternative examination coverage of approximately 99 percent BMV examination of the RPV head to include 100 percent of the RPV nozzles 360° at the nozzle/head interface and the areas upslope and downslope of the aforementioned inaccessible areas, provide reasonable assurance of the structural integrity of the RPV head, VHP nozzles, and welds. Further inspection of the VHP nozzles or RPV head surface in accordance with Sections IV.C.(1)(a) and IV.C.(1)(b)(i) of Order EA-03-009 would result in hardship without a compensating increase in the level of quality and safety. Therefore, pursuant to Section IV, paragraph F, of Order EA-03-009, good cause has been shown for relaxation of the Order, and the staff authorizes, for one 18-month operating cycle commencing with startup from the spring 2003 (SL2-14) refueling outage, the proposed alternative inspection for all CEDM head penetration nozzles and the RPV head surface at St. Lucie Unit 2, subject to the following two conditions that were agreed upon by the licensee by letter dated April 29, 2003:

- b. If the NRC staff finds that the crack-growth formula in industry report MRP-55 is unacceptable, the licensee shall revise its analysis that justifies relaxation of the Order within 30 days after the NRC informs the licensee of an NRC-approved crack growth formula. If the licensee's revised analysis shows that the crack growth acceptance criteria are exceeded prior to the end of the current operating cycle, this relaxation is rescinded and the licensee shall, within 72 hours, submit to the NRC written justification for continued operation. If the revised analysis shows that the crack growth acceptance criteria are exceeded during the subsequent operating cycle, the licensee shall, within 30 days, submit the

revised analysis for NRC review. If the revised analysis shows that the crack growth acceptance criteria are not exceeded during either the current operating cycle or the subsequent operating cycle, the licensee shall, within 30 days, submit a letter to the NRC confirming that its analysis has been revised. Any future crack-growth analyses performed for this and future cycles for RPV head penetrations must be based on an acceptable crack growth rate formula.

- c. Should there be any evidence of corrosive product upslope or downslope of the inaccessible areas, the relaxation is rescinded until such time that the licensee can provide adequate information to the staff that ensures that the RPV head is not degraded in the inaccessible areas. Since the licensee did not identify such evidence, this condition is moot.

Principal Contributors: Robert Davis, NRR
Allen Hiser, NRR

Date: May 29, 2003



Entergy Operations, Inc.
1340 Echelon Parkway
Jackson, MS 39213-8298
Tel 601 368 5758

Michael A. Krupa
Director
Nuclear Safety & Licensing

CNRO-2003-00034

August 27, 2003

U.S. Nuclear Regulatory Commission
ATTN: Document Control Desk
Washington, DC 20555-0001

SUBJECT: Entergy Operations, Inc.
Relaxation Request to NRC Order EA-03-009 for the Vent Line Nozzle

Arkansas Nuclear One, Unit 2
Docket No. 50-368
License No. NPF-29

Waterford Steam Electric Station, Unit 3
Docket No. 50-382
License No. NPF-38

REFERENCE:

1. Entergy Letter to the NRC, "Relaxation Requests to NRC Order EA-03-009," dated July 1, 2003 (CNRO-2003-00027)
2. Entergy Letter to the NRC, "Response to Request for Additional Information Pertaining to Relaxation Requests to NRC Order EA-03-009", dated July 24, 2003 (CNRO-2003-00030)

Dear Sir or Madam:


In Reference 1, Entergy Operations, Inc. (Entergy) had requested relaxation from Section IV.C(1)(b) of NRC Order EA-03-009 for Arkansas Nuclear One, Units 1 and 2 (ANO-1 and ANO-2), and Waterford Steam Electric Station, Unit 3 (Waterford 3). That relaxation request pertained to both the vent line nozzle and the in-core instrumentation (ICI) nozzles. In telephone calls held on July 14 and July 15, 2003, representatives of the NRC staff and Entergy discussed these requests. As a result of those discussions, Entergy submitted revisions to the requests for ANO-2 and Waterford 3 and withdrew the ANO-1 request in Reference 2.

In further discussions with the NRC, Entergy noted that it was considering additional analysis-based relaxations for the ICI nozzles. It was agreed that Entergy would consolidate the ICI nozzle relaxation in a single submittal. On that basis, please disregard the portion of the requests in Reference 2 that pertains to the ICI nozzles. Entergy requests NRC review and approval of only the vent line nozzle portion of that relaxation request. Entergy has updated the requests to remove the ICI information and the enclosed ANO-2 and Waterford 3 relaxation requests supercede the previous versions in their entirety.

Entergy requests approval of these proposed relaxation requests by September 18, 2003, in order to support inspection activities scheduled during the upcoming fall 2003 refueling outages at ANO-2 and Waterford 3. Entergy plans to submit the consolidated ICI nozzle relaxation request for ANO-2 and Waterford 3 shortly.

This letter contains no new commitments. Should you have any questions, please contact Guy Davant at (601) 368-5756.

Sincerely,



MAK/FGB/bal

- Enclosure:
1. Vent Line Nozzle Relaxation Request for Arkansas Nuclear One, Unit 2
 2. Vent Line Nozzle Relaxation Request for Waterford Steam Electric Station, Unit 3
 3. Summary of Commitments

cc: Mr. C. G. Anderson (ANO)
Mr. W. A. Eaton (ECH)
Mr. G. D. Pierce (ECH)
Mr. J. E. Venable (W3)

Mr. T. W. Alexion, NRR Project Manager (ANO-2)
Mr. R. L. Bywater, NRC Senior Resident Inspector (ANO)
Mr. T. P. Gwynn, NRC Region IV Regional Administrator
Mr. M. C. Hay, NRC Senior Resident Inspector (W3)
Mr. N. Kalyanam, NRR Project Manager (W3)

ENCLOSURE 1

CNRO-2003-00034

**ARKANSAS NUCLEAR ONE, UNIT 2
VENT LINE NOZZLE RELAXATION REQUEST**

**ENTERGY OPERATIONS, INC.
ARKANSAS NUCLEAR ONE, UNIT 2
VENT LINE NOZZLE RELAXATION REQUEST TO NRC ORDER EA-03-009**

I. COMPONENT/EXAMINATION

Component/Number: 2R-1

Description: Reactor Pressure Vessel (RPV) head penetration nozzles

Code Class: 1

References: 1. NRC Order EA-03-009, "Issuance of Order Establishing Interim Inspection Requirements for Reactor Pressure Vessel Heads at Pressurized Water Reactors," dated February 11, 2003

2. Letter 2CAN020304 from Entergy Operations, Inc. to the NRC, "Entergy Operations, Inc. – Answer to Issuance of Order Establishing Interim Inspection Requirements for Reactor Pressure Vessel Heads at Pressurized Water Reactors", dated February 28, 2003

Unit: Arkansas Nuclear One, Unit 2 (ANO-2)

Inspection Interval: Third (3rd) 10-Year Interval

II. REQUIREMENTS

The NRC issued Order EA-03-009 (the Order) that modified the current licenses at nuclear facilities utilizing pressurized water reactors (PWRs), which includes ANO-2. The Order establishes inspection requirements for RPV head penetration nozzles. ANO-2 is categorized as a "High" primary water stress corrosion cracking (PWSCC) susceptibility plant based on an effective degradation year (EDY) value greater than 12.

According to Section IV.C.1(b) of the Order, RPV head penetration nozzles in the "High" PWSCC susceptibility category shall be inspected using *either* of the following non-destructive examination (NDE) techniques each refueling outage:

- (i) Ultrasonic testing (UT) of *each* RPV head penetration nozzle (i.e., nozzle base material) from two (2) inches above the J-groove weld to the bottom of the nozzle and an assessment to determine if leakage has occurred into the interference fit zone, *or*
- (ii) Eddy current testing (ECT) or dye penetrant testing (PT) of the wetted surface of *each* J-groove weld and RPV head penetration nozzle base material to at least two (2) inches above the J-groove weld.

III. PROPOSED ALTERNATIVES

The ANO-2 RPV head has ninety (90) penetration nozzles that include eighty-one (81) Control Element Drive Mechanism (CEDM) nozzles, eight (8) Incore Instrument (ICI) nozzles, and one (1) vent line nozzle. Entergy Operations, Inc. (Entergy) requests relaxation from and proposes an alternative to the requirements of the Order as discussed below.

NDE Inspection Technique for the Vent Line Nozzle

Entergy understands that the Order requires the same technique, specified in Section IV.C(1)(b), be used to inspect the entire population of RPV head penetration nozzles; combining techniques or using one technique on one nozzle and the other technique on another nozzle is not permitted.

Entergy plans to inspect the CEDM and ICI nozzles using the UT inspection technique as specified in Section IV.C(1)(b)(i) of the Order or in accordance with approved relaxation requests. In lieu of using the UT inspection technique on every RPV head penetration nozzle, Entergy requests authorization to inspect the vent line nozzle and J-groove weld using the ECT technique per Section IV.C(1)(b)(ii) of the Order.

As required by the Order, a 60-day report for ANO-2 will be submitted and will include specific inspection information; i.e., type, extent, and results of inspections performed.

IV. BASIS FOR PROPOSED ALTERNATIVES

NDE Inspection Technique for the Vent Line Nozzle

The Order requires inspecting the entire population of RPV head penetration nozzles using only one of the techniques specified in Section IV.C(1)(b). This limits the licensee's options without measurably increasing the level of quality or safety. Entergy believes that using either inspection technique is sufficient to detect the PWSCC phenomena, and that no significant benefit is gained by requiring the same technique to be used on all nozzles.

Conditions at ANO-2 warrant using a different technique on different nozzles due to nozzle configuration. Specifically, the UT inspection probe used to examine the CEDM and ICI nozzles is not suitable for the leakage assessment due to the lack of an interference fit on the smaller vent line nozzle; therefore, Entergy proposes to use a different technique (ECT) to perform this inspection, as requested in Section III above.

V. CONCLUSION

Section IV.F of NRC Order EA-03-009 states:

"Licensees proposing to deviate from the requirements of this Order shall seek relaxation of this Order pursuant to the procedure specified below. The Director, Office of Nuclear Reactor Regulation, may, in writing, relax or rescind any of the above conditions upon demonstration by the Licensee of good cause. A request for relaxation regarding inspection of specific nozzles shall also address the following criteria:

- (1) The proposed alternative(s) for inspection of specific nozzles will provide an acceptable level of quality and safety, or
- (2) Compliance with this Order for specific nozzles would result in hardship or unusual difficulty without a compensating increase in the level of quality and safety."

Entergy believes the requested authorization to use ECT on the vent line nozzle (Section III above) maintains the level of quality and safety prescribed in Section IV.C(1)(b) based upon the justification provided in Section IV, above. Therefore, Entergy requests that the proposed alternative be authorized pursuant to Section IV.F of the Order.

ENCLOSURE 2

CNRO-2003-00034

**WATERFORD STEAM ELECTRIC STATION, UNIT 3
VENT LINE NOZZLE RELAXATION REQUEST**

**ENTERGY OPERATIONS, INC.
WATERFORD STEAM ELECTRIC STATION, UNIT 3
VENT LINE NOZZLE RELAXATION REQUEST TO NRC ORDER EA-03-009**

I. COMPONENT/EXAMINATION

Component/Number: MRCT0001

Description: Reactor Pressure Vessel (RPV) head penetration nozzles

Code Class: 1

References:

1. NRC Order EA-03-009, "Issuance of Order Establishing Interim Inspection Requirements for Reactor Pressure Vessel Heads at Pressurized Water Reactors," dated February 11, 2003
2. Letter WF3F1-2003-0014 from Entergy Operations, Inc. to the NRC, "Entergy Operations, Inc. – Answer to Issuance of Order Establishing Interim Inspection Requirements for Reactor Pressure Vessel Heads at Pressurized Water Reactors", dated February 28, 2003

Unit: Waterford Steam Electric Station, Unit 3 (Waterford 3)

Inspection Interval: Second (2nd) 10-Year Interval

II. REQUIREMENTS

The NRC issued Order EA-03-009 (the Order) that modified the current licenses at nuclear facilities utilizing pressurized water reactors (PWRs), which includes Waterford 3. The Order establishes inspection requirements for RPV head penetration nozzles. Waterford 3 is categorized as a "High" primary water stress corrosion cracking (PWSCC) susceptibility plant based on an effective degradation year (EDY) value greater than 12.

According to Section IV.C.1(b) of the Order, RPV head penetration nozzles in the "High" PWSCC susceptibility category shall be inspected using *either* of the following non-destructive examination (NDE) techniques each refueling outage:

- (1) Ultrasonic testing (UT) of *each* RPV head penetration nozzle (i.e., nozzle base material) from two (2) inches above the J-groove weld to the bottom of the nozzle and an assessment to determine if leakage has occurred into the interference fit zone, *or*
- (2) Eddy current testing (ECT) or dye penetrant testing (PT) of the wetted surface of *each* J-groove weld and RPV head penetration nozzle base material to at least two (2) inches above the J-groove weld.

III. PROPOSED ALTERNATIVES

The Waterford 3 RPV head has one hundred-two (102) penetration nozzles that include ninety-one (91) Control Element Drive Mechanism (CEDM) nozzles, ten (10) Incore Instrument (ICI) nozzles, and one (1) vent line nozzle. Entergy Operations, Inc. (Entergy) requests relaxation from and proposes an alternative to the requirements of the Order as discussed below.

NDE Inspection Technique for the Vent Line Nozzle

Entergy understands that the Order requires the same technique, specified in Section IV.C(1)(b), be used to inspect the entire population of RPV head penetration nozzles; combining techniques or using one technique on one nozzle and the other technique on another nozzle is not permitted.

Entergy plans to inspect the CEDM and ICI nozzles using the UT inspection technique as specified in Section IV.C(1)(b)(i) of the Order or in accordance with approved relaxation requests. In lieu of using the UT inspection technique on every RPV head penetration nozzle, Entergy requests authorization to inspect the vent line nozzle and J-groove weld using the ECT technique per Section IV.C(1)(b)(ii) of the Order.

As required by the Order, a 60-day report for Waterford 3 will be submitted and will include specific inspection information; i.e., type, extent, and results of inspections performed.

IV. BASIS FOR PROPOSED ALTERNATIVES

NDE Inspection Technique for the Vent Line Nozzle

The Order requires inspecting the entire population of RPV head penetration nozzles using only one of the techniques specified in Section IV.C(1)(b). This limits the licensee's options without measurably increasing the level of quality or safety. Entergy believes that using either inspection technique is sufficient to detect the PWSCC phenomena, and that no significant benefit is gained by requiring the same technique to be used on all nozzles.

Conditions at Waterford 3 warrant using a different technique on different nozzles due to nozzle configuration. Specifically, the UT inspection probe used to examine the CEDM and ICI nozzles is not suitable for the leakage assessment due to the lack of an interference fit on the smaller vent line nozzle; therefore, Entergy proposes to use a different technique (ECT) to perform this inspection, as requested in Section III, above.

V. CONCLUSION

Section IV.F of NRC Order EA-03-009 states:

"Licensees proposing to deviate from the requirements of this Order shall seek relaxation of this Order pursuant to the procedure specified below. The Director, Office of Nuclear Reactor Regulation, may, in writing, relax or rescind any of the above conditions upon demonstration by the Licensee of good cause. A request for relaxation regarding inspection of specific nozzles shall also address the following criteria:

- (1) The proposed alternative(s) for inspection of specific nozzles will provide an acceptable level of quality and safety, or
- (2) Compliance with this Order for specific nozzles would result in hardship or unusual difficulty without a compensating increase in the level of quality and safety."

Entergy believes the requested authorization to use ECT on the vent line nozzle (Section III, above) maintains the level of quality and safety prescribed in Section IV.C(1)(b) based upon the justification provided in Section IV, above. Therefore, Entergy requests that the proposed alternative be authorized pursuant to Section IV.F of the Order.

ENCLOSURE 3

CNRO-2003-00034

SUMMARY OF COMMITMENTS

SUMMARY OF COMMITMENTS

COMMITMENT	TYPE (Check one)		SCHEDULED COMPLETION DATE
	ONE-TIME ACTION	CONTINUING COMPLIANCE	
<p>For ANO-2, Enclosure 1, Section III:</p> <p>As required by the Order, a 60-day report will be submitted and will include specific inspection information; i.e., type, extent, and results of inspections performed.</p>	✓		60 days after startup from the next refueling outage
<p>For Waterford 3, Enclosure 2, Section III:</p> <p>As required by the Order, a 60-day report will be submitted and will include specific inspection information; i.e., type, extent, and results of inspections performed.</p>	✓		60 days after startup from the next refueling outage

Robert Davis x4028

Simon Sheng

ANO-2 RELAXATION REQUESTS, IN ORDER OF PRIORITY

SE INPUT DUE

D/NRR
(w/OGC)

1. Bare Metal Visual (BMV) - TAC MB8927

05/08/03 - initial application
06/26/03 - RAI response
08/02/03 - 3 proprietary reports (2CAN080303)
08/02/03 - 4 non-proprietary reports (2CAN080302)
08/27/03 - RAI response (2CAN080306)

09/17??

PD
(w/OGC)

2. Control Element Drive Mechanism (CEDM) Nozzles - TAC MB9542
(and TAC MB9644 for Waterford)

06/11/03 - initial application (some is proprietary)
08/27/03 - supercedes for ANO-2 only (some is proprietary),
3" thick (CNRO-2003-00033)

09/22??

I've already drafted proprietary letter

PD
(w/OGC)

3. In-Core Instrumentation (ICI) Nozzles - TAC MC0640

09/03/03 - initial application

09/26??

PD
(w/OGC)

4. Vent Line Nozzle - TAC MB9882 (and TAC MB9883 for Waterford)

07/01/03 - initial application
07/24/03 - RAI response, withdrew ANO-1
08/27/03 - supercedes for ANO-2 and Wat., withdrew ICI portion,
(CNRO-2003-00034)

09/22??, (SE almost done)

- Notes:
1. In order to save time, a formal memo from EMCB to PDIV-1 is not needed. Once EMCB management has reviewed the SE, e-mail the SE to the PM, and the PM will have EMCB on concurrence of the outgoing document.
 2. The ANO-2 outage starts 09/23. With an 18-day outage, restart would be 10/11.
 3. During a public meeting on 08/14, the EMCB/BC indicated that NRC needs 30 days after the last submittal to complete a review and issue a finding.